The Institute of Paper Chemistry

Appleton, Wisconsin

Doctor's Dissertation

The Compression Creep Properties of Wet Pulp Mats

Harry Douglas Wilder

June, 1960

THE COMPRESSION CREEP PROPERTIES OF WET PULP MATS

A thesis submitted by

Harry Douglas Wilder

B.S. in Ch. E. 1955, The University of Wisconsin
M.S. 1957, Lawrence College

in partial fulfillment of the requirements
of The Institute of Paper Chemistry
for the degree of Doctor of Philosophy
from Lawrence College,
Appleton, Wisconsin

June, 1960

TABLE OF CONTENTS

PRESENTATION OF THE PROBLEM

The application of a stress to individual filaments or fibers of cellulosic materials results in not only an immediate deformation but also in a time-dependent component. This deformation is dependent upon the stress applied, and on the molecular structure of the basic polymer chains involved, as well as the way in which these molecules are joined together in the final filament or fiber.

The system becomes more complex when dealing with a fiber network such as that encountered in a wet sheet of paper, since the deformation is now dependent upon the interactions between fibers as well as upon the behavior of the individual fibers. When dealing with an individual filament in tension, the manner in which this filament is stressed can be quite clearly defined, at least in a macroscopic sense. However, when any form of stress is applied to a complex fiber network, the stress within the individual fibers is not clearly defined, since the fibers are subjected to bending, compression, and tension forces although the over-all stress applied to the system may be entirely compressive in nature. When the void volume between the fibers is filled with water, the behavior becomes even more complex. In this case, any movement of this water relative to the fibers results in fluid drag forces being exerted on these fibers; such forces act in addition to the mechanical forces and tend to compress the system even further or to resist such compression, depending on the direction of the fiber-water movement.

The filtration operations involved in sheet formation from a dilute pulp suspension, as well as the removal of water at the suction boxes and in the presses, involve these mechanisms since in all cases the mat

structure is compacted by the application of forces which act in a direction perpendicular to the plane of the sheet. In the filtration operations, the driving force for such a compaction process is the pressure gradient set up across the sheet by either the table rolls (in the case of the fourdrinier) or by the application of a uniform vacuum to the wire side of the sheet. In the press section, the driving force is mechanical resulting from the mechanical compaction of the sheet by the press rolls.

In general, the rate of water removal can be expressed as

$$\text{rate} = \frac{\text{driving force}}{\text{resistance}}$$

with the driving force being introduced through the application of either a fluid pressure differential or by a mechanical compacting force. Since the resistance to fluid flow is a strong function of the void fraction of the sheet, any time-dependent mat "compression" would be important. The limited amount of information now available in the literature related to the behavior of fibrous structures under "compressive" stresses indicates that this time-dependent component of deformation is a significant fraction of the total observed deformation.

Thus, the practical aspect of the problem may be stated as follows. Since all of the stages of water removal depend upon the void fraction of the sheet, and therefore upon the amount of deformation which the sheet undergoes when subjected to the force used to cause water removal, an understanding of the stress-time-deformation behavior of wet pulp mats when subjected to "compressive" stresses is necessary before these water

removal mechanisms can be completely understood. In addition, it is of considerable theoretical as well as practical interest to determine, at least to a certain extent, what mechanisms are of importance in this deformation process. The use of experimental techniques which give a clear separation of the variables of time and deformation is desirable.

The compressive creep test, carried out under a constant applied load, allows for such a separation, and will be employed in this work. Since changes in the interrelation between these variables is expected as the stress history is changed, and since all practical applications do involve such changes, this work will cover a variety of such stress histories, ranging from an essentially unstressed mat to one which has undergone several stress-stress removal cycles. From such a study, it is hoped that certain of the mechanisms involved can be understood in at least a qualitative manner. Also, it is hoped that the actual creep behavior can be described well enough so that numerical estimates can be made of the importance of creep in industrial processes involving water removal from the water-saturated sheet.

INTRODUCTION AND HISTORICAL REVIEW

This introductory section will be divided into three parts. The first section will deal with a general discussion of the properties of viscoelastic materials, with special emphasis on the behavior as observed using the creep test under constant applied load. Next, a section will be devoted to a review and discussion of the work which has been done on the behavior of fibrous systems under "compressive" loadings. Finally, a section will be devoted to the indirect evidence obtained from drainage studies which indicates that the time-dependent component of deformation is of importance in determining the rate of water flow through the sheet.

PROPERTIES OF VISCOELASTIC MATERIALS

When a material such as steel is tested for deformation under an applied load, it is observed that up to a certain limit the deformation observed is proportional to the load applied. Over rather extended time intervals there is no significant change in the magnitude of this deformation as long as the load is maintained constant. However, with many materials such as rubber, plastics, and paper, there is a significant change in the magnitude of the deformation with a change in the time of continuous loading. Since such behavior is somewhat analogous to the flow of a fluid under applied shear, this type of behavior is termed "viscoelasticity."

There are three types of mechanical tests used to describe the time-dependency of stress or strain. They are the stress relaxation test, the creep test, and the load-deformation test. The first two allow for separation of either stress and time or strain and time, while maintaining the third variable constant. These tests are discussed in detail in the literature (1, 2, 3). The creep test will be employed in this work, so a brief description of this test is included.

The creep test consists of the application of a constant load to the specimen and the measurement of the deformation as a function of time. The load is usually applied in tension, since this type is the easiest to apply and the resulting specimen deformation is relatively easily obtained. Although this test allows for the separation of the load-time-deformation variables, it has the inherent disadvantage that the specimen geometry changes due to deformation of the specimen during the test period.

In such a complex system the definition of stress within individual fibers is very difficult. Since the creep test is relatively simple to carry out experimentally and does allow for the separation of the time and deformation variables, this test will be employed in this work.

It has been pointed out that most of the creep work has been carried out using a single filament or fiber under tension. It is apparent from a consideration of the physical complexity of a material such as a sheet of paper or a mat of wet pulp fibers that a strict analogy cannot be drawn to the simple single filament system. Such an attempted analogy would be similar to comparing the behavior of a single cellulose molecule to the whole pulp fiber. A basic study of the mechanisms of deformation would have to include the contributions of the cellulose molecule itself, the fibrils which are made up of these molecules (and the crystalline and amorphous regions), the fibers made up of these fibrils, and the action of the fibers with respect to the system as a whole.

While the mat itself is subjected to a "compressive" stress, the individual fibers within the mat are subjected to tension, compression, bending, and shear. Many attempts have been made to fit the properties of such viscoelastic systems to simple mechanical models made up of dashpots and Hookean springs. In certain instances, it has been possible to correlate the experimental results with such models. However, as the system becomes more and more complex, it is necessary to add more mechanical units, and finally it becomes necessary to correct for the "non-Newtonian" behavior of the viscous elements. Although such an approach may yield equations which fit the data, such equations seem very empirical in nature. It is felt that if an empirical approach is required

(and in a system as complex as the one dealt with here this is almost certain to be the case) no explanation based on a quantitative treatment involving springs and dashpots should be used. Such an approach has the disadvantage of appearing to explain the basic mechanisms involved, and could very probably lead workers away from more fruitful avenues of approach.

RESPONSE TO STRESS

When a viscoelastic material is subjected to a stress, the total observed deformation can be divided into three parts. These include the immediate elastic deformation, the delayed elastic deformation, and the nonrecoverable deformation. A very good discussion of these components is given by Brezinski (2), with special reference to cellulose systems. Only a brief review will be given here.

These three components can be understood if we consider the time-strain relationship obtained when a specimen is subjected to a constant stress for a time, t, and is then unloaded. Upon application of the stress at zero time, the specimen undergoes an immediate elastic deformation. This deformation continues with time and, although it never ceases completely, it appears to approach a limiting value. The total deformation is thus the sum of the immediate elastic deformation and the total delayed deformation. If the load is now removed, the immediate elastic component is recovered, and the delayed recovery begins. Again, a limiting value is approached, and in the general case it is observed that not all of the initial delayed deformation is recovered. Thus, the total initial deformation is composed of the delayed elastic deformation (that portion which is recovered following the removal of the load) and the nonrecoverable deformation.

The immediate elastic deformation is due to the deformation of primary and secondary valence bonds and changes in primary and secondary valence bond angles. Although easy to visualize, the measurement of this deformation is very difficult due to the interference of delayed deformations and also because of the mechanical problems involved in such a measurement. The modulus of elasticity calculated by such a measurement will depend very strongly on the type and number of bonds present per unit volume. Thus, highly crystalline cellulose exhibits a much higher modulus than does a highly amorphous material. Brezinski, when studying the creep properties of paper under tension, found that the apparent elastic modulus (measured by extrapolation of creep data to zero time) decreased greatly as the relative humidity increased. Since the presence of water decreases the tendency for the existence of hydrogen bonds between fibers and fibrils, such results would be expected. When dealing with wet fibers in "compression," a low value would also seem probable.

"Delayed elastic deformation" in itself means little unless the conditions of recovery are stated. It is often possible to increase this component (at the expense of the nonrecoverable deformation) by increasing the temperature or some other variable which may increase the recovery. No definite boundary can be drawn between recoverable and nonrecoverable deformations (often referred to as primary and secondary creep). Such delayed elastic behavior is usually attributed to a change in configuration in the amorphous or less-ordered regions of the cellulose system. In these regions, there is much more randomness of orientation than in the crystalline regions and, although the molecules

are bonded to adjacent molecules at points along their length, there are segments which are unbonded and which may move or "jump" to new positions. When there is no external force present, the system is at equilibrium and these jumps are of a random nature. However, when a stress is present, the jumps are predominantly in a direction so as to relieve the applied stress. When the stress is removed, the molecules tend to return to their original random orientation.

When the molecules have oriented themselves as described above, there is less randomness (or more order) in the molecular orientation. This brings more of the molecules into contact with each other, and an increase in the degree of crystallinity may result. If such crystallization is permanent under the conditions of the experiment, it will lead to permanent deformation. Often permanent deformation of this type may be reduced or eliminated by carrying out the recovery measurements at elevated temperatures or humidities, since the vibrational energy of the molecular segments is increased by the former while the tendency to form secondary bonds is greatly reduced by the latter.

In the case of a wet fiber mat, it seems doubtful that any such irreversible crystallization would occur, since the fibers' bonding potential is largely satisfied by water molecules. Since the presence of water also decreases the bonding in the amorphous regions, it seems probable that this system would exhibit greater delayed elastic deformation than the corresponding "dry" system.

"Permanent set" can also result from the "viscous flow" of molecules through the amorphous regions of the polymer. However, the molecules of

cellulose are longer than the length of a crystallite, and therefore one chain may extend through several amorphous-crystalline combinations. The flow of such a molecule is restricted by the portion present in the crystalline regions, so that true viscous flow is not likely in this case.

In a system such as a wet fibrous mat, the behavior of the fibers relative to neighboring fibers must also be considered. Thus, though the deformation within a particular fiber may be entirely recoverable, the deformed fiber might slip entirely past its neighboring fibers and assume a new equilibrium position somewhat lower in the mat structure. When the stress is removed, this fiber might return to its original shape, but due to its change in position in the mat an over-all nonrecoverable deformation could occur. Or, depending on the location of the fiber relative to its neighbors and also on the stress applied to this fiber, only one end might slip to a new position while the rest of the fiber remained securely held by its neighbors. In this case, the removal of the stress would probably result in the return of the fiber to its original position, unless of course the deformation within the fiber were not completely recoverable or the displaced end became caught and was not free to relieve the stresses introduced during the creep test.

Mechanical Conditioning

Since the amount of "flow" that can occur in a material such as cellulose is limited by the presence of crystalline regions, it would seem that such flow would occur predominantly during the first loading cycle. Tests (1, 2) involving repeated loading-unloading cycles have shown this to be the case; generally, after two or three cycles there is little nonrecoverable deformation. Such treatment is known as "mechanical conditioning,"

and a great deal of the study given to creep properties of materials has been carried out using a mechanically conditioned sample. (A mechanically conditioned sample is not conditioned against stresses higher than those used in the conditioning process, since a higher stress may break weaker linkages and allow further nonrecoverable deformation to occur.)

One of the most interesting and valuable contributions of such studies on mechanically conditioned samples is the Boltzmann Superposition Principle. This principle was proposed by Boltzmann in 1874 and states, in effect, that (3, page 55) the deformation at any instant of a body manifesting primary (recoverable) creep is due not only to the load acting at that instant but also to the entire previous loading history. As an example of the application of this principle, let us consider a specimen (which is known to obey the principle) subjected to the loading schedule shown in Fig. 1.

It is seen that the removal of a stress is represented by the application of a negative stress of the same magnitude. The total deformation at any time is equal to the sum of all the deformations due to all previous stresses, allowing of course for the appropriate times over which each has acted.

A mathematical treatment of this principle is given in many references, and a brief summary of the treatment given by Leaderman (1, page 20) is presented here. When a stress is applied to a specimen, the instantaneous deformation is given by $J\sigma/E$, where J is a factor, σ the applied stress, and E the appropriate modulus of elasticity. It is further

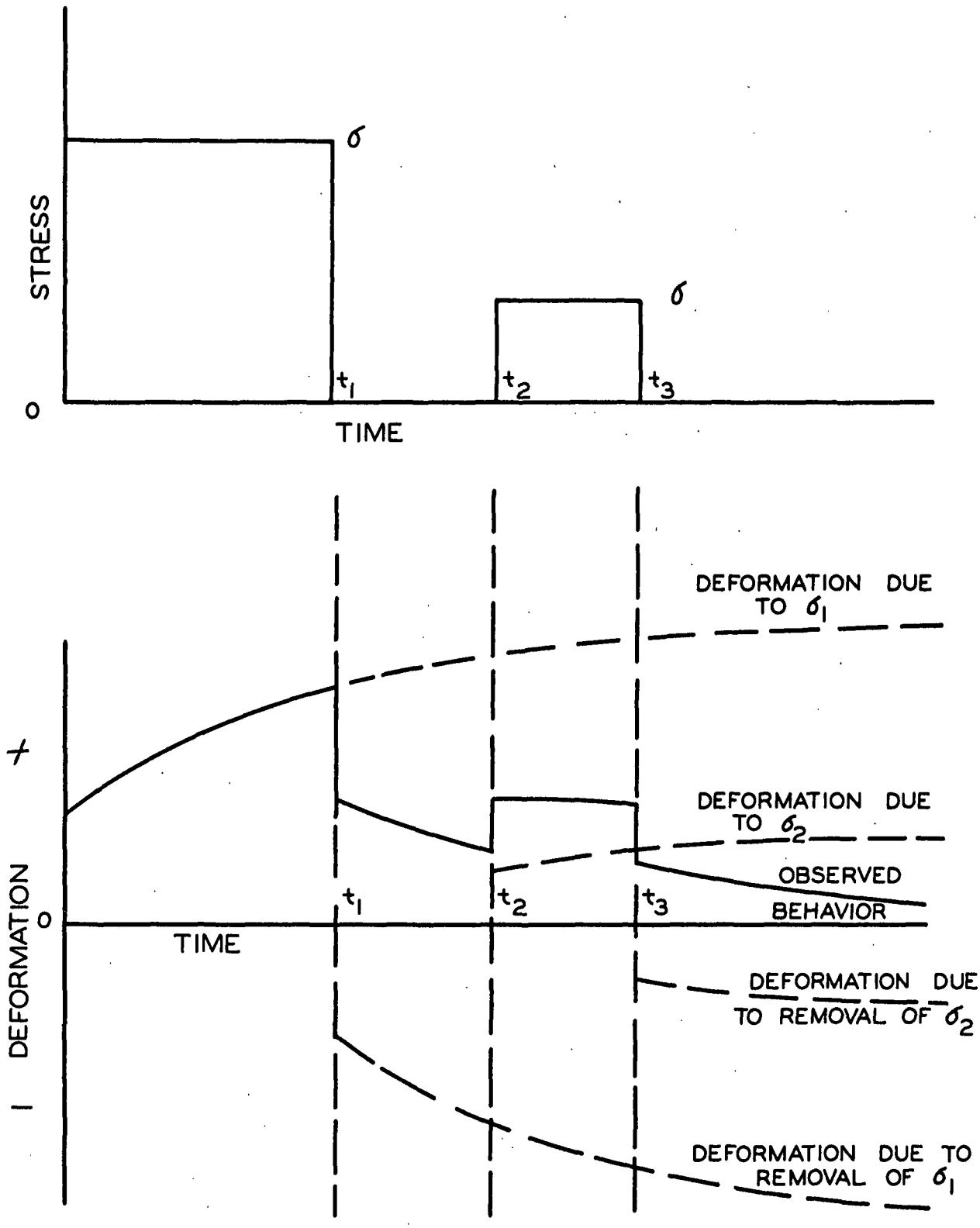

Figure 1. Behavior of a Material Obeying the Boltzmann Superposition Principle

assumed that the magnitude of the delayed elastic deformation is proportional to the immediate elastic deformation (or to the applied stress). This delayed deformation can then be written as:

$$\left(\frac{J\sigma}{E}\right)\beta \cdot f(t)$$

where β is a constant and $f(t)$ merely indicates that this deformation is some function of time. Then the total deformation at time t due to a stress σ is given by:

$$\Delta L = \frac{J\sigma}{E}[1 + \beta \cdot f(t)]. \qquad (1)$$

If the stress is continually changing with time, $(d\sigma/dt)(dt)$ represents the infinitesimal increase in stress over time dt at time t, and if the total time is designated by t', then

$$(\Delta L)_{t'} = \frac{J}{E}\left[\sigma_{t'} + \beta \int_0^{t'} \frac{d\sigma}{dt} \cdot f(t' - t)\, dt\right] \qquad (2)$$

where $\sigma_{t'}$ represents the stress at time, t', and $(t' - t)$ represents the time elapsed since the stress, $(d\sigma/dt)(dt)$, was applied. Leaderman also gives examples of modified forms of this equation which may be applied where the instantaneous deformation is proportional to the stress, while the delayed deformation is proportional to the product of a function of the stress and a function of the time under stress (1, page 159). Such modified forms are usually termed "nonlinear."

The applicability of this principle is checked by one of two methods. If the deformation characteristics are determined by a number of long-time

creep tests at different stresses, the deformation due to short-time cyclic tests using these stresses should be predictable. A comparison of the actual and calculated deformations would then prove or disprove the theory. Also, if the principle does apply, the creep and recovery curves of long-duration experiments should be identical (since the removal of the stress is equivalent to the addition of a negative stress of the same magnitude). The principle has been proven valid for a number of materials under tension and torsion (1). Steenberg (4) has found it to hold for a mechanically conditioned paper under tension after the first few minutes of each cycle. Ivarsson (5) studied the stress-strain characteristics of cellulosic sheets in compression at a constant rate of strain, and found that after the first cycle the load-time curve (time being proportional to strain) for the loading and unloading portions of the cycle were almost identical in form. This indicates that the principle is also applicable in this case. Brezinski (2) carried out several long-duration, multiple-cycle creep tests and found that although the creep-recovery curves approached each other more closely as more cycles were carried out, at the higher stresses a difference still existed after six cycles. At lower stresses, the two curves agreed very well. It thus appears that the applicability of this principle depends not only upon the amount of mechanical conditioning but also on the stresses involved.

Behavior of Materials Prior to Mechanical Conditioning

Although the superposition principle is of interest once the nonrecoverable deformation has been eliminated by mechanical conditioning, the condition usually encountered during forming and pressing operations would be one

of either no or only partial mechanical conditioning. At the same time, laboratory drainage measurements are carried out on an essentially unconditioned sample, since the stress is never released during the entire operation. Therefore, it is also necessary to consider the first-creep properties of the material. When first-creep deformation is plotted as a function of the logarithm of time, a sigmoidal curve is obtained:

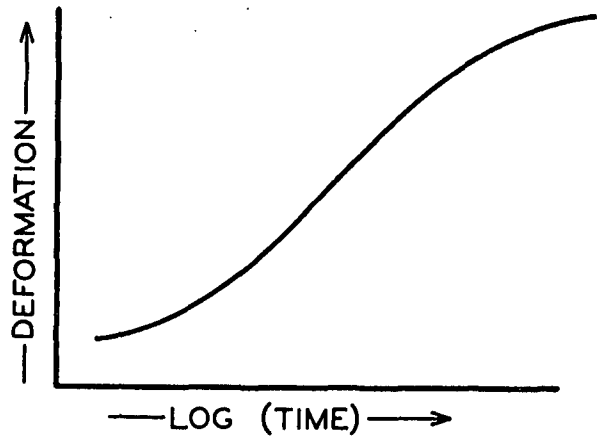

Figure 2. Usual Shape of First-Creep Curve

This is the general form of the curve, and if a material could be studied at all times from zero to infinity, such a curve would usually be observed. However, since the various creep mechanisms discussed previously may act at different times for different materials or at different temperatures and humidities, only certain portions of this over-all curve may be observed experimentally. Leaderman (1) has shown that the initial and final portions of the curve are best described by a power law, while the central portion is described by a logarithmic law. Brezinski (2) has carried out a very complete study of the first-creep behavior of paper under tension and has found that at low applied stresses and relatively short times, the total first-creep deformation is described by a power equation. At

longer times or at higher stresses, the total creep function was found to be logarithmic, with the slope of this logarithmic curve being directly proportional to the applied stress. Brezinski reported no leveling off of the curve at the longer times employed in his work. Tobolsky and Eyring (6) also report such behavior "under conditions of high stress," and interpret it as an indication that primary bonds are being broken after a certain time period.

It has been mentioned that Brezinski found a direct relationship between the slope of the logarithmic creep curve and the applied stress. Catsiff, et. al., (7) worked with single nylon filaments and found the same increase in rate of creep as the stress applied to the filaments was increased. Leaderman (1) shows that increases in temperature have much the same influence as increases in applied stress when dealing with rubber. Catsiff, et.al., reasoned that if the creep rate was a direct function of the applied stress, then by shifting the creep curves along the time and strain axes it should be possible to fit all the data to a single "master-creep"curve. The shift required in the strain dimension was found to be linear with the applied stress at low stress values, but at higher stresses a limiting "shift factor" was required. The immediate elastic deformation was also found to be proportional to the applied stress, indicating an elastic modulus independent of stress.

Brezinski (2) also found that the creep of paper over a wide range of tensile stresses could be correlated using a master creep curve. The curves were first reduced to a single slope by dividing the strain observed by the applied stress. Then one curve was selected as the base for the master curve, and the other curves were shifted in log (time)

until they coincided with this base curve. The time shift (actually a shift in log time) is also a linear function of the initial applied stress. As a result of this work, it is concluded that all portions of the creep curve will occur at any initial stress, and are linearly related to the initial stress, although they will occur at different experimental times for different stresses. Again, the immediate elastic deformation is also found to be a linear function of initial stress, indicating a constant modulus.

BEHAVIOR OF FIBROUS SYSTEMS UNDER COMPRESSIVE LOADS

Almost all of the work on the viscoelastic behavior of paper or cellulosic fibers has been carried out using relatively dry paper in tension. Studies have also been made at higher moisture contents using sheets in tension, and a great increase in deformation is indicated. However, in these cases once the interfiber bonding is weakened or destroyed, the fiber itself has little influence on the sheet elongation. In the case of fibrous systems in compression, the interfiber bonds are, of course, important in determining the creep behavior, but in this case the fibers are preferentially oriented with their length dimension perpendicular to the direction of the applied stress. These fibers will then act as a very complex system of beams, supported at various points by the fibers beneath them. This difference in the fundamental nature of the fiber behavior makes it very dangerous to draw conclusions from work done on tension applied parallel to the plane of the sheet and to apply such conclusions to the present problem.

Very little work has been done on the behavior of cellulosic systems under compressive stresses, and even less is known about the behavior of wet systems under these conditions. Gavelin (8) has studied the creep and stress-relaxation of newsprint. The creep studies were carried out using a rather crude technique; the newsprint was kept in large rolls, and the change in roll diameter was measured as a function of time following the application of a load. Little can be concluded from these results except that a large portion of the deformation was elastic and considerable permanent deformation resulted from the first cycle.

Ivarsson (5) studied the compression of cellulose fiber sheets by the application of a constantly varying rate of strain. Although it is difficult to draw quantitative conclusions from this type of measurement, certain trends are evident. The material appeared to be mechanically conditioned following one cycle. Increasing the applied maximum stress increases the compression and the permanent set, but the "relative permanent set" (the ratio of permanent set to total initial deformation) is less load-dependent. As the moisture content is increased, the values for absolute compression and permanent set increase. In the range of five to eighty per cent moisture (based on dry fiber), the absolute compressibility (deformation/initial caliper) increases initially but levels off at higher moisture contents. At constant moisture, this value decreases with beating. The relative permanent set reaches a maximum at about ten to fifteen per cent moisture and then decreases slowly. Beating has little effect on this value.

Christensen and Barkas (9) have studied the compression of wet fibrous webs using a surface tension method of compressing the system. An unbeaten bleached sulfite pulp was employed. While their work deals with the so-called "equilibrium" conditions and does not include the time variable, some aspects of their findings are of interest. When the loading-unloading cycles were extended over several complete cycles, it was found that the mat was compressed less during the second cycle than during the first. This is in direct opposition to the behavior of most viscoelastic materials, and the authors attribute this behavior to fiber entanglement plus possible increased bonding. When the pulp was beaten, it was found that the mat was more readily deformed. This is apparently

due to decreases in fiber rigidity as a result of the beating operation. [Work carried out at the Institute (10) indicates that the beating of an unbleached pulp increases its compressibility but that a bleached pulp is not affected.] In this work, the amount of deformation was calculated using a direct measure of the decrease in mat thickness and also by measuring the amount of water removed from the mat and calculating deformation, assuming no change in mat area during compression. Since both values agreed very well, this indicates that there is little change in mat diameter even when the mat edges are not restricted. This finding is of importance in the design considerations to be discussed in a later section.

Ingmanson and Whitney (11) report that when a water-saturated mat of red oak kraft pulp is placed under a constant "compressive" stress, the solids concentration within the mat is a linear function of the logarithm of the time of stress application.

Seborg and co-workers (12-14) have carried out several experiments concerning the recovery of wet fibrous mats from compressive deformations. Their assumption has been that this recovery is a function of the fiber "stiffness." In addition to recovery measurements, they measured the stiffness of individual fibers by subjecting them to bending. These measurements were also made under conditions of complete water saturation. Through these two types of measurements and a comparison of the results of each, the following conclusions were reached (southern pine pulps were used):

1. When considering the recovery from deformation, sulfate summerwood fibers were more than twice as recoverable as sulfite summerwood fibers. Sulfate springwood fibers were third, and sulfite springwood fibers were least recoverable.

2. Measurements on fiber stiffness ranked the four fiber types in the same order. However, the stiffness measurements showed a much greater difference between sulfate and sulfite fibers than did the recovery tests.

3. As the temperature of the recovery tests was increased, the per cent recovery decreased linearly over the range of 13-41°C.

4. As the mat basis weight was decreased, recovery increased. Since this increase was very large in the range of basis weights encountered on paper machines, this point must be considered in the design of the experimental program.

5. As the freeness increases, there is a very marked increase in the recovery value.

6. As the duration of the compression portion of the cycle was increased, recovery decreased.

7. In general, pulps could be ranked in order of decreasing recovery as follows: kraft> sulfite> groundwood.

One obvious limitation of this work is that, following the initial mat deformation, no precautions were taken to prevent air from entering the pad during recovery. This introduces surface tension effects as a variable.

The use of recovery tests as a possible measure of the stiffness of the fibers making up the mat was first introduced by Brown (15). Although he eliminated time effects by taking readings at certain predetermined times, he was aware of their existence. When describing the procedures used in carrying out these tests, he states:

"The pulp sheet should not be measured until it has been under full pressure one minute since it takes some time to reach minimum thickness. Following load removal, some pulps are still increasing in thickness four minutes later, but the major increase in all cases occurs in the first minute."

From this summary of the results reported in the literature, it is seen that very little work has been done with time as a variable. However,

all indications are that time is an important variable to be considered in this system. The other results presented here indicate that the deformations introduced by the application of "compressive" stresses are similar to those observed with most systems involving viscoelastic materials in that both recoverable and nonrecoverable deformations are encountered.

TIME-DEPENDENT DEFORMATION:
INDIRECT EVIDENCE FROM DRAINAGE STUDIES

A great amount of work has been carried out at the Institute in the field of fluid flow through porous media. Indications have been found through these studies that a time-dependent deformation may be present in the case of wet fibrous systems while such systems are subjected to the fluid drag forces present during the fluid flow. This evidence will be discussed.

When considering fluid flow through a fibrous network, the rate equation is expressed in terms of the usual driving force-resistance concept. The following form is usually employed:

$$\frac{dV}{dt} = \frac{A \cdot \Delta P_f}{(W/A)R\mu} \qquad (3)$$

where dV/dt is the volumetric rate of flow through a filter bed having an external cross-sectional area, A, and a dry weight, W. The pressure drop (driving force) across the bed is ΔP_f and the fluid viscosity is μ. R is termed the "average specific filtration resistance" of the bed (11). With an incompressible material such as sand, this resistance term remains essentially constant during the course of the filtration and the flow rate is directly proportional to the pressure drop and the area available for flow and inversely proportional to the mass of solid particles in the bed.

Ingmanson (16) has employed the Kozeny-Carman equation to relate the specific filtration resistance of a fibrous system to certain physical properties of the bed. The resulting equation may be written:

$$R = \frac{kS_w^2 \Delta P_f}{\int_0^{\Delta P_f} [(1 - vc)^3/c] dP} \qquad (4)$$

where k is the Kozeny constant, S_w the specific surface, v the effective specific volume, and P the mechanical compacting pressure at some point in the bed at which the fiber concentration is given by c. The integration is required since the compacting pressure varies throughout the thickness of the pad, from zero at the top surface to ΔP_f at the bottom. It is seen that if all of these quantities remain unchanged by the time of stress application, then the resistance to flow should not change with time. However, if the mat solids concentration, c, increases with time due to increased mat deformation, the resistance, R, must increase. In all work described here, c has been assumed independent of time, and has been related to the compacting pressure by the equation:

$$c = MP^N \qquad (5)$$

where M and N are constants. This equation is often referred to as the "compressibility equation." Two methods are employed in the laboratory to study this drainage behavior, one being carried out at a constant flow rate and the other at a constant pressure drop across the fibrous mat. Both use Equation (5) in conjunction with Equations (3) and (4) to determine specific volume and specific surface. When the specific volume, v, is determined by each of these methods, it is observed that the value obtained using the constant pressure drop technique is considerably higher than that obtained under conditions of constant rate. At

the same pressure drop, the filtration resistance obtained at a constant pressure drop is consistently higher than the corresponding constant rate value (11).

Let us consider an element of the bed located just above the bottom of the mat and of infinitesimal thickness. In a constant pressure drop process, this element is subjected to a constant stress throughout the experimental run. However, in a constant-rate experiment, the stress on this element is building up throughout the run, since if (dV/dt) is to remain constant as (W/A) increases, ΔP_f must also increase. (The same effect is felt by elements located nearer the top of the bed, except in this case there is also some change in stress during the constant pressure drop method, since the mat is continuously being built up during the filtration process and the stress at any point is a function of the mass fraction of solid material above this point.)

When Equation (5) is used to relate mat solids concentration and compacting stress, the constants are evaluated by compressing a mat under a mechanical load and after several minutes recording the deformation. Thus, if time is an important variable, then this technique yields a value of c which is higher than the true value at some shorter time. In the constant pressure drop work, each element within the bed is subjected to the same load for a longer period of time than in the constant rate work; therefore, c would be higher in this case. Since $v \cdot c$ appears in the filtration equation, it is noted that the use of a higher value of c would result in a lowering of v. Since the value of c calculated from Equation (5) is more in error in the case of the constant rate method, this method would yield a value of v lower than

that obtained by the other means. Similar considerations explain the difference in filtration resistance at equivalent pressure drops. Since the constant rate measurements are considerably displaced from the experimentally determined concentration-stress relationship, the bed has less chance to compact, and the resistance is lower than with the other method.

Another example of the time dependence of filtration resistance can be found in the constant pressure drop filtration data. If Equation (3) is rearranged and written in incremental form, it becomes:

$$\frac{1}{\Delta V/\Delta t} = \mu \frac{(W/A)R}{A \cdot \Delta P_f} \quad . \qquad (3')$$

However, when the slurry is dilute, the basis weight (W/A) is proportional to the volume of filtrate collected. Then this equation may be written:

$$\frac{1}{\Delta V/\Delta t} = B'RV \qquad (3'')$$

where B' is a constant equal to $\mu C/A^2 \Delta P_f$ and C is the slurry consistency. For a constant pressure drop experiment, if the left side of this equation is plotted against the total volume of filtrate, V, a straight line should be obtained. However, data obtained in this manner (11) indicate that the slope of the line (and consequently the value of R) increases as the filtration is carried out. This can also be attributed to a time effect.

Since the times involved in these filtration measurements are of the order of four to ten minutes, it is probable that a considerable

amount of the total deformation as determined by the static "compressibility" tests has already occurred, at least in those portions of the mat which were laid down early in the run. However, during drainage at the table rolls of the fourdrinier, the filtration time is very short and the time effect becomes even more important. Taylor (17) has shown that the maximum pressure differential available at a table roll is given by:

$$(\Delta P_f)_{max.} = \frac{1}{2}\rho u^2 \qquad (6)$$

where

ρ = white water density, g./cc., and

u = wire velocity, cm./sec.

Taylor also related the total filtration resistance, R_t, of the mat to the machine speed, table roll radius, and drainage rate. This total filtration resistance is related to the specific filtration resistance, R, by:

$$R_t = W'_{av} R \qquad (7)$$

where W'_{av} represents the arithmetic average of the mat basis weight entering and leaving the table roll area. Measurements made on a machine at Gilbert Paper Company (18) make it possible to calculate the average specific filtration resistance on the machine, and a comparison of these results with those obtained in the laboratory at equivalent pressure drops shows that the laboratory-obtained resistance is about eight times as great as that calculated for the machine. As least five factors might be partially responsible for this result. First, it is possible that water removal on the fourdrinier wire occurs by a different

mechanism than filtration as carried out in the laboratory. Second, since the basis weight on the machine is much lower than that encountered in the laboratory measurements, there would be a much greater chance for fines loss on the machine. Such fines losses would reduce the filtration resistance.

Burkhard and Wrist (19) have succeeded in measuring the pressure profiles along the table roll region, and found that just as the wire passes over the top dead center of the table roll there is a pressure exerted upward from beneath the wire. This might act to expand the mat and make it more permeable. However, it seems more likely that the entire web would be lifted up. A fourth possibility is that, in the table roll area, fibers which were subjected to the drag forces would be partially supported by neighboring fibers which were outside this zone of drainage. This would tend to keep the sheet more porous, and drainage could occur more rapidly.

The fifth possibility is that creep is an important factor in determining drainage behavior. Since the drainage time at each table roll (estimated from Wrist's data) varies from about 0.005 seconds at a wire speed of 500 feet per minute to about 0.002 seconds at a wire speed of 2500 feet per minute, there is very little time for the mat to compress under machine conditions.

This introduction and review has attempted to present the general aspects of the behavior of viscoelastic materials, with special emphasis on work which was concerned with creep behavior of fibrous structures under "compressive" stresses or on work which had a direct

bearing on the behavior of such a system. Since it is also of importance to point out the value of such work from a practical standpoint, several examples were presented which indicate that the time-dependent component of deformation is of importance in both laboratory and machine drainage studies.

APPARATUS: CONSTRUCTION AND OPERATION

PRELIMINARY CONSIDERATIONS

Prior to the actual design and construction of the apparatus to be used in the main body of this work, preliminary work of an exploratory nature was carried out using the filtration apparatus of the Chemical Engineering Group at the Institute (11). Mats were formed using the filtration technique and "compressions" were carried out by inserting a permeable piston into the filtration tube following mat formation and adding the desired weights to this piston arrangement. During this work, the sides of the mat were restricted from any outward movement by the presence of the Lucite filtration tube. Mat thicknesses were measured with a cathetometer. Classified and unclassified bleached sulfite pulp and nylon fibers were used in this work. As a result of these experiments, the following difficulties and limitations were observed.

First, some difficulty was encountered in obtaining mats of reproducible "compression" behavior. It is known that the amount of fiber flocculation which occurs during the formation operation has an effect on the properties of the resulting mat. In filtration work, mats are usually formed from 0.01%-consistency stock to minimize this flocculation tendency. However, in this work the mats must be formed under very low pressure drops so that as little precompaction of the mat occurs as possible. Therefore, very low flow rates were necessary, especially when dealing with the unclassified pulps of relatively high filtration resistance, and considerable flocculation

was observed at 0.01% consistency. It was concluded that in future work, consistencies should be chosen so that the flocculation effects were minimized. The choice of fiber to be used is also an important consideration here.

In these preliminary tests, it was observed that when the piston was removed from the mat following creep measurements, the recovering mat exhibited a "hump" in the center of the tube. This indicated that the recovery near the edges was hindered by the frictional drag forces between the outer fibers of the mat and the walls of the filtration tube containing the mat. When the mat was removed from the tube and immersed in water, no such edge effects were observed. Some very interesting work along similar lines is reported by Train (20), who studied the transmission of forces through a powder mass during the process of pelleting. The author reports that the internal stresses are highest at the outside edge of the pellet just below the compression member, and this is attributed to a build-up of frictional forces in the areas of maximum relative movement between the powder particles and the cylinder walls. Such edge effects were eliminated in the final apparatus by removing the restraining tube prior to mat compression.

The preliminary work also indicated that a manually operated measuring device such as the cathetometer used here would be of little value if deformation readings were to be taken at relatively short times (less than ten seconds). Since this low time range is of particular interest, it was felt that an electrical measuring system would be more appropriate.

CREEP-TESTING APPARATUS, DESIGN AND OPERATION

In the design and construction of this apparatus, the following objectives were achieved:

1. The elimination of any changes in temperature during the creep test.

2. The elimination of any edge effects due to mat-cylinder friction and also possible friction between the piston sides and the cylinder.

3. Allowance for a precompaction of the mat prior to the actual compression measurements (this is to overcome any nonuniform compaction introduced by the mat-forming operation, and also to keep the mat from being disturbed around its unconfined edges during the initial rapid stages of deformation).

4. Provision of a swift and accurate method of measuring mat deformation, both at short and long times.

5. The ability to use relatively small compressive loads.

6. Once the compressive portion of the cycle is completed, it must be possible to remove the compressive load and to study the mat recovery over the same time range.

7. Following the creep and creep-recovery tests, it must be possible to remove the mat from the apparatus to allow it to be dried for basis-weight determination.

The essential features of the creep-testing apparatus are shown in Figs. 3, 4, and 5. A description will be given here of the operations involved in forming and testing a wet mat, so that the functioning of the apparatus may be better understood. Detailed descriptions of pulp-preparation procedures will be found in the section on experimental procedures.

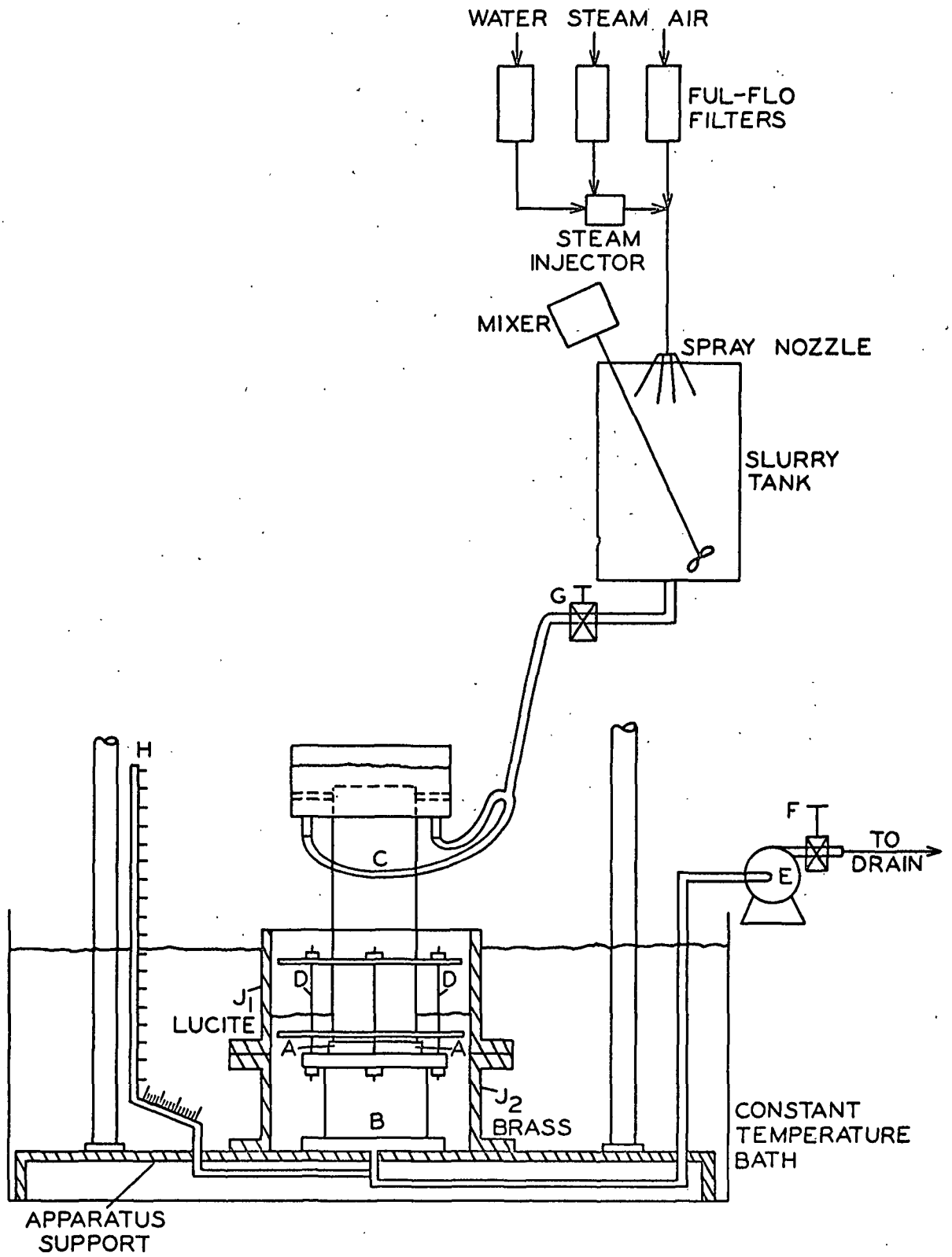

Figure 3. Creep Testing Apparatus, During Mat Formation

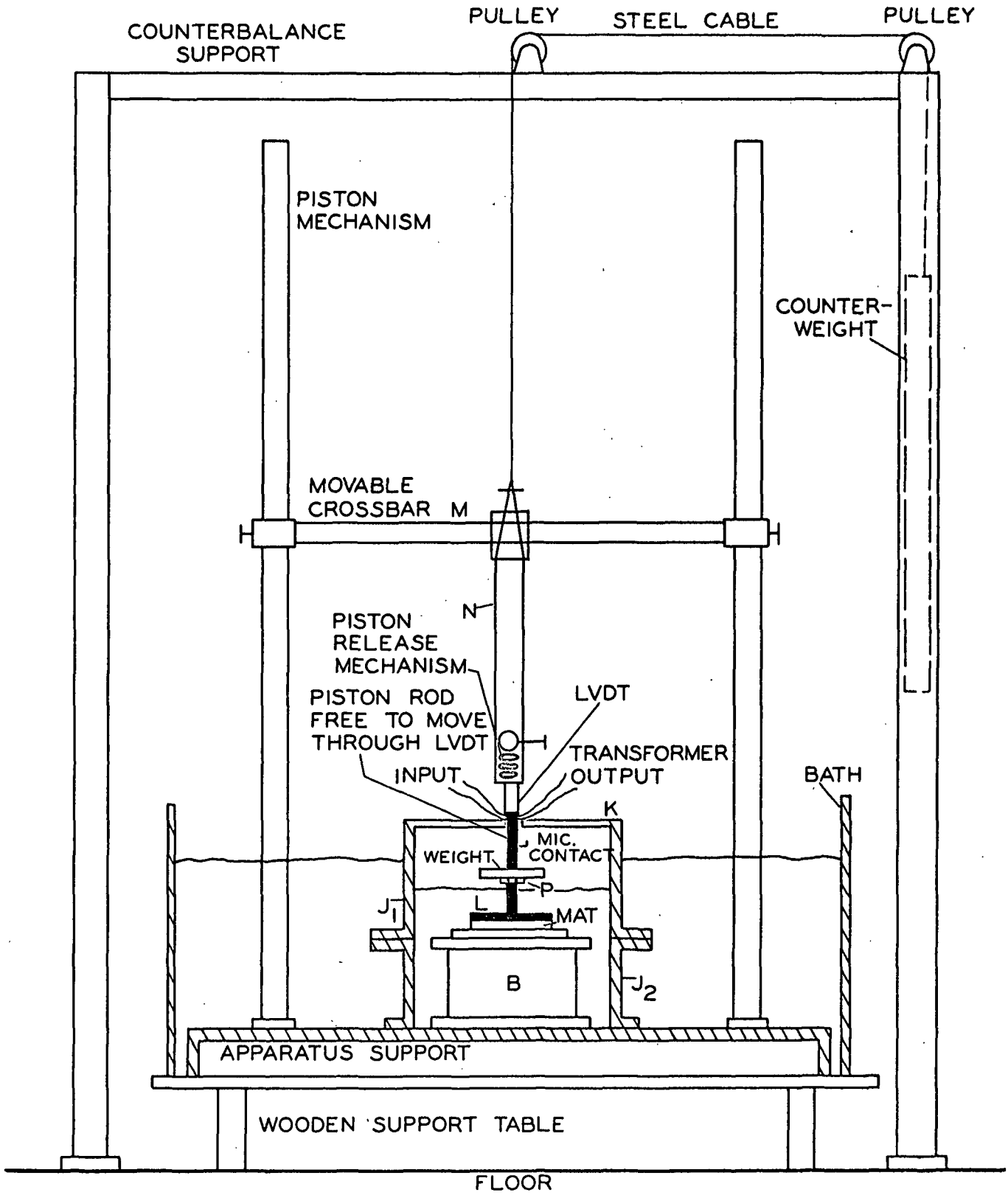

Figure 4. Creep Testing Apparatus, During Mat Compression and Recovery

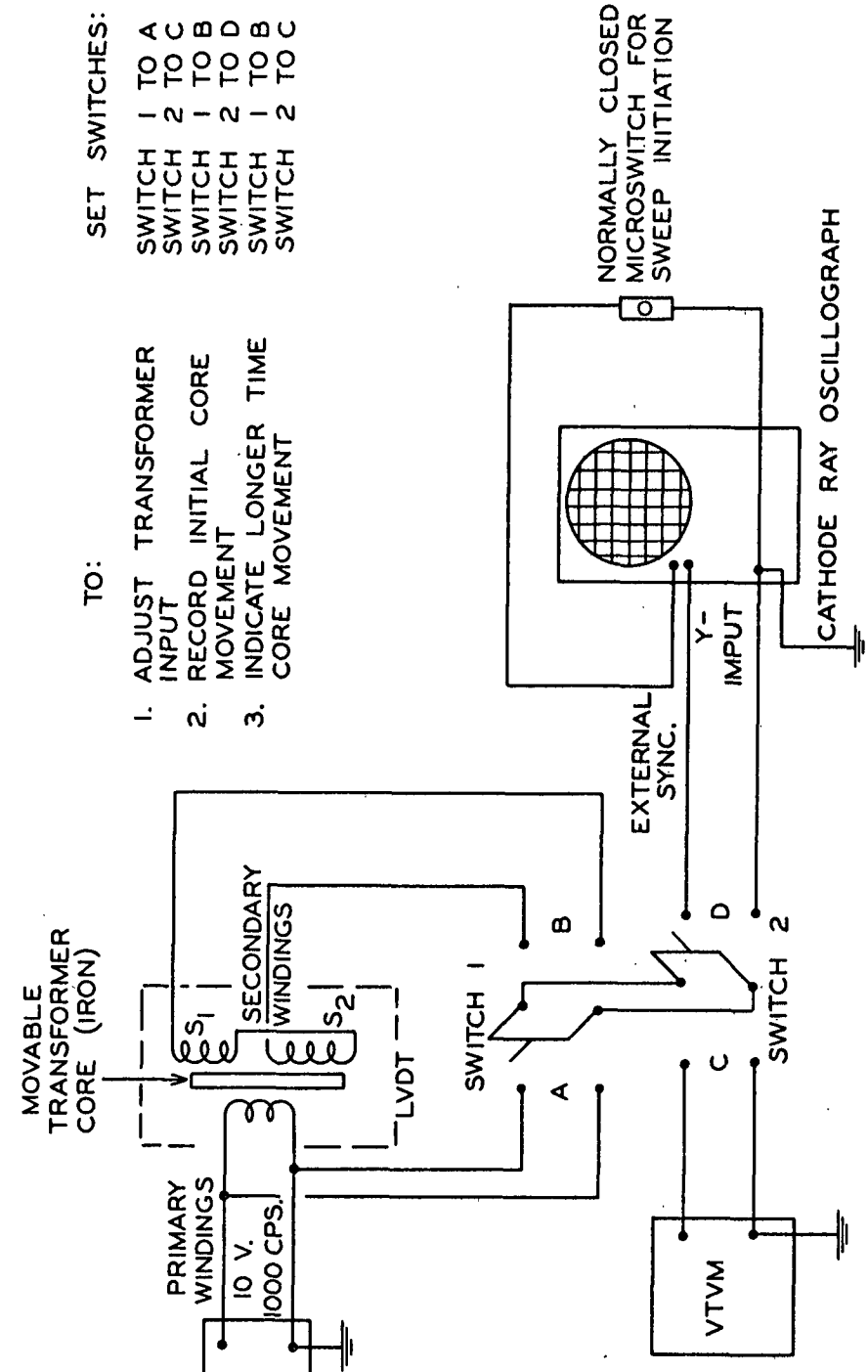

Figure 5. Circuit Diagram of Measuring Circuit Used With Linear Variable Differential Transformer (LVDT)

MAT FORMATION

The fifty-gallon stainless steel slurry tank is filled with sufficient water to give a slurry consistency of approximately 0.005%. The water is heated to slightly above room temperature by injecting steam into the water line with a Penberthy steam injector, and air is then injected through a small orifice to strip dissolved gases from the water. The water, steam, and air are all filtered through Ful-Flo brass constructed filters prior to the mixing step. The heated, deaerated water is then sprayed into the top of the slurry tank. The water is agitated with a reduced speed 1/4-horsepower Lightnin' mixer to remove entrapped air, and the pulp slurry is added. Mixing is continued for about ten minutes prior to mat formation.

The forming septum, A, is constructed of brass plate drilled to allow water passage. The upper face of the septum is covered with a 100-mesh screen which is clamped tightly into place on the septum. The septum is secured to the lower brass-flanged cylinder, B, by four brass screws (Figs. 3 and 4). Before the mat is formed, the septum position is measured by placing the piston on the septum and measuring the distance between the micrometer support, K, and the micrometer contact on the piston rod with a depth micrometer which can be read to 0.001 inch and estimated to 0.0001 inch. Contact between the micrometer and the piston rod is indicated electrically by having a d.c. circuit close when contact is made; a milliammeter is used to indicate circuit closure.

The filtration tube, C, is then lowered onto the gasketed septum and secured by four threaded brass rods, D. Two baffled inlets are provided in the filtration tube to reduce uneven flow. The forming septum

is then wet from below with deaerated water so that no air bubbles will become trapped in the septum and cause an uneven flow.

The filtration tube is filled with slurry and the centrifugal pump, E, is started. The flow from the pump is regulated by the throttling valve, F, and the flow to the tube by the valve, G. These input and output flows are balanced so that a constant head is maintained in the filtration tube and so that a maximum mat frictional pressure drop of one centimeter of water is observed on the manometer, H. The mat formed by this process has a diameter of five inches, and the formation time is approximately thirty minutes for a mat containing five grams of ovendry fibers.

TEMPERATURE CONTROL

In order to maintain a constant temperature during the creep tests, the entire mat-containing apparatus is placed in a glass temperature bath equipped with two centrifugal circulating pumps, a cooling coil supplied with well water, and two 125-watt heaters. A thermoregulator and electronic relay are employed with the heaters to control the temperature to within $\pm 0.05°C.$ of the desired value. Since the mat itself cannot be exposed to the agitation caused by the circulation pumps, it was necessary to surround the mat-containing section by the guard cylinder, J. The top portion of this cylinder, J_1, is made of Lucite tubing so that the mat can be more readily observed. However, Lucite is not a good conductor of heat, and since the control of the mat temperature depends upon the ability of the heat to flow into or out of the mat compartment through the guard cylinder, the bottom portion of the

cylinder, J_2, is made of brass. These cylinders are gasketed so there is no leakage of liquid between the water bath proper and the mat compartment. Temperature measurements made during actual runs indicate that the compartment temperature is within 0.05°C. of the bath temperature.

PREPARATION OF THE MAT FOR TESTING

It has been mentioned that the mat is formed under a fluid friction pressure drop of not more than 1 cm. of water. However, even this small force serves to compress the mat, and unless some means of correcting for this "precompressive stress" is employed, the first compression measurements will in reality be at least partially second compression measurements. Another difficulty involved is that when the filtration tube is removed prior to compression, the mat is disturbed if some method is not used to hold it in place. Therefore, the unweighted piston, L, is lowered inside the filtration tube by means of the movable crossbar, M, until the weight of the piston is supported entirely by the mat. Allowing for the buoyancy of that portion of the piston submerged in water, this piston exerts an apparent stress of 1.216 g./sq. cm. (based on the total pad area). The piston is made of aluminum, with one section of the piston rod being made of iron and serving as the core for the linear variable differential transformer (LVDT) to be described later. The piston face is drilled with holes and covered with a tight-fitting 150-mesh screen to allow water passage during the compression. The screen is held tight by means of a ring which fits around the outer edge of the piston and is held in position by small screws. The over-all piston weight was carefully controlled to be as

light as possible but to be heavy enough to offset the maximum pressure drop observed during the mat formation. During this piston-lowering step, the piston is kept from falling onto the mat by the piston release mechanism. This consists of two tapered steel rods which run through slots in the vertical member, N, on which a pin through the upper piston rod can rest. Once the piston comes into contact with the mat, the rods no longer contact each other and the piston is supported by the mat.

The annulus between the guard cylinder and the filtration tube is now filled with water to the same level as the liquid in the filtration tube, and the filtration tube is removed by sliding it upward and securing it to the crossbar, M. In this position, it is out of the way and does not interfere with any future operations.

Before the compression measurements can be made, sufficient time must be allowed for the liquid inside the mat compartment to reach the bath temperature and for the piston weight to compress the mat until any further compression due to the unloaded piston is negligible during the actual compression run. Three hours has been found to be a sufficient waiting period. At this point, the mat is at the desired temperature, and the entire mat has been compressed under a uniform stress which is slightly higher than the maximum stress encountered during the mat-formation process. Using this as an arbitrary "zero load" point, the compression measurements can be carried out.

MAT COMPRESSION, RECOVERY, AND THEIR MEASUREMENT

The vertical member, N, which is connected rigidly to the crossbar, M, is equipped with a means of holding the piston in a fixed position until its release. This member also is equipped with the primary and secondary coils of a linear variable differential transformer (LVDT) whose primary coils are activated by an input of ten volts at 1000 cycles per second supplied from a Hewlett-Packard Audio Oscillator. The iron core which is a portion of the piston rod passes inside these coils, and the output of the secondary coils is a function of the position of the piston. The voltage output-position relationship for this arrangement has been accurately calibrated by connecting the piston rod to a depth micrometer and measuring output voltage as a function of the micrometer reading. The relationship is linear over most of the range, but a slight deviation from linearity is observed near the null point. (Theoretically, when the iron core is centrally positioned in the coils, the output should be zero.) However, the values are reproducible over the entire range of operation, so that a calibration over this near-null range allows one to use the measurements in this range as well. (Since the output is small near this null point, greater reading accuracy can be obtained by operating in this range.)

The relative position of the iron core with respect to the transformer (which determines the output voltage) can be varied by means of an adjustment nut on the end of the piston rod. This is adjusted to give the desired initial voltage. The initial mat thickness is

then determined by another measurement with the depth micrometer as previously described for determining the septum position. With the piston held in this position, the desired weights are added to the weight spindle, P. This apparatus was designed to be operated at compressive stresses ranging from zero to 100 g./sq.cm. of mat surface. When the compression is to be made, the piston is simply released. A similar procedure is used to study recovery; the piston is held at the desired position, the output voltage adjusted to the desired value, and the piston is released. By using the depth micrometer to indicate the initial mat thickness, and by using the transformer voltage changes to indicate changes in mat thickness, the mat thickness at any measured output voltage can be calculated.

In order to measure mat deformation and recovery as a function of time, one must be able to determine the output voltage accurately over the time intervals desired. For times of five seconds and above, the output voltage is measured using a Ballantine Model 300 AC Electronic Voltmeter, which operates over ranges of 0.01, 0.10, 1.0, 10, and 100 volts full scale. However, it is desirable to obtain measurements at times much shorter than this, since a large fraction of the total deformation has occurred in five seconds. For these short time measurements, the transformer output is fed to the Y-input of a type 304-A DuMont Cathode-Ray Oscillograph. The "x" axis is used as the time axis by use of the external sync control. A normally closed microswitch is connected in series with the external sync and Y-input ground terminals of the oscillograph. When this switch is pushed and released, one sweep across the scale is produced. The vertical width of the envelope

at any time is directly proportional to the voltage; whereas, the horizontal position is proportional to the time. The Y (voltage) axis of the oscillograph was calibrated by applying ten volts at 1000 c.p.s. to the input coil of the LVDT. (In all cases, the input voltage was adjusted to ten volts at 1000 c.p.s). Then the piston was moved up and down relative to the LVDT, and the voltage output at any core position was compared to the width of the envelope obtained on the Y-axis of the oscillograph. The width of this envelope was directly proportional to the output voltage as determined by the vacuum tube voltmeter. The linearity of the time (X) axis was checked by photographing the oscilloscope trace when the sweep was fast enough to distinguish the wave form of the output voltage. The distances between the peaks of these waves was constant across the entire width of the screen. Since this distance is inversely proportional to the frequency of the output, this indicates that this axis is directly proportional to time. The time for each sweep is determined by timing 100 sweeps; the corresponding time equivalence of each screen division can then be computed. The sweep time can be adjusted; a sweep time of about 0.5 seconds was used during the compression runs while about 0.75 second was used during recovery measurements. Longer times (slower sweeps) can be obtained by use of an external capacitance, but such adjustments did not seem necessary in this work. The instrument is equipped with a numbered, edge-illuminated scale so that no external scale is needed.

A type 302 (Polaroid Land) DuMont Oscillograph-Record camera is fitted to the oscillograph to record the envelope produced as the

piston is released. Since only one sweep is utilized, the camera need not be synchronized with the piston release but is set on time exposure. The initial voltage is adjusted so that the null point will be approached or passed during the time of the sweep. The voltage values corresponding to various times are read from the resulting photograph using a microscope with a magnification of 26.3 equipped with a scale mounted in the eyepiece which allows interpolation between the oscillograph scale lines.

MAT REMOVAL

When the compression and recovery measurements have been completed, the piston is removed from the mat surface and the water is removed from the mat compartment by the same centrifugal pump used during the mat formation. The septum screws are then loosened, the septum (with the mat adhering) is removed from the apparatus and the mat is removed and dried. It has been found that the mat is more readily removed if the water is not sucked completely through the mat by the pump.

This section has outlined the apparatus and the experimental steps used in the measurement of mat compression and recovery. An estimation of the maximum errors resulting from these operations will be found in the appendix.

FIBER SELECTION AND PREPARATION

GENERAL

There are many factors which must be considered when selecting the fiber system which is best suited for a study such as this. These factors will be considered briefly in this section.

The first problem involves the decision as to whether an actual pulp fiber should be used or some synthetic fiber. Since the viscoelastic properties of a system such as a wet fibrous mat are certain to be dependent upon the molecular structure of the basic polymer(s) involved as well as on the way these molecules are combined to form the final fiber, the use of a synthetic fiber which differs from a natural fiber in both basic chemical structure and fiber make-up would not give results which would be immediately applicable to a pulp system. On the other hand, if nylon were chosen, it would be possible to work with a greatly simplified system since such fiber properties as length, diameter, and density could be held to very close limits throughout the entire mat structure. As will be seen, such a uniform system would have definite advantages if the behavior is to be considered from a more theoretical standpoint. It was decided that this work would be carried out using natural pulp fibers rather than a synthetic, since the great lack of understanding of the actual mechanisms involved would of necessity limit the amount of theoretical interpretation which could be given to the results obtained. The results obtained with a natural pulp fiber would be readily applicable to the more practical aspects of the problem,

and as will be seen also serve to indicate how this general problem might now be attacked in a more fundamental manner.

The next problem is one of deciding which type of pulp fiber is to be used. There are several considerations which would indicate that as large and stiff a fiber as possible should be used. It has been mentioned that it is desirable to form the mat under as little fluid pressure drop as possible to keep mat compaction during this operation at a minimum. If a large, stiff fiber is used, this decreases this pressure drop in two ways. First, such large fibers have a low specific surface, which decreases the filtration resistance. Second, if the fibers are stiff, they compact less at any applied stress so that the void fraction within the bed is higher and there is more area available for fluid flow. The work by Seborg and co-workers (12-14) has shown that summerwood fibers are stiffer than springwood, and that kraft pulp fibers are stiffer than sulfite fibers. Also, an unbleached fiber would be stiffer because the lignin acts as a cementing material which holds the fiber together. Of course, large-diameter fibers would be stiffer than those of small diameter since the moment of inertia of a cylinder is proportional to the fourth power of the radius. It is also an advantage to use all large fibers rather than a whole pulp, since the possibility of a nonuniform distribution of fibers of varying dimensions throughout the mat from top to bottom could be introduced during the formation process.

A second problem is also encountered which can be minimized through the use of large, stiff fibers. During the rapid initial stages of mat

compression, there must be a significant amount of movement of water relative to the fibers in the mat. This will introduce drag forces, and the rate of initial mat compaction may be controlled by these forces rather than by the creep properties of the mat. One way of minimizing this effect is to use very low basis weights, since then there is distance required for water-fiber movement in order to reach the same degree of compaction. However, when the mat becomes very thin, it is difficult to obtain accurate measurements of changes in mat thickness. Also, it is possible that if very low basis weights are employed, the deformation mechanism may change, since now the fibers on the top and bottom of the mat will exert a larger percentage contribution to the over-all mat behavior. Under the conditions of these tests, these fibers would be subjected to a different type of loading than those in the mat interior, so it is necessary that their contribution to the over-all behavior be quite small. The best way of minimizing this effect would again seem to be to use fibers which have very low resistance to flow but high resistance to compaction under applied stress. This again indicates the value of using a stiff, large fiber.

As a result of these considerations, it was decided that an unbleached kraft pulp prepared from the summerwood portion of a species containing large-diameter fibers should be used. The following section will describe the preparation of this pulp.

FIBER PREPARATION

Three logs of Virginia loblolly pine (Pinus taeda) were chosen which exhibited rapid growth and large annual rings. Although pulp was

prepared from all three logs, all the work reported here was carried out on fibers obtained from one log. A cross-sectional view of this log is shown in Fig. 6.

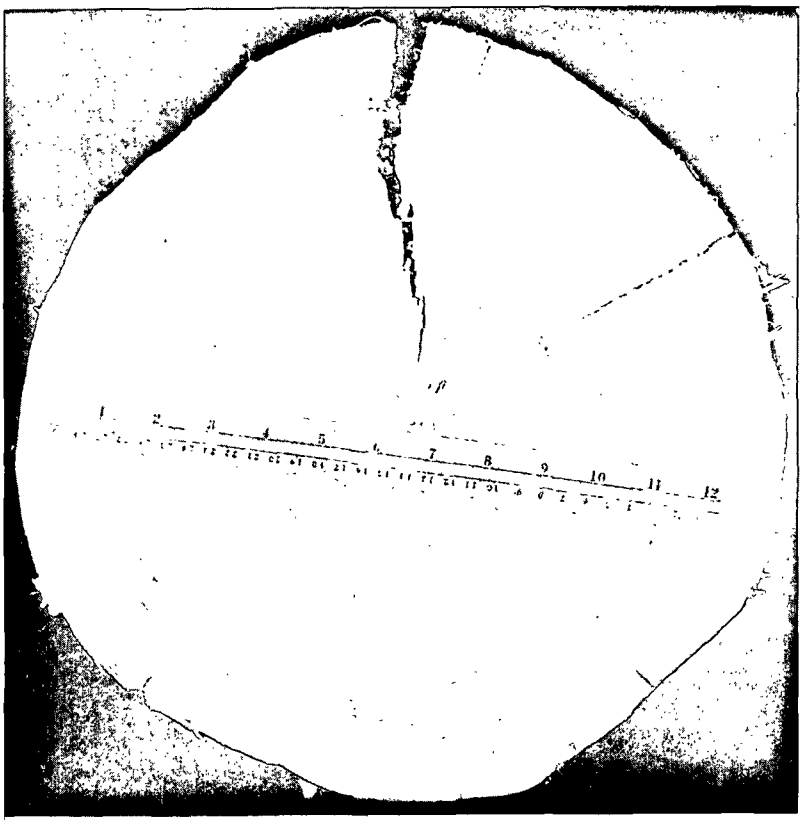

Figure 6. Cross-Sectional View of Log Used for Pulp Preparation

This log was approximately fourteen inches in diameter and contained summerwood rings of approximately 1/4-inch thickness, with springwood rings of approximately 3/16-inch thickness. The log was barked with a draw-shave and split into quarters. Half the log was sawed into disks approximately one inch in thickness. The springwood and summerwood were then separated using a wood chisel. The summerwood chips were cooked by the kraft process under the following conditions:

Chemical composition of cooking liquor:

25% active alkali (as NaOH)

25% sulfidity (as NaOH)

4-1/2 to 1 liquor-to-wood ratio

Cooking schedule:

75 minutes to 172°C.

70 minutes at 172°C.

relieve to 75 p.s.i.g.; blow

The pulp produced in this way had a permanganate number of 31.0 (using the 40-ml. permanganate test). The pulp was screened, centrifuge-dried to about 20% o.d. solids, and stored. This pulp was then classified in the Bauer-McNett classifier. Ten-gram (o.d.) charges were employed and 14-, 35-, 65-, and 150-mesh screens were used. (All work reported in this thesis was done with the 14-mesh fraction.) Prior to the classification, the pulp was treated for fifty counts in a British disintegrator at 0.5% consistency to break up any fiber bundles present in the pulp. The classification of each ten-gram charge was carried out for fifteen minutes (Institute Method 415). About 90% of the pulp charged was retained on the 14- and 35-mesh screens, with about equal amounts on each. Each fraction was then dewatered to approximately 20% solids and stored with 1% formaldehyde to prevent biological decomposition.

The fractions retained on the 14- and 35-mesh screens were characterized by measuring the hydrodynamic specific surface and specific volume. Due to the very low filtration resistance of these fractions, the constant-rate technique of Ingmanson and Whitney (11) could not be employed.

Instead, the permeability technique (21) involving mechanical pre-compression of the mat and measurement of the frictional pressure drop at various flow rates was used. The results obtained with the 14-mesh fraction, together with those reported by Ingmanson (11) for red oak kraft pulp, are given in Table I.

TABLE I

SPECIFIC SURFACE AND SPECIFIC VOLUME OF TEST PULPS

Pulp	Specific Surface, S_w, sq. cm./g.	Specific Volume, v, cc./g.
Red oak kraft (11)	10,600	2.78
Loblolly pine summerwood, on 14 mesh	4,080	3.62

Note: The values given for the 14-mesh fraction were obtained using the Kozeny-Carman equation, and allowing for changes in the Kozeny constant with changes in mat porosity (22).

These results indicate that the desired low filtration resistance was obtained. Also, since the fibers present are thick-walled summerwood fibers with a rather high lignin content, they should exhibit a high stiffness.

Fiber length and width measurements were carried out on this 14-mesh fraction of the pulp by the Fiber Microscopy Group at the Institute. The following average values were obtained:

Arithmetic-average fiber length = 2.34 mm.
Weighted-average fiber length = 2.48 mm.
Arithmetic-average fiber diameter = 40.1 microns
Weighted-average fiber diameter = 43.6 microns

When the fibers are to be used to form a mat, the desired amount is weighed out and placed in two liters of water. This slurry is treated for fifty counts in the British disintegrator and is then deaerated under vacuum until very few bubbles can be observed in the slurry. The pulp is now ready for the mat-forming operation.

EXPERIMENTAL RESULTS AND DISCUSSION

PRELIMINARY INVESTIGATIONS

Before the actual creep studies can be started, it is necessary to check the reproducibility of results obtained and also to study the effect of changes in mat dimensions on the deformation-time behavior. This section will be devoted to this preliminary work.

REPRODUCIBILTY OF RESULTS

As a means of checking the reproducibility of the results obtained, three mats were formed using the techniques described previously. The temperature in this work, as with all the work reported in this thesis, was maintained at 25.00± 0.05°C. First, compression and recovery measurements were made on each mat; since the same apparent stress was applied in each case and all mats were of approximately the same basis weight, the variations between runs should be within the error limits defined in the appendix. The results of the two compressive and three recovery series are shown in Fig. 7, together with the estimated maximum experimental errors introduced. It will be observed that the data for both the creep and recovery portions of the cycle are within the range of predicted experimental error.

EFFECT OF BASIS WEIGHT ON CREEP BEHAVIOR

The effect of basis weight on creep behavior is of importance from several standpoints. It has been seen that the literature (12-14) indicates the occurrence of a marked change in recovery properties of wet

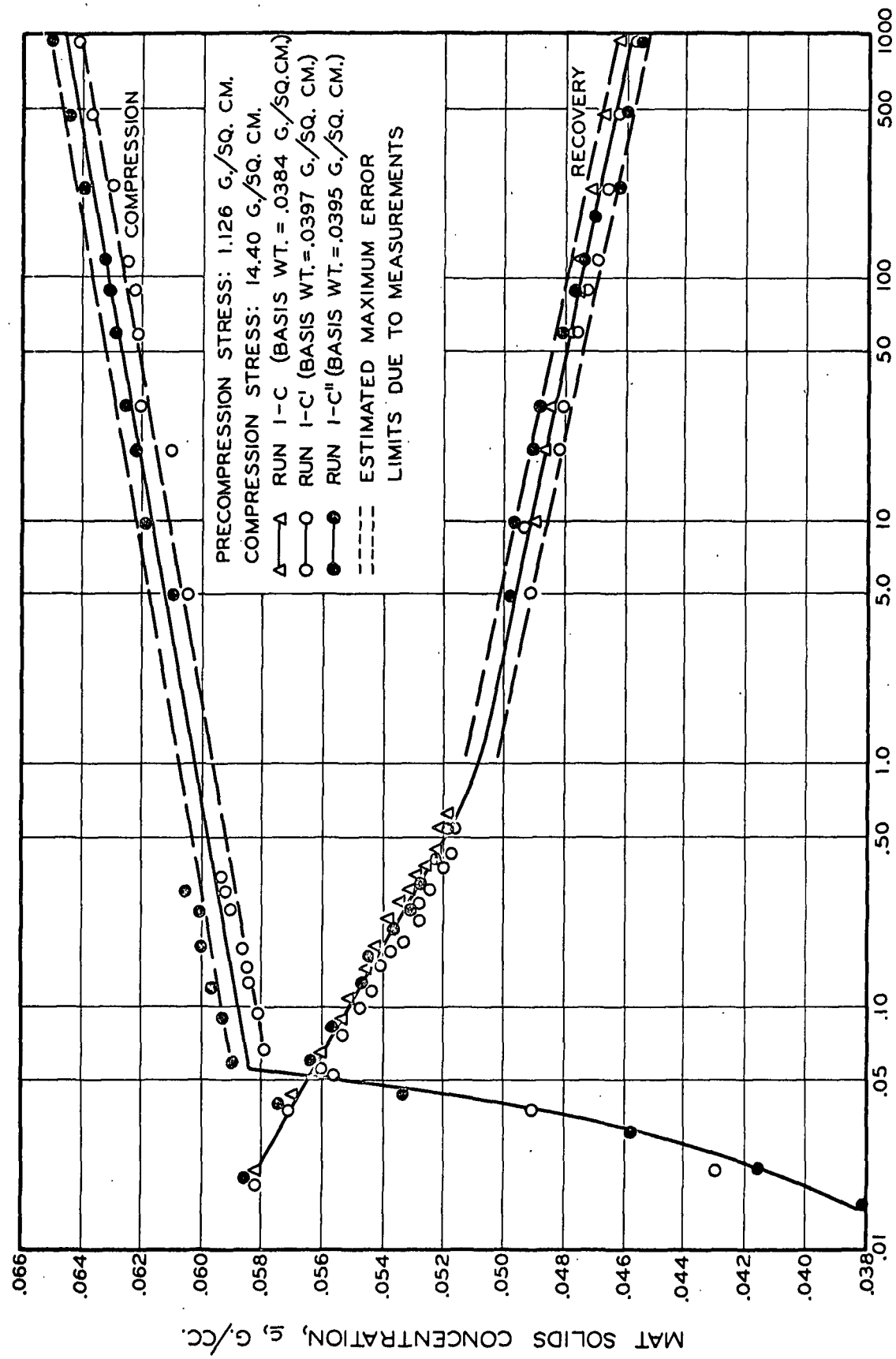

Figure 7. Reproducibility of Creep and Creep Recovery Data

mats as the basis weight decreases. Since the work reported in this thesis has been carried out in the range of basis weights over which this change was observed, it is important to know if basis weight must be held within very close limits in order to obtain consistent results. Also, the effect of basis weight must be considered if any attempt is to be made to use data obtained at relatively high basis weights to predict the mat behavior at the low basis weights encountered on the paper machine.

A third consideration involves the actual deformation-controlling mechanism at short times. If it is assumed that the rate of mat compression is not controlled by the rate at which fiber-water movement can occur but rather by the creep properties of the fibers within the mat, then regardless of the basis weight, the same percentage change in mat thickness should be observed at any constant time and applied apparent stress. (The term, "apparent stress," is used to designate the compressive stress applied to the mat. Since this stress is not the stress present in the individual fibers, the term, apparent stress, seems appropriate.) Therefore, the solids concentration, c, should be independent of basis weight when compared at equal times and applied apparent stress. However, if it is assumed that the rate of water expulsion from the mat (in a direction perpendicular to the plane of the mat surfaces) controls the deformation rate, a mat of higher basis weight will exhibit a lower amount of deformation than one of a lower basis weight because the water-fiber movement must take place over a longer path and more water must be squeezed from the mat.

As a means of checking these possibilities, creep-creep recovery runs were carried out using apparent stresses of 14.40 and 4.77 g./sq. cm., the former being used at basis weights of approximately 0.054, 0.040, and 0.016 g./sq. cm., the latter at basis weights of 0.040 and 0.020 g./sq. cm. Each run was carried out for one compression-recovery cycle. The results of this work are shown in Fig. 8 (compression) and Fig. 9 (recovery).

At short times (less than 0.1 sec.) a decrease in basis weight results in a significant increase in the amount of deformation at any time. When a certain low basis weight is reached, an actual cycling or vibration effect can be noted (Runs 1-F and 1-J). This indicates very strongly that the water-fiber movement is an important factor in controlling this initial rapid deformation. If the system is considered from the standpoint of a vibratory system, the behavior observed in Runs 1-F and 1-J would be termed a damped vibration. The mathematical analysis of the two types (vibratory and nonvibratory) of systems shown by this work (23) shows that in order for oscillation to occur, the elastic behavior of the system must become greater than the damping or viscous portion. In the present instance, this means that the elastic properties of the fibers in the bed become predominant over the viscous drag forces created by water-fiber movement as the basis weight (and the total amount of water-fiber friction) decreases. This behavior will be treated in greater detail when the short time behavior is discussed.

The longer time-creep data show that the differences between runs are much less pronounced than during the earlier stages. This is due to

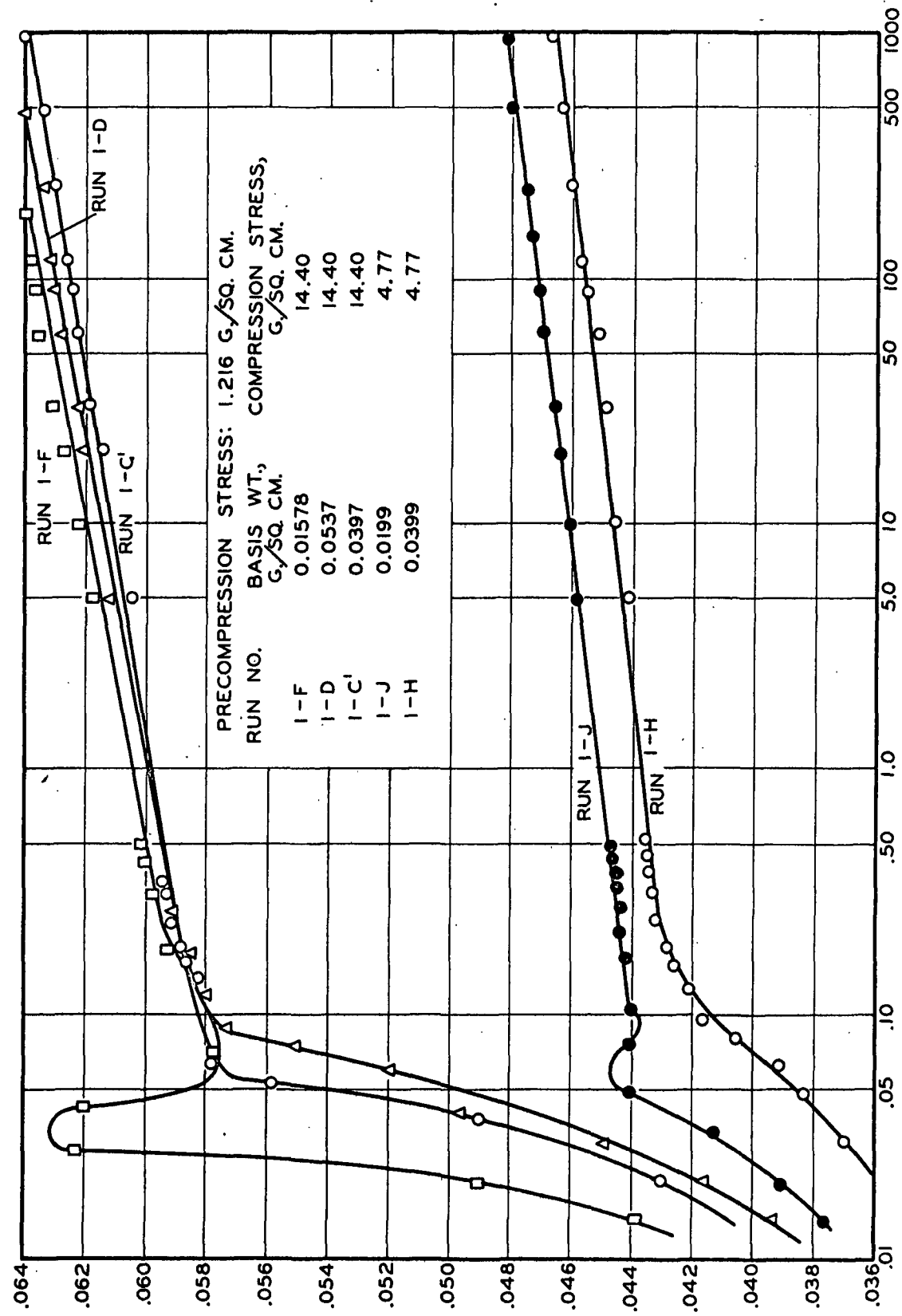

Figure 8. Effect of Basis Weight on Mat Compression Properties

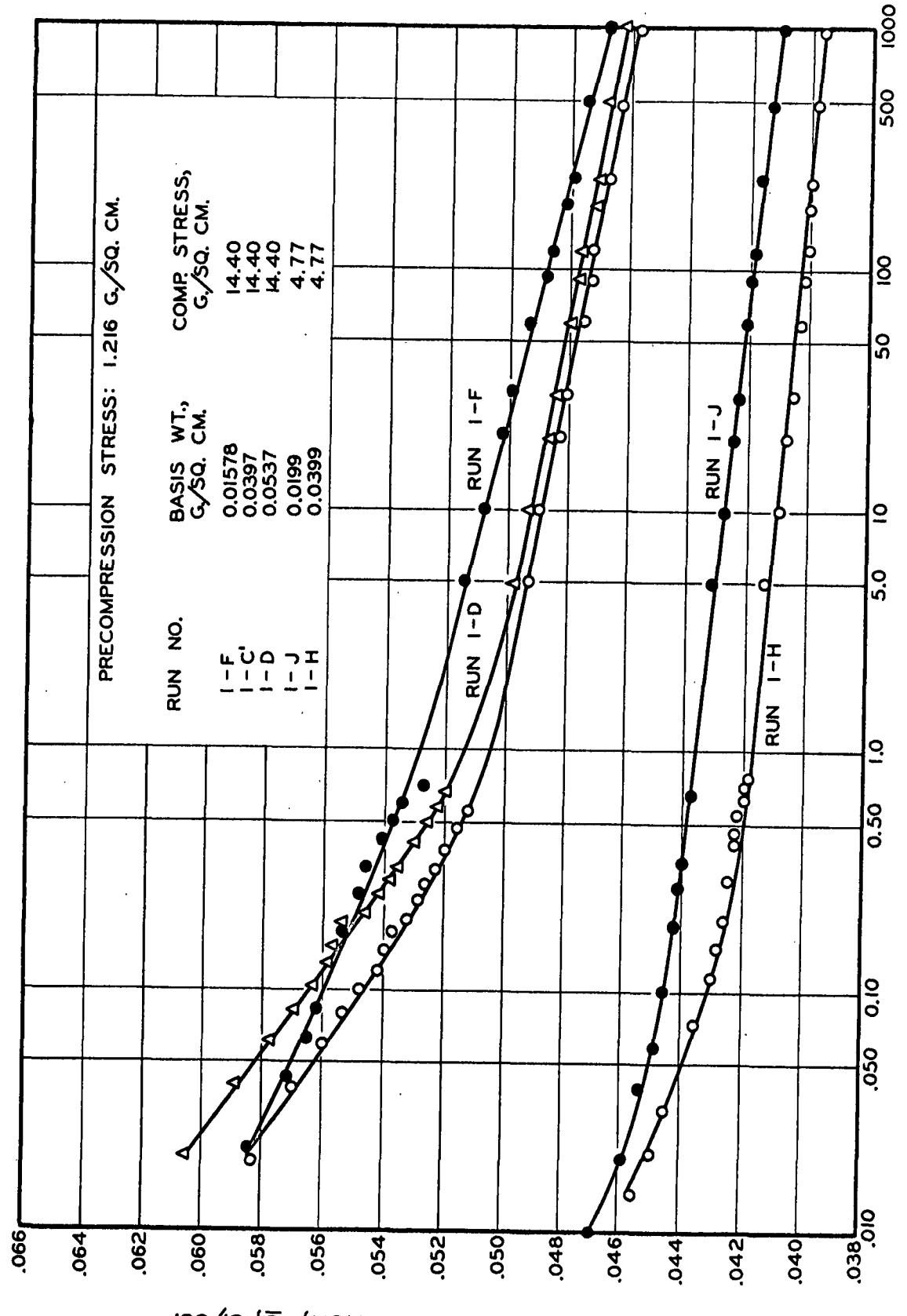

Figure 9. Effect of Basis Weight on Wet Mat Recovery Properties

the fact that oscillations have damped out and creep is controlled by the mechanical properties of the fiber network. Fluid flow is unimportant at long times.

The slight differences between the results of the various creep tests (somewhat greater than the amount attributable to experimental error) and the even greater differences observed with the corresponding recovery runs are undoubtedly a result of changes which have occurred during the initial rapid stages of compression. Under conditions favorable to rapid initial piston movement (low basis weights), the piston plus the attached weights develop a considerable amount of kinetic energy. When the fibers in the mat begin to exert an opposing force to this piston movement and the piston is reduced in velocity, an additional force is transmitted to the fibers due to the large inertia of the piston. Since the deformation of viscoelastic systems is generally "due not only to the load acting at that instant but also to the entire previous loading history" (3), this additional force at the beginning of the sequence results in an increase in deformation over the rest of the cycle over the deformation observed when the initial compaction is not as rapid. The additional force due to this effect can be calculated, and is as high as 100% of the force due to the static weight of the applied apparent stress; such forces certainly are not negligible.

If the differences in creep and creep-recovery curves are due to these initial forces and not to inherent differences in the mechanical behavior of the fibrous structure itself at different basis weights, then a static loading test designed to eliminate this initial rapid

movement should yield identical results at various basis weights; conversely, if the fibrous structure itself is responsible for the differences, they should still be present during such a static experiment. To check these possibilities, the ordinary "compressibility" measurements used in filtration work to relate mat fiber concentration to applied apparent stress (11) were made at basis weights of approximately 0.08 and 0.02 g./sq. cm. The mats were formed, the first stress was applied, and in fifteen minutes the mat thickness was measured. The next increment in stress was added, and the procedure was repeated. An apparent stress range of from 4 to 60 g./sq. cm. was covered. The results of the two runs are shown in Fig. 10. It will be noted that any differences between the two runs are negligible; it happens that the higher basis weight mat was slightly more readily deformed than the lower basis weight mat. Since this is in direct opposition to the results obtained when the mat was compressed rapidly during the early compression times, it may be concluded that changes in the water-fiber friction properties during the rapid initial deformation and not in the mechanical properties of the fibrous network are responsible for the observed differences.

If actual fiber deformation rather than water-fiber friction controlled the mat deformation at short times, it would be expected that at the lowest times a value approximating an immediate elastic deformation would be observed, and that measurements made at still lower times would not deviate greatly from this value. However, the results of Fig. 8 indicate that, for both compressive apparent stresses, this

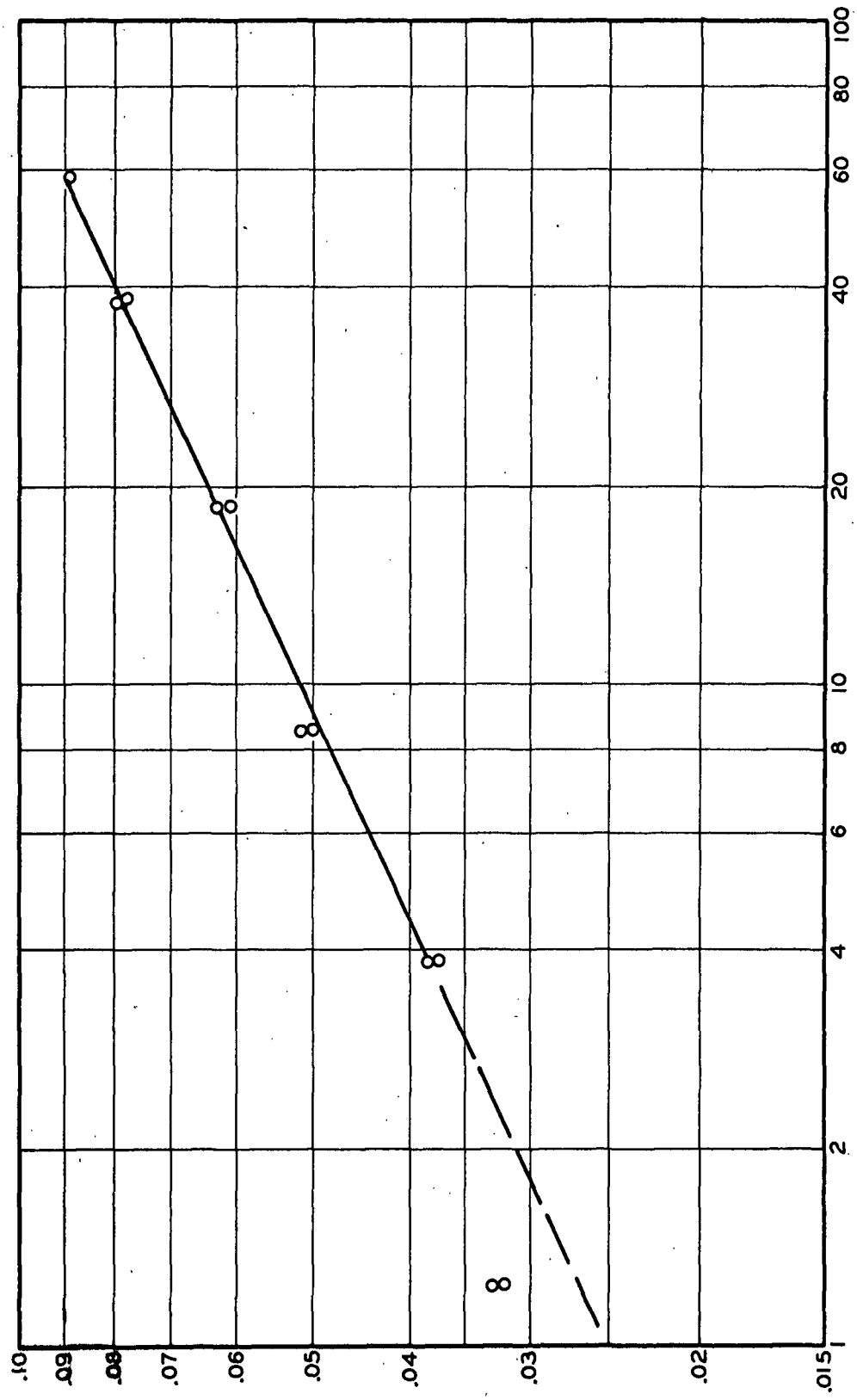

Figure 10. Variation of Compressibility Measurements with Basis Weight

limiting low time value is merely the mat thickness at zero time. This lends further support to the conclusion that this early compression is controlled to a large extent by the rate of water movement through the mat.

Further evidence that the straight-line relationship between the mat solids concentration and the logarithm of time of stress application would extend to times shorter than about 0.1 sec. was obtained when one mat was accidentally subjected to a short time stress while it was being readied for the creep tests. In this case, the straight-line portion of the curve began at about 0.04 sec. (see Fig. 11). Since the initial solids concentration was higher in this case, once the compression was begun it was necessary to squeeze less water from the mat before the entire compressive load was supported by the fiber structure. In this way, the true properties of the fibrous structure became apparent in less than half the time usually required.

EFFECT OF MAT DIAMETER ON CREEP BEHAVIOR

In the work involving the effect of basis weight on creep and creep recovery, the observed changes were attributed to the flow of water relative to the fibers in a direction perpendicular to the mat surface plane. However, since these measurements are made without confining the mat edges, it is also possible for water to be squeezed from the mat in this direction. Such flow would not only influence the rate of compression, but might also disturb the fibers in the outer regions of the mat. A series of three runs was made to study these effects. Mats of diameters smaller than that of the filtration tube were formed by

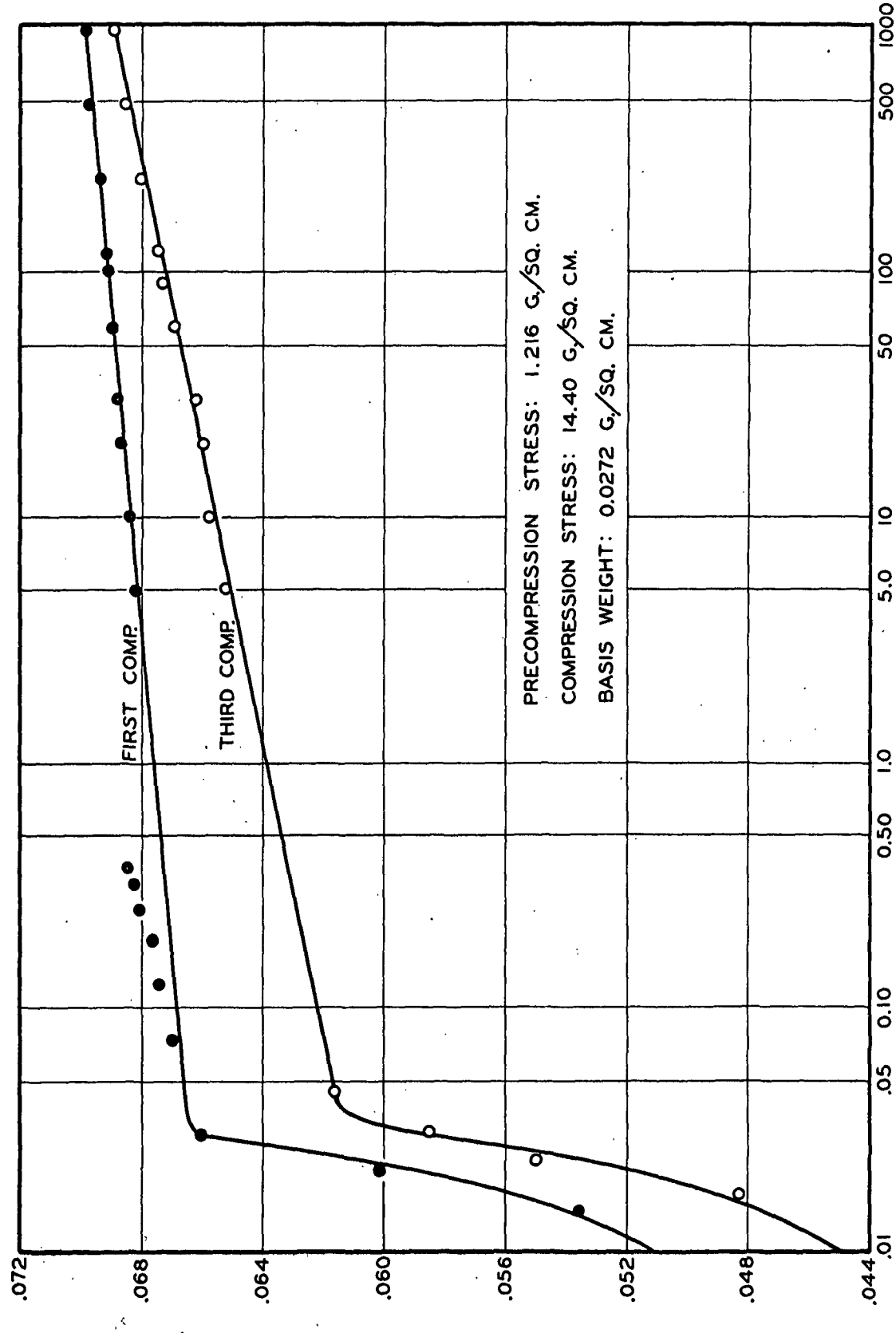

Figure 11. Extention of Linear Creep to Shorter Times Using a Prestressed Mat

inserting glass cylinders approximately four inches in length into the filtration tube and supporting them on the septum. The mat is then formed by filtration, with the cylinder forming a partition between the inner circular mat and that portion formed outside the cylinder. The water is then drained below the top of the cylinder, and the portion of the mat outside the cylinder is removed. The cylinder is carefully lifted out leaving a mat of the desired diameter. Since pistons of the same diameter as the glass cylinders were not available, it was necessary to remove the glass cylinders without any precompression load on the mat, and then to lower the piston onto the expanded mat. Both the removal of the cylinder and the placement of the piston almost certainly disturbed the mat somewhat more than when the piston is in place before the cylinder is removed.

The results of these compression-recovery runs (Runs 2-A, 2-B, and 2-C) are shown in Figs. 12 and 13. It will be observed that the creep curves for Runs 2-A and 2-C (representing the extremes in mat diameters) are in quite good agreement, while Run 2-B deviates considerably from the others. The recovery curves are closer together, but here again, the intermediate-diameter mat gives results outside the range of the extreme diameters. At short times, the creep curves of all three mats are in rather good agreement; since this would be the period when any transverse water flow would be expected to give large differences in results, this supports the hypothesis that water flow from the mat edges is negligible.

Although the results of the runs are not within the limits of experimental error defined in the appendix, it is felt that this is due

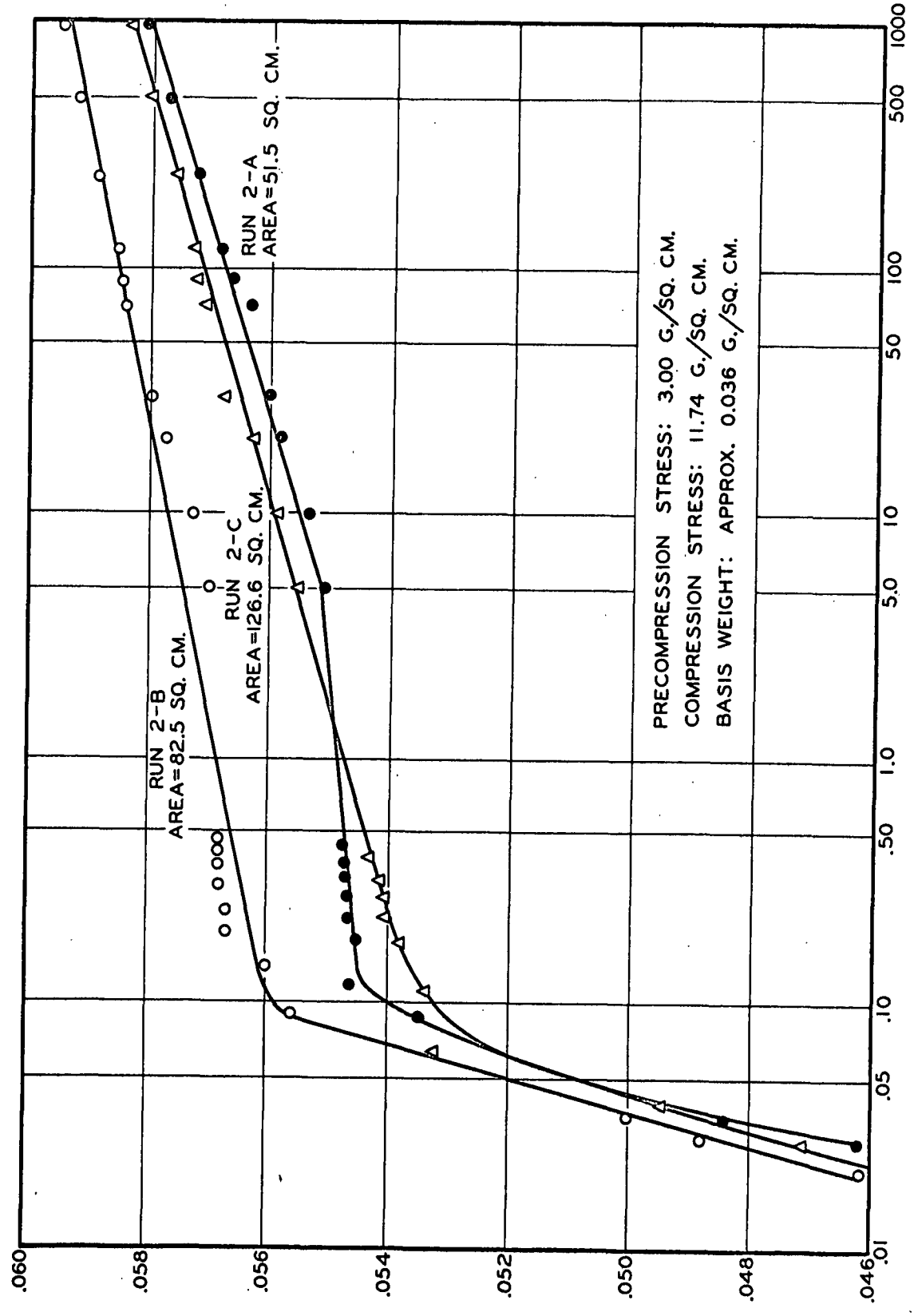

Figure 12. Effect of Mat Area on Compression Properties of Wet Mats

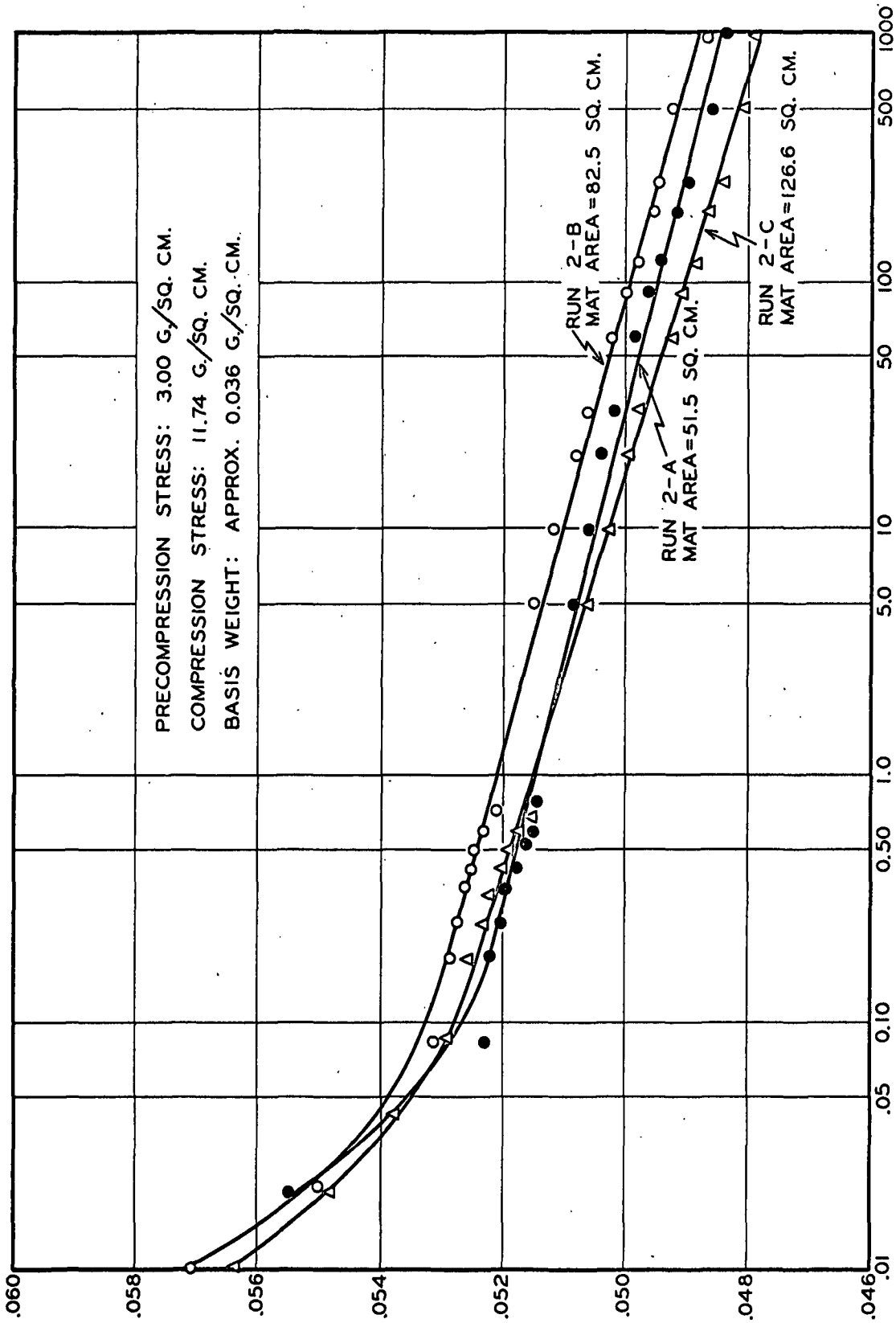

Figure 13. Effect of Mat Area on Recovery Properties of Wet Mats

not to any effect of transverse water flow but rather to increased disturbances introduced in the mats by the additional operations involved in mat formation. It is therefore concluded that water flow in this direction is probably a negligible effect. It may also be concluded that any disturbance or bulge at the unrestricted mat edge caused by an outward expansion of the mat is also probably negligible. Since the differences observed here are larger than those attributable to measurement error alone, and since errors introduced by possible mat disturbance cannot be estimated, it cannot be definitely stated that mat diameter is an unimportant variable.

The conclusions of this preliminary work may be summarized as follows.

1. Reproducible results can be obtained using the procedures and methods outlined previously.

2. Mat basis weight has no effect on the creep properties of the fibrous mat structure. However, increases in basis weight result in an increase in the amount of water-fiber movement during the initial rapid stages of deformation and for this reason the time-deformation curves may be of somewhat different forms at different basis weights. This subject will be dealt with further in a later section.

3. Experiments carried out on mats of varying diameter were not conclusive since mat disturbances during preparation introduced an error of unknown magnitude. However, since the creep and creep-recovery results did not rank the mats in order of increasing mat

diameter, it is probable that very little water flow occurs out through the unrestricted mat edges and that any bulging at the edges of the mat has very little effect on the creep behavior of the mat.

FIRST AND SECOND CREEP AND CREEP RECOVERY; EFFECT OF REPEATED CYCLING

GENERAL

The study of the first creep behavior of a material must necessarily involve all of the possible creep mechanisms which exist in the material. Following the first creep-creep recovery cycle, at least a portion of the nonrecoverable creep will have been eliminated and will not be encountered in subsequent cycles. Therefore, a study of the first creep and first creep-recovery behavior of the wet fiber network will be valuable in estimating the maximum possible creep rate and in studying the importance of nonrecoverable deformation during this first cycle under varying values of applied apparent stress.

In a large majority of viscoelastic systems, most of this nonrecoverable or secondary creep occurs during the first creep test. Therefore, a study of second creep and creep recovery would be of interest since the importance of this nonrecoverable portion of the first creep behavior would become more apparent. From the practical standpoint, the effect of the second stress application as well as subsequent applications is of value, since the production of the paper sheet involves many such applications and removals of stress. From a more basic standpoint, a comparison of the results obtained for first and second creep and creep recovery may be useful in helping to understand the mechanisms involved in this deformation process.

It would be of considerable interest to extend this study through several creep-recovery cycles beyond the second. However, in this thesis,

only the first two cycles will be studied over a range of applied apparent stress. The behavior of a mat subjected to several such cycles at one applied apparent stress is also included; this series of cycles was employed in an attempt to reach a state of mechanical conditioning.

The first and second creep work was carried out using five values of applied apparent stress ranging from 5 to 90 g./sq. cm. of external mat area. Basis weights of these mats were in the range of 0.04-0.08 g./sq. cm. (within the range shown to have a negligible effect on mat "compressibility"). Each apparent stress was employed over two five-hour cycles; first creep was studied for two and one-half hours as were second creep and first and second creep recoveries.

An attempt was made to obtain the creep and recovery data at short times (less than one second) by using the oscillograph camera to record the data. This was successfully accomplished at the two lowest values of applied apparent stress (5.99 and 10.85 g./sq. cm.). However, as the applied apparent stress was increased, the case of an underdamped vibration was again observed. Also, the initial rapid deformation resulted in water flow laterally through the mat edges and a corresponding disturbance of the fibers in this zone. This behavior made it necessary to apply the higher apparent stresses by lowering the weighted piston onto the mat surface manually. This eliminated the rapid initial compression and the undesirable mat disturbance, but made it impossible to obtain creep data at times shorter than five seconds following stress application. All recovery measurements were made over the entire time range starting at about 0.1 sec., since this mat disturbance problem is not encountered during the recovery portion of the cycle.

DATA OBTAINED

The results of this portion of the study are shown graphically in Fig. 14 (first and second creep) and Fig. 15 (first and second creep recovery). It will be noted that both the first and second creep and creep-recovery curves can be well approximated by straight lines on the mat solids concentration—log time plots over the time range of about 0.5 sec. to the termination of each run. The more rapid deformation during the early portion of the creep studies is probably attributable to the relative movement of water and fiber during this time period, as will be shown. The recovery curves also show a sharp deviation from the straight-line behavior at short times. Although these data cannot be handled in the same manner as the short-time creep data, evidence will be presented which makes it seem likely that this deviation from linearity can also be attributed to the control of the early recovery by the relative fiber-water movement and not by the structural properties of the mat itself.

Figures 14 and 15 show that not only the amount of creep (or recovery) but also the rates (as indicated by the slopes of the curves) of creep and recovery are a function of the applied apparent stress. This indicates the possibility of the existence of a general relationship between applied apparent stress, deformation (as indicated by the solids concentration within the wet mat), and time of stress application. Such a relationship would be similar to the type obtained if a master creep curve were constructed from the data.

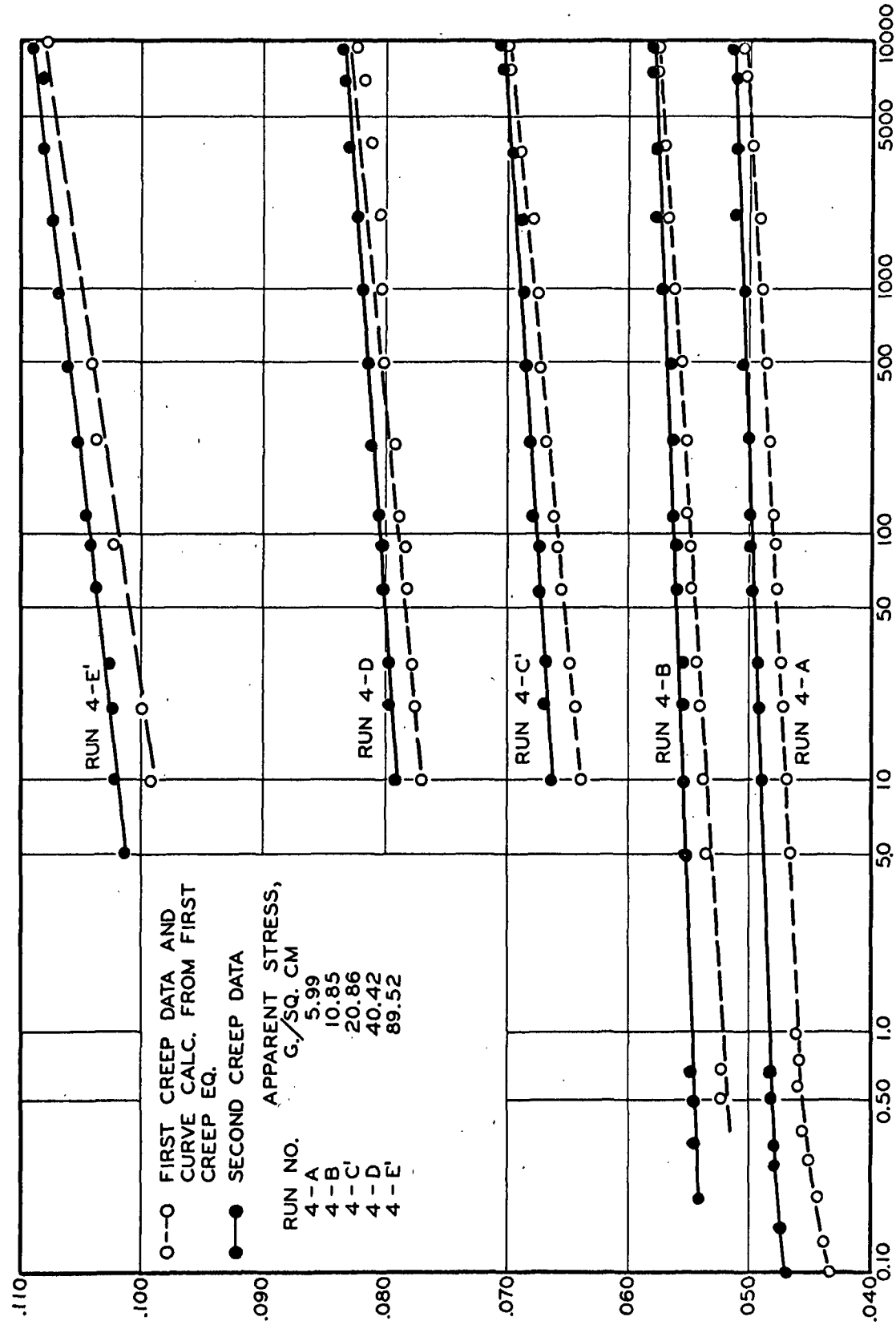

Figure 14. First and Second Creep Behavior of Water-Saturated Pulp Mats

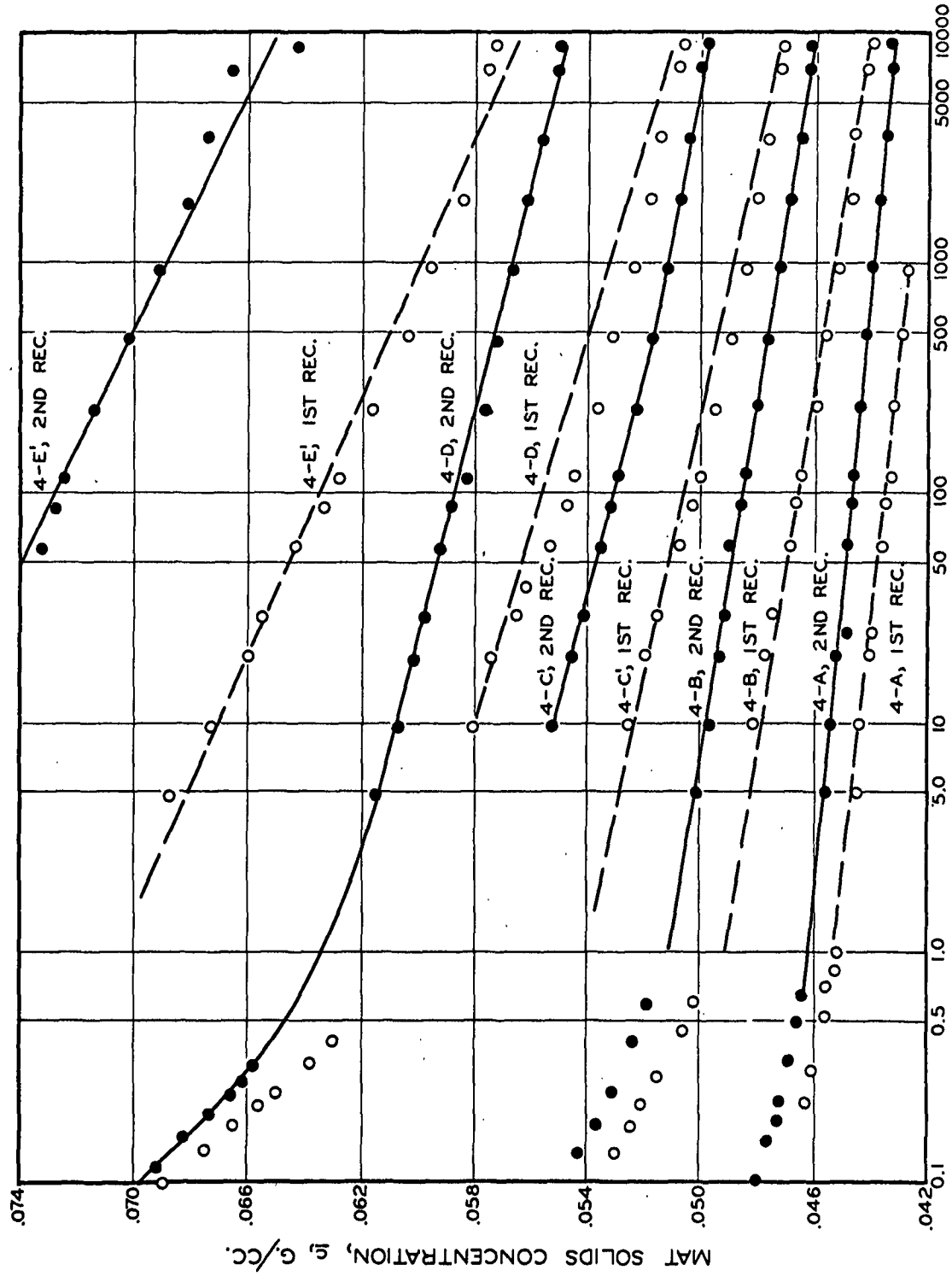

Figure 15. First and Second Creep Recovery of Water-Saturated Pulp Mats

Since the relationship

$$c = MP^N \tag{5}$$

has been used with considerable success to correlate the mat solids concentration, c, and apparent stress, P, over a wide range of apparent stresses and for a large number of different pulps, it is felt that this equation is probably a special simplified form of a more general equation which also includes time as a variable. It was found (see Appendix I for methods of evaluation) that the exponent, N, is independent of time while the constant multiplier, M, can be expressed as a function of time by:

$$M = A + B \log t \tag{8}$$

where A and B are constants independent of time and apparent stress, and t represents the time of stress application. It is also necessary to include a third constant in Equation (5), designated as c_o. If this general relationship were found to apply even as the apparent stress approached zero, this new constant would represent the mat solids concentration at zero compacting stress. At the present time, the applicability of such a relationship to very low stresses has not been substantiated; therefore, this constant should be considered to be empirical in nature but with some possible theoretical significance.

If these modifications are now substituted into Equation (5), it becomes:

$$c - c_o = (A + B \log t)P^N. \tag{5'}$$

One other comment should be made concerning the general form of this equation. If time is set equal to zero, the time function in this

equation no longer has any meaning. This should not be considered a weakness of this equation: the data from which the equation was derived were obtained at times ranging from no less than 0.1 sec. to several hours. Although it has been hypothesized that this relationship does hold down to times considerably shorter than 0.1 sec., it is to be expected that deviations would be encountered at very short times. If this limitation is kept in mind, there need be no speculation concerning the behavior of this relationship at zero time.

If the constants of Equation (5') are evaluated for the first creep data, the equation becomes

$$\underline{c} - 0.0208 = (0.01227 + 0.000487 \log \underline{t})\underline{P_t}^{0.403}. \qquad (9)$$

Values of $\underline{c}$ calculated using the $\underline{P}$ values employed during the first creep work are plotted with the original data on Fig. 14 for comparison purposes. It will be observed that very good agreement is obtained; the calculated values agree with those obtained experimentally within the limits of possible experimental error. (In this equation, $\underline{P_t}$ refers to the total applied apparent stress, or the sum of the precompression stress applied with the unloaded piston and the compressive stress added as extra weights.)

It is interesting to consider the possible significance of the value of $\underline{c_o}$ (0.0208 g./cm.^{3}) obtained in this way. As will be shown later, a true value of this quantity would be very useful when the deformation mechanisms are considered from a more theoretical standpoint. Ingmanson and Whitney (11) have estimated this value of solids concentration in a completely unstressed mat to be between 0.018 and 0.023 g./cc. for a

bleached spruce sulfite pulp. This would indicate that the value of 0.0208 may be of more significance than merely an empirical constant. Daily and Bugliarello (24) have used an "elastic counterrotation" test to determine the point at which pulp systems begin to have mechanical strength. They observe this to take place at a value of c of about 0.002 g./cc., which is much lower than the c_o value obtained in this work. However, with this method of evaluation, the fibers were free to rotate in three dimensions; in the present case, fiber orientation is limited primarily to the plane of the mat surface. Mason (25) has calculated the point at which the fiber interaction should become important by comparing the volume of the sphere swept out by a freely rotating fiber to the volume of the fiber itself; when the slurry reaches this consistency, fiber interaction should occur. A similar estimation can be made here, except that the volume swept out by the rotating fiber will now be confined to one plane. Thus,

$$\text{fiber volume} = \pi r^2 b \qquad (10)$$

where

r = fiber radius, and

b = fiber length;

and

$$\text{volume of rotation} = \pi(b/2)^2(2r) \qquad (11)$$

where $\pi(b/2)^2$ represents the area of the circle defined by the fiber rotation and $2r$ is the fiber thickness. Then the solid fraction at

which interaction between fibers should begin is given by

$$\underline{v}\underline{c}_o' = \frac{\pi \underline{r}^2 \underline{b}}{\pi(\underline{b}/2)^2 2\underline{r}} = \frac{2\underline{r}}{\underline{b}}$$

or

$$\underline{c}_o' = \frac{2\underline{r}}{\underline{v}\underline{b}} \qquad (12)$$

where $\underline{v}$ represents the specific volume of the fibers, or 3.62 cc./g. in this case. If this equation is to yield a value of approximately 0.02 for $\underline{c}_o'$, it is seen that the length-to-diameter ratio, $\underline{b}/2\underline{r}$, must be about 14:1. Average fiber length and diameter values for the pulp used in this work give a ratio of about 57:1 which corresponds to a $\underline{c}_o'$ value of about 0.005. This value is considerably below the value of $\underline{c}_o$ obtained from the first-creep equation. However, this treatment assumes that the fiber is rigid and does not bend. If we assume that the effective length, $\underline{b}$, is halved due to fiber curvature, $\underline{c}_o'$ is increased to about 0.010. While this is still below the value obtained by the use of the creep data, it is seen that it is of the same order of magnitude. Also, it must be remembered that the value calculated in this way represents the minimum value possible; the actual concentration at zero stress might be greater than this calculated value. It is seen from these examples that there is at least some basis for assuming a theoretical significance for the constant, $\underline{c}_o$.

When considering first-creep recovery, a second factor must be taken into account, this being the nonrecoverable portion of the observed creep. When both first creep and first-creep recovery measurements are allowed to proceed for a period of two and one-half hours

(as was the case in this work), the nonrecoverable creep (taken as the solids concentration following the recovery cycle, $\underline{c}_f$, minus the solids concentration before the first creep is begun, $\underline{c}_i$) can be represented by the equation:

$$(\Delta \underline{c})_{n.r.} = \underline{c}_f - \underline{c}_i = 0.00450 \underline{P}_r^{0.360}. \qquad (13)$$

In this equation, $\underline{P}_r$ represents the apparent stress removed prior to the recovery portion of the cycle; $\underline{c}_i$ represents the mat solids concentration after the addition of the precompression stress (represented by the unweighted piston) and is not the same quantity as the $\underline{c}_o$ which appears in Equation (9). $\underline{c}_i$ is determined experimentally and has the value of 0.0340 g./cc. It must also be remembered that this equation applies only for the times used in the creep and creep-recovery tests. If creep were allowed to proceed for longer times, there would undoubtedly be more nonrecoverable creep; if the recovery were allowed to proceed for longer times, there would be less nonrecoverable creep.

If this nonrecoverable portion of the creep-recovery behavior is combined with the equation used to describe the time-dependent portion of the recovery (which takes the same form as the equation used to represent first creep), the entire recovery behavior can be represented by the equation:

$$\underline{c} - \underline{c}_i = \underline{c} - 0.0340 = 0.00450 \underline{P}_r^{0.360} + (0.00158 - 0.000408 \log \underline{t}) \underline{P}_r^{0.486} \qquad (14)$$

where t represents the time following removal of the apparent stress, P_r. Results obtained using this equation are included on Fig. 15 for comparison purposes. The method of evaluating the constants of this equation is described in the appendix. (This equation applies only to final straight-line portion of the recovery curves.) Such a technique cannot be applied to the earlier portion of the curves; it is felt that these early curves are again controlled by the relative fiber-water movement and not by the structural properties of the mat itself. If this short time recovery data is plotted as the logarithm of mat solids concentration versus the logarithm of time, this entire initial portion plots as a straight line, indicating that the same mechanism is controlling over this entire range.

The successful correlation of these results using a more general form of the familiar "compressibility" equation serves as a further indication of the general applicability of an equation of this form and also lends support to the possibility of the theoretical significance of such an equation. This will be treated further in a later section.

It seems probable that similar correlations could be obtained for the second creep and second creep-recovery data. However, this will not be done here; the value of these data will be seen when possible mechanisms of compression are discussed.

DISCUSSION OF RESULTS OF CREEP AND RECOVERY WORK

The preceding section has dealt with the quantitative treatment of the first and second creep and creep-recovery data. In addition, certain

statements have been made concerning the possible theoretical significance of these empirical equations. A later section will be devoted to a more thorough quantitative treatment of their possible theoretical significance. This section will deal with the qualitative aspects of the possible mechanisms involved in mat creep and creep recovery.

All types of fiber network deformation can be classed in one or more of three general types of behavior. This classification scheme is based on the changes which would be observed if the whole fiber were considered in a macroscopic sense; all the possible intrafiber deformations such as molecular segment motions, fibril motions, etc., could occur under any of these classifications as well. Figure 16 gives a schematic representation of these possible types of deformation.

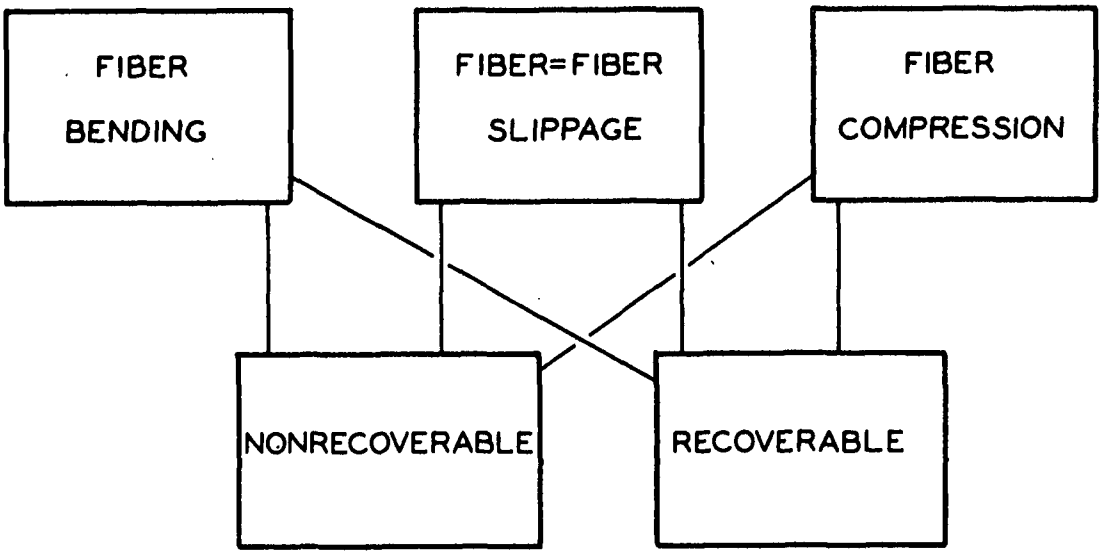

Figure 16. Schematic Representation of Fiber Network Deformations

It is seen that there is no clear-cut distinction between mechanisms which might yield recoverable deformations and those which would yield nonrecoverable deformations. For example, if one fiber were to slip completely past another during the creep portion of the cycle, this fiber would be under little or no induced stress, although the over-all effect would contribute to mat deformation. Once the applied stress is removed prior to the recovery measurements, there would be no force tending to restore this particular fiber to its original position; hence, such a deformation would be essentially nonrecoverable. However, if this fiber were held on one end through its contacts with two or more adjacent fibers, the slippage of the free end relative to its neighbors would result in a stress being set up within the fiber; when the recovery cycle was begun, at least a portion of this deformation would be recovered because of this restoring force within the fiber. Slippages of fibrils within the fibers and of molecular segments within the fibrils could result in the introduction of nonrecoverable deformations even when no movement of one entire fiber relative to other fibers is observed.

The complications of such a system do not end here. In addition to the above considerations, one or two of these deformation mechanisms may lead to the third. For example, the bending or compression of a fiber may so change its own geometry and its geometry relative to adjacent fibers that fiber slippage may result. On the other hand, nonrecoverable fiber slippage during one creep cycle would result in a repositioning of the fiber involved and during subsequent creep cycles this fiber would be subjected to different amounts and distributions of compressive and bending loadings.

From this introduction, it is apparent that the mechanisms of deformation are very complex and are changed from one creep-creep recovery cycle to the next if any individual fiber is considered. Therefore, it is possible to consider only the behavior of the entire structure as being composed of a statistical distribution of these different types of deformation. Although all of these mechanisms contribute to both the recoverable and nonrecoverable deformations, it is not possible to separate the contributions of each mechanism to each of these two categories of over-all structural behavior. With these considerations in mind, we shall now consider the results of the first and second creep and creep-recovery measurements.

The first and second creep and creep-recovery curves for run 4-B (applied apparent stress = 10.85 g./cm.^{2}) are reproduced in Fig. 17. This same general behavior is observed with all of the runs of this series. The observations which can be made concerning these curves are:

a. The first and second creep curves tend to approach the same value of mat solids concentration at longer times.
b. The slope of the first creep curve is significantly higher than that of the second.
c. The first and second recovery curves are essentially parallel to each other throughout the entire linear portions of the recovery curves.
d. The slope of the recovery curves is higher than the slope of the corresponding creep curves.

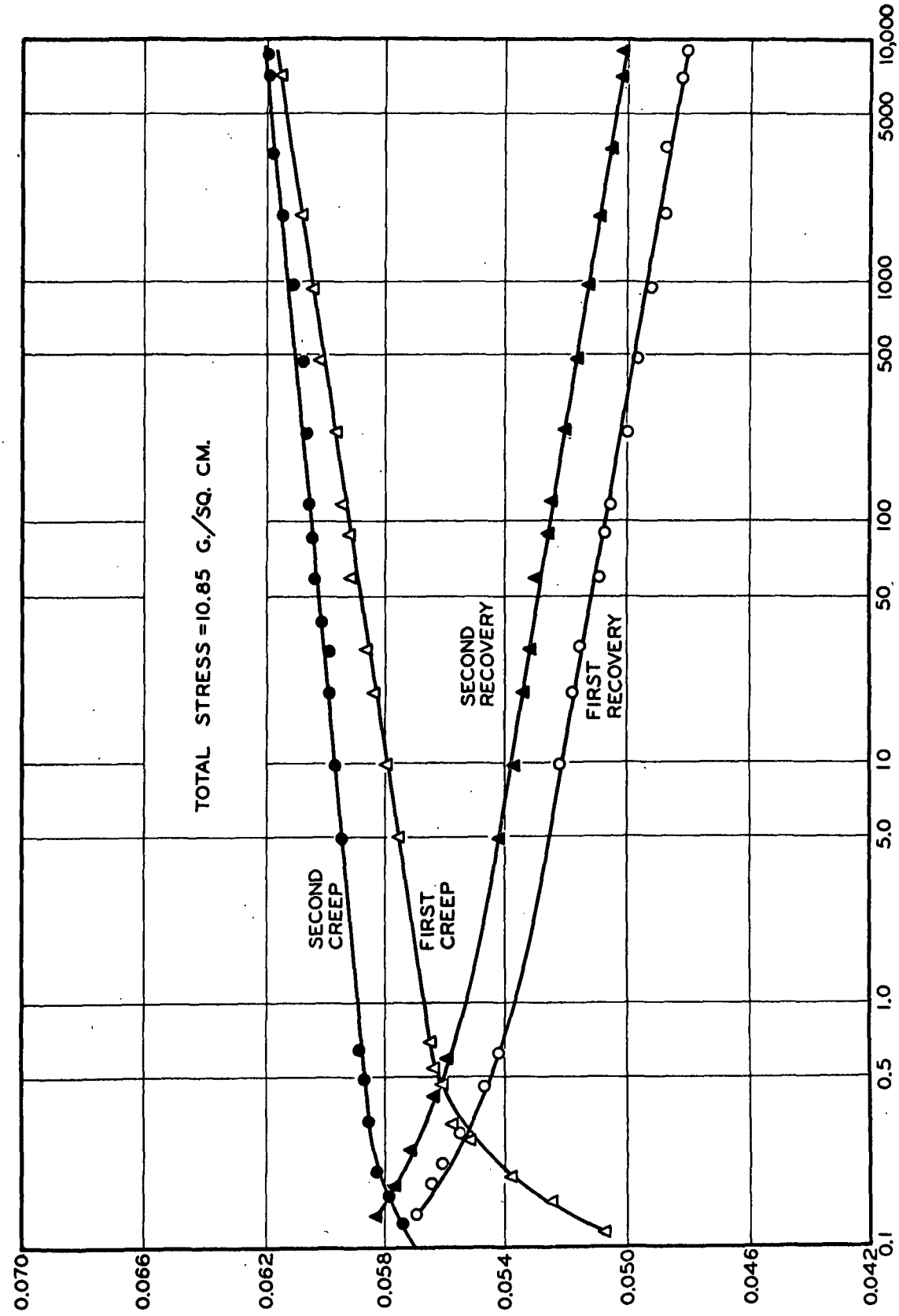

Figure 17. First and Second Creep and Creep Recovery Data

In addition to these observations, the following observations are introduced here from the results of the work carried out on repeated cycling of a mat through eight creep-creep recovery cycles. These cycles were carried out using an applied apparent stress of 34.04 g./cm.^{2}; each creep and creep-recovery run was carried out over a 24-hour period. The results of these multicycle runs are shown in Fig. 18 (creep behavior) and Fig. 19 (creep-recovery behavior).

e. Following the first four cycles, very little change is observed in the creep results.

f. The creep-recovery curves show a tendency to shift toward higher mat solids concentration values for the first six cycles.

g. In these repeated cycling runs, which were carried out over a total of 48 hours for each complete cycle as contrasted with five-hour cycles for the first and second creep and recovery runs discussed in this section, the slope of the recovery curves gradually decreased as more cycles were carried out. However, the slopes of the recovery curves in the 48-hour cycles were almost twice as great as that obtained for the 5-hour cycle.

The following statements can be made concerning the implications of these results. First, the higher slope of the first creep curve coupled with the fact that the two curves approach each other at longer times indicates that the creep rate is higher during the first creep test than during any of the subsequent creep runs. This increased rate of

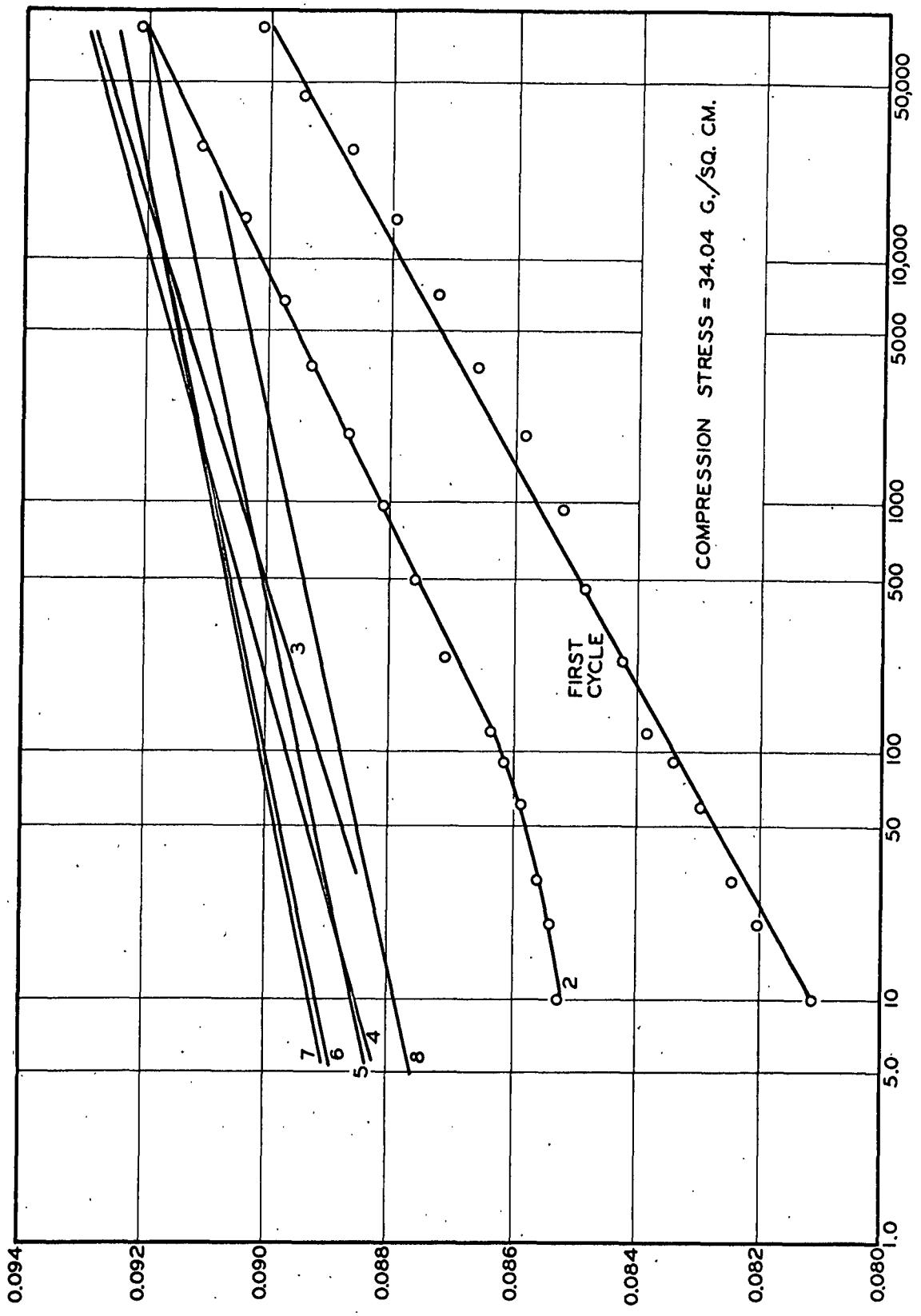

Figure 18. Wet Mat Behavior During Repeated Cycling (Compression)

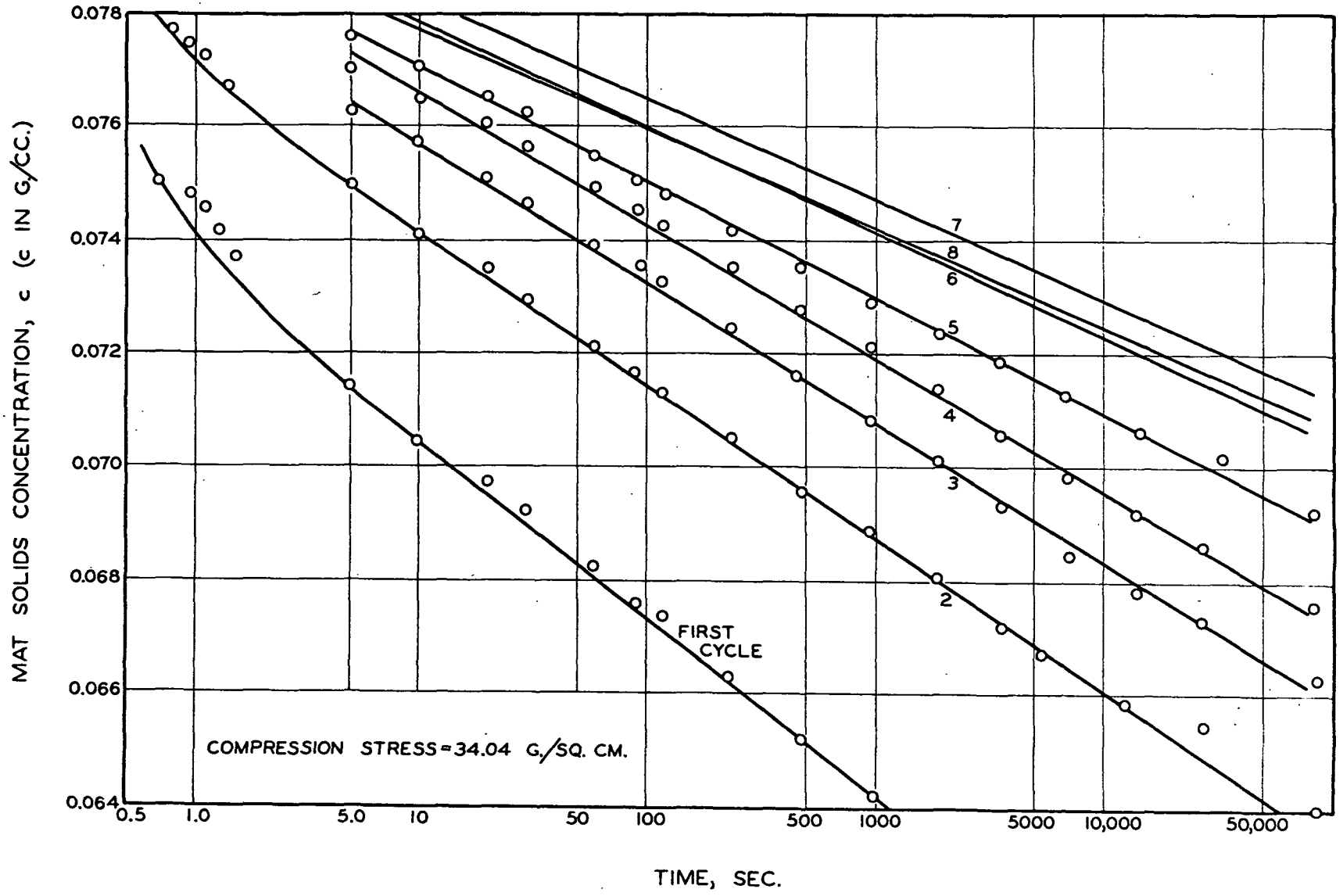

Figure 19. Wet Mat Behavior During Repeated Cycling. (Recovery)

creep during the initial test is probably due to the large amount of secondary (nonrecoverable) creep which takes place during this initial step. This change in the creep curves is also noted in the longer duration, multicycle runs. Each succeeding cycle produces a creep curve which is more nearly identical to the one preceding it, but the curves do not become identical (within experimental error) until four cycles have been carried out.

A similar behavior is observed with the creep-recovery curves. The shift toward higher mat solids concentrations with each succeeding recovery step indicates again that secondary creep is still in evidence after six cycles. However, the slopes of the first and second creep-recovery curves are much more nearly equal than those for first and second creep. Since the slope gives a measure of the rate of the various mechanisms involved, it appears that the recovery mechanisms change much less in nature than do the creep mechanisms over the first two cycles. Again, this is probably due to the large amount of secondary creep encountered in the first creep cycle.

The time of the complete cycle is also of importance, since an increase in cycle time from five to twenty-four hours results in an approximate doubling of the slope of the recovery curve. This means that the rate of the various recovery mechanisms actually increases with increasing time of creep.

The difference in slopes between creep and creep-recovery curves is also very interesting. With most materials, these slopes are identical, at least when dealing with a mechanically conditioned specimen. Since

the Boltzmann Superposition Principle states that the removal of a stress is equivalent to the application of a negative stress, this implies that the shapes of the creep and creep-recovery curves must be identical. This in turn implies that the slopes at corresponding points on both curves must be equal; since the creep curves obtained here are straight lines, the slopes of these lines should be equal for both creep and creep recovery. It will be observed that this difference in slopes is in evidence even after the mat has been essentially mechanically conditioned as well as during the initial cycles. Of course, this creep data is calculated in terms of mat solids concentration while the usual form is to represent it in terms of change in dimension. However, if these same data are plotted as mat thickness (or reciprocal mat solids concentration) versus log time, the same very marked change in slopes is apparent. Thus, there is apparently some restraining force which prevents the mats from recovering as much initially as they are initially compressed during the creep process; as recovery is allowed to continue, the rate of recovery is higher than the corresponding creep rate.

There appear to be at least two possible explanations for such behavior. First, it is possible that water movement into and out of the fiber lumen during creep and creep recovery could be of importance in determining the mat behavior. Conceivably, such water movement might be more nearly instantaneous during the compression process since any small obstacles to flow might be pushed outward by the water. When recovery was begun, such obstacles might be pulled into the areas available for flow and cause a reduced initial change in mat dimensions;

however, at longer times, this flow would control the recovery rate and would make it appear that the recovery was proceeding at a more rapid rate than would otherwise be the case.

This explanation seems rather unlikely for two reasons. First, if such water flow were responsible, it seems doubtful that there would be change in the rate of recovery in going from a 5- to a 24-hour cycle time. Approximately the same flow resistance would be encountered in either case, so that the rates should remain approximately equal. Second, if such flow were controlling, it would be expected that a point would ultimately be reached at which the actual fiber recovery would assume control; a marked change in the appearance of the curve would be expected at this point. Of course, it might be argued that this point is not reached during the first 24 hours of recovery.

This increase in slope during recovery has also been reported by Leaderman for nylon filaments under high tensile stresses (1, p. 197) in the range of 5×10^5 to 1×10^6 g./sq. cm. of filament cross section. However, these differences decreased as the humidity of the specimen surroundings was increased (1, p. 228). The same type of behavior was exhibited by silk filaments (1, p. 130, 138) and viscose (1, p. 145). When the duration of the creep test with nylon was decreased (1, p. 217), the initial recovery increased, approaching the initial deformation value obtained during creep. (Leaderman used the deformation at fifteen seconds following stress application or removal as an indication of the initial behavior to eliminate errors resulting from any attempted extrapolations to shorter times.)

Leaderman interprets these results to mean that the fiber is "stiffer" when the load is removed than when it is added due to a gradual increase in the degree of crystallinity while under stress. Following stress removal, decrystallization takes place accompanied by a gradual disappearance of the new secondary bonds formed during creep (1, p. 204, 205).

Since the results reported by Leaderman and interpreted as being due to reversible changes in crystallinity are qualitatively similar to the results obtained for wet mat creep and creep recovery under conditions of first creep as well as with a mechanically conditioned mat, it is of value to consider the wet fibrous system itself at this point to see if such increases in crystallinity are plausible. The presence of water would be expected to decrease the chances for any increase in crystallization since water would tend to form a sheath around the cellulose chains and keep them from coming into close contact. Since the secondary valence forces such as those responsible for the formation of hydrogen bonds between hydroxyl groups of adjacent cellulose molecules are active only over very short distances [van der Waals forces may be expected whenever two chain segments approach to within about 4 or 5 A., but the presence of hydrogen bonds necessitates not only the close approach of chains but also the correct positioning of appropriate reactive groups (3, p. 5)], such water barriers would greatly reduce the tendency of any such secondary bond formation.

The stresses involved in the creep work would also be of great importance in determining the amount of induced crystallinity. A considerable amount of chain alignment would be required if the chains were to

be brought close enough together to be held by secondary valence forces. Leaderman reported this apparent increase in crystallinity when stresses in the range of 5 - 10 x 10^5 g./sq. cm. were used; at lower stresses, this behavior was not in evidence and recovery and creep curves were of the same shape and slope. In the present work, apparent stresses in the range of 5-90 g./sq. cm. of external mat area were employed, but these values alone tell us very little about the actual stresses set up within the fibers making up the mat. In a later section, the fibrous network is treated as a system of beams subjected to loads which introduce bending moments. Equation (50) which has been derived in this section can be used to estimate the load which is applied at each point of fiber-to-fiber contact; according to this equation:

$$\delta \underline{P} = \frac{\pi^2 \underline{r} \underline{P} \rho_{\underline{f}}}{4 \underline{b} \underline{c}^{\alpha} (\underline{c}_o')^{1-\alpha}} \qquad (50)$$

where

$\delta \underline{P}$ = the load applied at each fiber-to-fiber intersection, g.,

$\underline{r}$ = fiber radius, cm.,

$\underline{P}$ = apparent stress applied to the bed, g./sq. cm.,

$\rho_{\underline{f}}$ = fiber density, g./o.d. fibers/cc. of wet fiber volume $\cong \frac{1}{\underline{v}}$

$\underline{b}$ = fiber length, cm.,

$\underline{c}$ = mat solids concentration, g./cc.,

$\underline{c}_o'$ = mat solids concentration at zero compacting load, g./cc.,

and α = a constant.

For purposes of simplification, α will be assumed to be approximately equal to unity. For the fibers used in these studies, the following constants may be assumed:

$\rho_f \cong 0.276$ g./cc.

$b = 0.25$ cm.

$r \quad 2 \times 10^3$ cm.

If P is taken at 50 g./sq. cm. and c is assumed to be 0.08 g./cc., Equation (50) shows that a load of approximately three grams is present at each fiber-fiber intersection. For a beam restrained at both ends, the maximum bending moment is given by the expression (28):

$$M_{max.} = \frac{\delta P \cdot \ell}{8} \tag{15}$$

where ℓ represents the unsupported fiber length. The maximum stress is given by

$$\sigma_{max.} = \frac{M_{max.} y}{I} \tag{16}$$

where y represents the distance from the neutral axis to the remotest element of the beam and I represents the moment of inertia about this neutral axis. For a beam of circular cross section, $I/y = \pi r^3/4$. Therefore,

$$\sigma_{max.} = \frac{4M_{max.}}{\pi r^3} = \frac{\delta P \cdot \ell}{2\pi r^3} \tag{17}$$

However, from Equation (47) with $\alpha = 1$,

$$\ell = \frac{\pi}{2b} \cdot \frac{c_o'}{c} \cdot \tag{47}$$

Thus, Equation (17) becomes

$$\sigma_{max.} = \frac{\delta P \cdot c_o'}{4r^3 bc} \cdot \tag{18}$$

If c_o' is assumed to be 0.02 g./cm.^{3}, and the other values are substituted into Equation (18), it is found that the maximum stress due to fiber bending under this load is about 1×10^8 g./sq. cm. This is a very large stress, and may be an indication that this treatment does not apply to this system. In this discussion it will be assumed that such a value is reasonable, but it should be kept in mind that there is little real evidence to support such an assumption. If this can be taken as an accurate estimate of the stress actually encountered, it is seen that very high stresses are actually set up in the fibers. It should be kept in mind that the application of such beam equations to this fiber network has several limitations and the validity of such an approach has been shown in only a qualitative fashion; further verification of such an approach is necessary before the certainty of such an approach can be established. If a similar calculation is carried out using the equations for actual compression of the fibers at the points of fiber-fiber contact, a maximum stress of about 2×10^6 g./sq. cm. is obtained. Thus, it appears that although the apparent stresses applied to the bed are not large, very large stresses may be set up at points within the fiber. These values

would tend to support the hypothesis that an actual increase in crystallinity might result from these creep loads. At the present time, no definite statements can be made as to whether crystallinity actually does change during the course of the creep test. However, the results obtained are in very close agreement with those obtained for nylon filaments under high tensile stress. One possible method of checking the possibility of crystallinity changes would be the use of X-ray to detect such changes. However, the actual changes might be quite small and could be masked by other effects such as changes in fiber orientation. The establishment of the exact reason for this behavior would be an important contribution to the knowledge of the viscoelastic properties of wet fibrous cellulosic networks.

As a result of this discussion, the following conclusions may be drawn:

1. First creep proceeds at a significantly higher rate than any of the subsequent creep tests. This is probably due to the larger amount of secondary (nonrecoverable) creep which is present during the initial creep test.
2. After four creep-creep recovery cycles, very little change is observed in the creep curves. Recovery curves become essentially superimposable after six cycles. Thus, for the conditions of applied apparent stress and time of stress application used (34.04 g./sq. cm.; 24 hours creep), the mat is essentially mechanically conditioned after six cycles.

3. The influence of the duration of the creep test on the rate of recovery, together with the differences in creep and recovery rates, is analogous to the behavior of nylon under high tensile stresses. Such behavior could be attributed to increased crystallinity during the creep test and a decrease in crystallinity during recovery. However, further work is necessary before this hypothesis can be proved or disproved.

THE MECHANICALLY CONDITIONED STATE

It has been shown that after approximately six creep-creep recovery cycles a state is reached in which the creep and creep-recovery curves are reproducible with each subsequent cycle. It is of interest to study the behavior of the mat once it has reached this state of mechanical conditioning. Therefore, a series of creep and creep-recovery measurements of 2-1/2 hour duration were carried out on the mechanically conditioned mat using four values of apparent stress ranging from 5 to 34 g./sq. cm. Duplicate runs were made at each apparent stress to check the maintenance of a mechanically conditioned state. The results of the creep measurements are shown in Fig. 20; the creep recovery data are shown in Fig. 21.

The same general equation, Equation (5'), was used to correlate the data, using the methods described in the appendix for evaluating the constants. The following equation was obtained for the creep behavior:

$$\underline{c} = 0.06738 + (0.00387 + 0.000174 \log \underline{t})\underline{P_r}^{0.462} . \qquad (19)$$

(In this equation as well as in the equation given below for creep recovery, $\underline{P_r}$ refers to the apparent stress applied at the start of the deformation test and removed at the start of the recovery test; the pre-compression stress is not included in this term.)

Values of $\underline{c}$ calculated using Equation (19) are included in Fig. 20 for comparison purposes.

For creep recovery, a somewhat different method is used for evaluating the constants of the recovery equation; this method is also

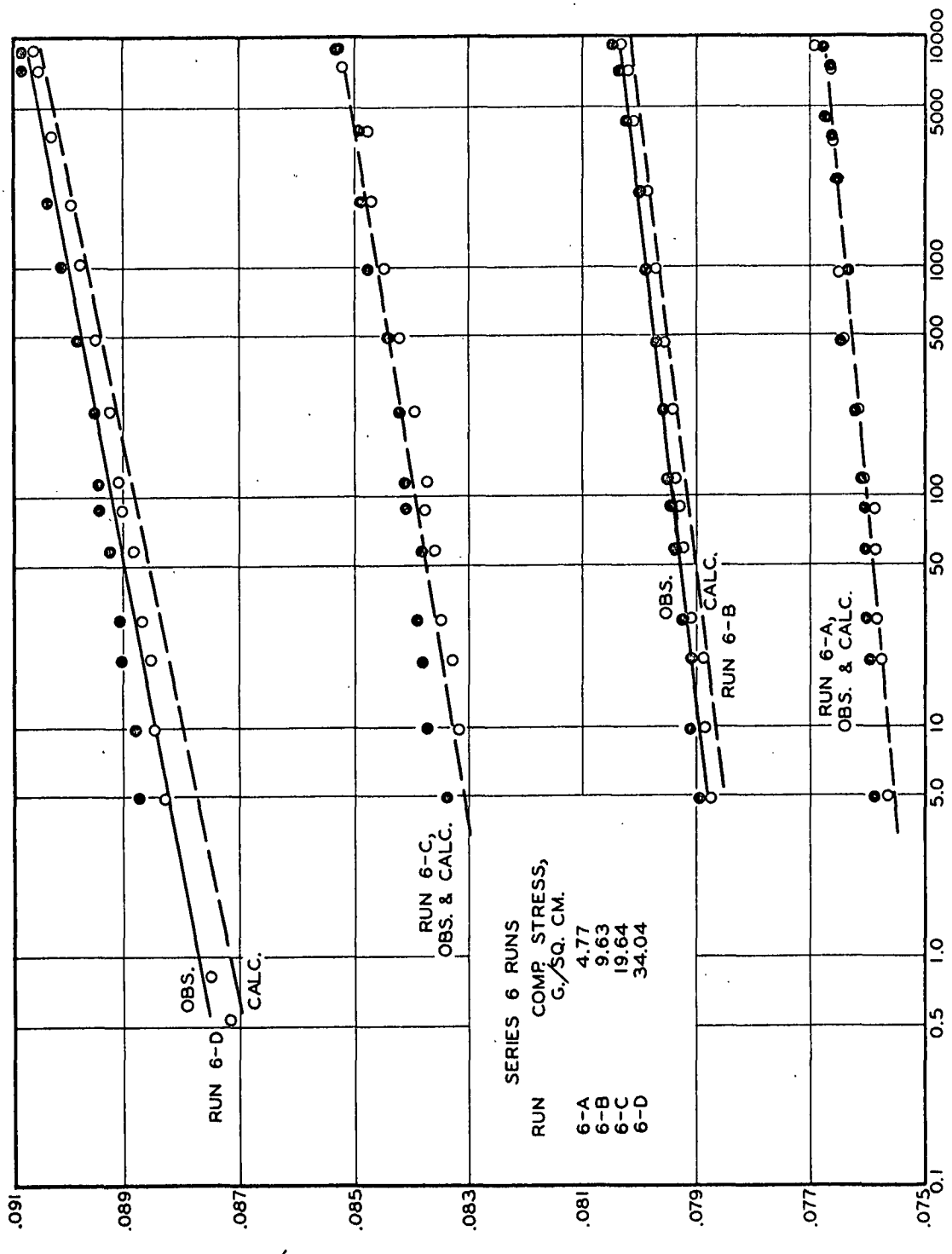

Figure 20. Creep Measurements on Mechanically Conditioned Mats

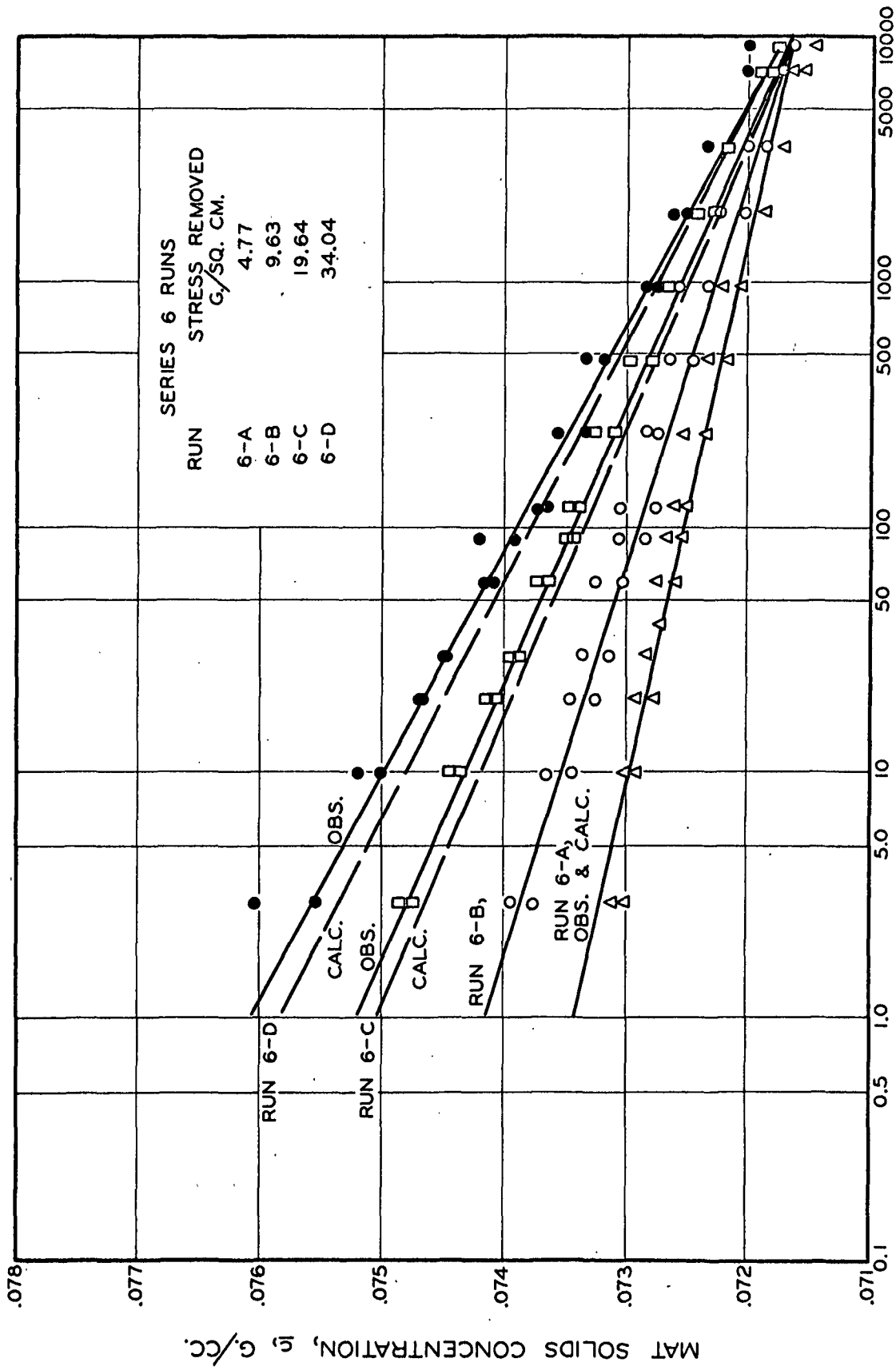

Figure 21. Creep Recovery Measurements on Mechanically Conditioned Mat

included in Appendix I. In this particular case, this method of data treatment gave calculated results which were in better agreement with the experimental results than those calculated by the other method. The following equation was obtained as a result of the application of this method to the recovery data:

$$\underline{c} = 0.07162 + (0.000865 - 0.000215 \log \underline{t})\underline{P_r}^{0.462}. \qquad (20)$$

Values of $\underline{c}$ calculated using Equation (20) are included in Fig. 21 for comparison purposes.

The observed and calculated results are seen to be in good agreement over the apparent stress and time ranges studied. The rather good reproducibility of results (as evidenced by the data obtained during the duplicate runs), together with the good agreement between observed and calculated results, indicate that the mat has reached a state of essentially complete mechanical conditioning.

The exponent, $\underline{N}$, is constant at 0.462 for both creep and creep recovery. However, the time effect (or the slopes of the creep and recovery curves) is again seen to be greater during recovery. Also, if the curves for creep and recovery at the highest apparent stress are compared with those obtained during the final cycles of the mechanical conditioning treatment (which were carried out at the same apparent stress but for 24-hour periods rather than 2-1/2 hours), it will be seen that, while the creep curves are of essentially the same slope and are in the same range of $\underline{c}$ values, the creep-recovery curve for the short time run has a much lower slope and also a larger initial change in $\underline{c}$

at relatively short times. These results are in qualitative agreement with those previously discussed for first creep and first-creep-recovery behavior, and again it appears that the longer creep cycle "stiffens" the fibers so that they exhibit less initial recovery. This effect then appears to disappear with time of recovery, so that the fibers recover at a more rapid rate following the longer creep test.

If the slopes of the first-creep curves are compared with those obtained with the mechanically conditioned mats, it is seen that the slope during first-creep work is more than twice as great as that observed with the mechanically conditioned mats. This indicates that the creep mechanisms are proceeding at a much greater rate during the first-creep cycle. It could be supposed that this difference in rates is due to the elimination of the nonrecoverable portion of creep but that the other mechanisms still proceed at much the same rate in both cases. However, the amount of nonrecoverable creep increases as the mat becomes conditioned; therefore, the term "nonrecoverable creep" really has no significance here unless the defining conditions are stated. The slopes of the first-recovery curves are also almost twice as great as those obtained with the conditioned mat. Since the recovery curves are a measure of the "recoverable" portion of creep, it is seen that the rates of those creep mechanisms which might be termed "recoverable" are also decreased very significantly by the conditioning process. Similar observations are reported by Susich (26).

It must be concluded that all mechanisms (both recoverable and nonrecoverable) are reduced in both magnitude and rate by the mechanical conditioning process. The term "nonrecoverable" has little meaning unless the exact conditions of the test are stated.

IMPORTANCE OF CREEP DURING THE INITIAL RAPID STAGES OF MAT COMPRESSION

Through the use of simple creep experiments, it has been possible to characterize the creep behavior of wet mats from times ranging from about 0.1 second up to 24 hours. The behavior over this time range has been shown to be independent of mat basis weight over the range studied and it has been concluded that this deformation behavior is controlled by the mechanical properties of the mat structure. However, at times shorter than 0.1 second, the relative amount of deformation at any time following the start of the test increases as the basis weight decreases. At such short times, it would be expected that the rate of mat deformation would be at least partially controlled by the relative movement between fiber and water and the resulting frictional drag forces.

It is the purpose of this section to obtain a quantitative interpretation of this initial stage of deformation, and to determine the relative importance of the two possible controlling mechanisms: creep and water-fiber flow.

MATHEMATICAL CONSIDERATIONS

The first and most simplified treatment of this behavior can be made by assuming that creep during this initial period is relatively unimportant in comparison to the deformation process as controlled by water-fiber movement. In the treatment which follows, the following assumptions must be made:

1. The frictional pressure drop across the piston screen is negligible.

2. The fiber (solids) concentration in the mat at any time is uniform (does not vary from the top to the bottom of the mat).

3. The acceleration of water and fiber during this stage is a negligible effect.

The first assumption can be checked by assuming the total rate of piston fall to be controlled merely by the resistance to flow of water through the piston screen. If this is done, it is seen that for such a mechanism the deformation rate would be many times greater than that observed.

The importance of the maximum force required to accelerate fiber and water can be estimated by considering the total mass of the fiber and water within the bed and comparing this to the mass of the piston and attached weights which will also be accelerated during this process. Such a comparison shows that this effect could be no greater than five per cent of that due to the piston and attached weights; for purposes of simplification, this term will also be neglected.

Since this treatment assumes that all water-fiber movement occurs in a direction parallel to the piston movement, any flow of water through the mat edges is neglected. This assumption may not be entirely valid, since the experiments relating creep to mat diameter were not conclusive as to the importance of such flow through the edges. However, the results did indicate that such behavior was probably not of great importance.

Since the relative velocity between fibers and water will vary from a maximum at the piston face to zero at the septum which supports the mat (no water flow is permitted out through this supporting septum during mat

deformation), the use of an average relative velocity would simplify the mathematical manipulations which are to follow. If it is assumed that the mat solids concentration is constant throughout the bed at any instant, then the velocity of the fibers within the bed (relative to a fixed point outside the bed) must be a linear function of the relative distance above the septum. If we let G represent the volume fraction of either component (fiber or water), V their volume rate of flow, and u their actual velcoity, and the subscripts, $_f$ and $_w$, refer to fiber and water respectively, the following equations can be written.

The volume rate of flow at any time and at any point in the bed must be of equal magnitude but opposite direction for fibers and water. If A refers to the total bed area measured perpendicular to the direction of flow, then

$$V_f = V_w,$$

$$V_f = G_f u_f A,$$

$$V_w = G_w u_w A, \text{ and}$$

$$u_w = u_f (G_f / G_w). \tag{21}$$

However, the relative velocity between fiber and water is given by:

$$u_{rel.} = u_f + u_w = u_f + u_f (G_f / G_w) = u_f \left(\frac{G_w + G_f}{G_w} \right).$$

But, by definition, $G_w + G_f = 1$, so that

$$u_{rel.} = \frac{u_f}{G_w}. \tag{22}$$

Equation (22) can be used to calculate the relative velocity at any point within the bed if the fiber velocity is known along with the volume fraction of water at this particular point.

If the location of the point under consideration is defined as in the sketch below, then the fiber velocity, u_f is related to the veloc-

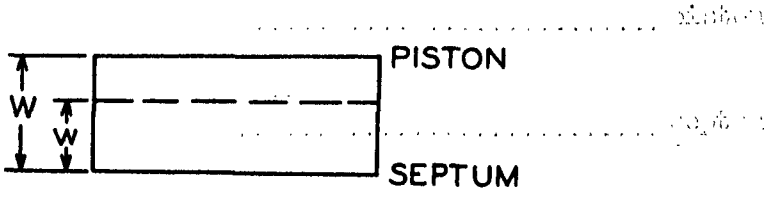

ity of the piston, u_p, by the relationship

$$u_f = u_p\left(\frac{w}{W}\right). \qquad (23)$$

To obtain an average fiber velocity over the entire mat, this expression is written in differential form and integrated across the mat:

$$(u_f)_{av} = \frac{\int_{w=0}^{w=W} u_f \cdot dw}{W} = \frac{u_p \int_0^W \frac{w}{W}\, dw}{W} = \frac{u_p}{2} \qquad (24)$$

If this value of average fiber velocity is substituted into Equation (22), the average relative velocity is:

$$(u_{rel.})_{av} = \frac{u_p}{2G_w}. \qquad (25)$$

The filtration equation, which may be used to estimate the resistance to water-fiber movement, can be written in the form:

$$q = dV/dt = A\Delta P_f/\mu(W/A)R = A\Delta P_f/R' \qquad (26)$$

where

q = dV/dt = volume rate of flow, cc./sec.,

A = mat area, sq. cm.,

ΔP_f = frictional pressure drop resulting from the fiber-water movement.

μ = fluid viscosity,

R = specific filtration resistance, and

R' = modified filtration resistance, = $R(W/A)\mu$.

Equation (26) applied to the flow of water through a fibrous mat; here the fibers are considered fixed so that the relative velocity is determined entirely by the water flow. Thus, in this case, the volume flow rate, q, is related to the relative velocity of Equation (22) by the relationship:

$$u_{rel.} = q/G_w A = \Delta P_f/R'G_w \qquad (27)$$

and the frictional resistance force is given by:

$$F_1 = A \cdot \Delta P_f g = (u_{rel.})_{av} R'G_w A g = \frac{u_p R'A g}{2}. \qquad (28)$$

The modified resistance, R', can also be expressed as a function of G_w and G_f by the equation:

$$R' = K \cdot vc/(1 - vc)^3 \qquad (29)$$

but $vc = G_f$ and $(1 - vc) = G_w$, so that Equation (29) becomes

$$R' = KG_f/G_w^3 \qquad (29')$$

and Equation (28) becomes:

$$F_1 = \Delta A \cdot P_f g = \frac{KG_f^3 Au_p g}{2G_w^3}. \qquad (28')$$

When writing a force balance for the deformation behavior of this system, the restraining force due to the mechanical strength of the fibrous structure itself must also be included. At present, the correct value of this term is very difficult to obtain, since the mat is subjected to several stresses during this initial period and each stress acts over a different increment of time. Since the first creep equation employs the total apparent stress added to the mat and does not separate this from the precompression stress, errors would result when applying such an equation to very short times. Also, questions would arise as to just what times should be used in such an evaluation. If creep is to be considered of minor importance during this initial stage, the use of the stress-solids concentration relationship obtained during the "compressibility" measurements in the calculation of this restraining force should yield results which are not greatly in error. These values are used in the calculations which are included in this section; the force calculated in this way will be designated as F_2.

Taking these two restraining forces, F_1 and F_2, into account, and writing the over-all force balance on the bed (taking the downward direction of the piston movement as positive), we have:

$$F = ma = m\left(\frac{du_p}{dt}\right) = mg - \frac{KG_f^3 Au_p g}{2G_w^3} - F_2 \qquad (30)$$

Equation (30) states that the total downward force is equal to the force due to the mass of the piston and the attached weights, m, minus the restraining forces resulting from the water-fiber frictional force and the mechanical strength of the mat itself.

The validity of Equation (30) can be checked by calculating the constant, K, from the experimental data at several times following the piston release and then comparing this calculated value with the value calculated from theoretical considerations. As will be shown, all the quantities in Equation (30) with the exception of K can be evaluated from the experimental data.

THEORETICAL VALUE OF K

K was defined by Equation (29) as

$$K = R'(1 - vc)^3/vc.$$

However, from Equation (26),

$$R' = R\left(\frac{W}{A}\right)\mu$$

or

$$K = R\left(\frac{W}{A}\right)\mu(1 - vc)^3/vc = R\left(\frac{W}{A}\right)\mu G_w^3/G_f. \qquad (31)$$

Also, from the Kozeny equation,

$$R = kS_w^2 c/(1 - vc)^3 = kS_w^2 c/G_w^3 \qquad (32)$$

but $G_f/v = c$, so

$$\underline{R} = \underline{k}\underline{S}_{\underline{w}}^{2}\underline{G}_{\underline{f}}/\underline{v}\underline{G}_{\underline{w}}^{3} : \qquad (32')$$

Substituting this value of $\underline{R}$ into Equation (31), we obtain:

$$\underline{K} = \underline{k}\underline{S}_{\underline{w}}^{2}(\underline{W}/\underline{A})\mu/\underline{v} \qquad (33)$$

where

$\underline{k}$ = Kozeny "constant,"

$\underline{S}_{\underline{w}}$ = specific surface = 4080 sq. cm./g.,

$\underline{v}$ = specific volume = 3.62 cc./g., and

μ = fluid viscosity = 8.94×10^{-3} poise.

The Kozeny "constant", $\underline{k}$, is not a true constant but has been found (22) to be related to the bed properties by the equation,

$$\underline{k} = \frac{3.50(1-\underline{vc})^{3}}{(\underline{vc})^{1/2}}[1 + 57(\underline{vc})^{3}]. \qquad (34)$$

Using Equation (33), $\underline{K}$ can be calculated for any particular basis weight and compared to the experimentally determined value.

EXPERIMENTAL VALUES OF $\underline{K}$

By the use of Equation (30), $\underline{K}$ can be evaluated from experimental data. However, it will be noted that this evaluation requires the determination of the slope of the experimental deformation-time curve and then this data must be plotted versus time and the second derivative determined by taking the slope of this second plot. Since the error introduced by such a graphical approach can be appreciable, a polynomial

containing five terms and of the following form was fitted to the experimental curve.

$$s = a + bt + ct^2 + dt^3 + et^4 \qquad (35)$$

where

s = distance of piston travel, cm.,

t = time of piston travel, sec., and

a, b, c, d, and e represent constants.

This allows one to take both the first and second derivatives of s with respect to t analytically rather than graphically.

This procedure was applied to two experimental runs; basis weights of 0.0537 and 0.0399 g./sq. cm. and compressive loads of 1975 and 758 grams were used. The results of the application of this analytical method to each of these two runs are shown in Table II (Run 1-D) and Table III (Run 1-H). The theoretical values of K, calculated using Equation (33) and the appropriate basis weights, are included for comparison with the experimentally determined values.

DISCUSSION

The calculated and experimentally determined values of the constant, K, are seen to be in reasonably good agreement over the final portion of both runs. The values calculated at points corresponding to the shorter times are in fair agreement. In these cases, the calculated values of K are lower than the theoretical values.

TABLE II

ATTEMPTED VERIFICATION OF EQUATION (30) USING POLYNOMIAL (RUN 1-D)

Equation for Experimental Data: $s = 1.4968 - 10.121t - 6.528t^2 + 958t^3 - 4426t^4$

$m = 1975$ g.; $v = 3.62$ cc./g.; $S_w = 4080$ sq. cm./g.; $W/A = 0.0537$ g./sq. cm.

t, sec.	ds/dt	d^2s/dt^2	G_f (= vc)	G_w (= $1-vc$)	k	K/g (theor.)	F_1/g	F_2/g	F_1/g (calc.)	K/g (calc.)
0.0149	9.737	-60.71	0.1423	0.858	6.72	15.1	141K	527	1570	11.1
0.0224	9.172	-88.92	0.1505	0.850	6.62	14.9	142K	610	1544	10.9
0.0298	8.429	-110.89	0.1628	0.837	6.33	14.2	147K	797	1400	9.5
0.0447	6.549	-137.49	0.1792	0.821	6.07	13.6	135K	1113	1138	8.5
0.0597	4.435	-140.44	0.1877	0.812	5.94	13.4	99K	1278	979	9.9
0.0745	2.479	-119.94	0.1992	0.801	5.85	13.1	61K	1535	681	11.2
0.0893	0.999	-76.16	0.207	0.793	5.77	13.0	29K	1763	365	12.6
0.1192	0.489	0	0.210	0.790	5.73	12.9	13.2K	1825	150	11.5

From Equation (34): $$k = \frac{3.50G_w^3}{G_f}[1 + 57G_f^3]$$

From Equation (33): $$K_{theor.} = kS_w^2(W/A)\mu/v$$

From Equation (28'): $$F_1 = \frac{KG_fA(ds/dt)g}{2G_w^3}$$

From Equation (30): $$(F_1)_{calc.} = mg - m\left(\frac{d^2s}{dt^2}\right) - F_2$$

TABLE III

ATTEMPTED VERIFICATION OF EQUATION (30) USING POLYNOMIAL (RUN 1-H)

Equation for Experimental Data: $s = 1.1860 + 3.164t - 400.20t^2 + 7733t^3 - 45470t^4$

$m = 758$; $v = 3.62$; $S_w = 4080$; $W/A = 0.0399$ g./sq. cm.

t, sec.	ds/dt	d^2s/dt^2	G_f ($= \frac{}{vc}$)	G_w ($= 1-\frac{}{vc}$)	k	K/g (theor.)	F_1/g	F_2/g	F_1/g (calc.)	K/g (calc.)
0.00788	1.179	473	0.1217	0.878	7.49	12.5	20.4K	190	202	9.9
0.01575	4.40	205	0.1244	0.876	7.39	12.4	51.6K	253	346	6.7
0.01236	5.19	9.2	0.1285	0.872	7.29	12.2	63.8K	329	422	6.6
0.0315	4.28	-119	0.1339	0.866	7.04	11.8	56.0K	403	448	8.0
0.0472	2.05	-58.2	0.1393	0.861	6.92	11.6	28.3K	486	317	11.2
0.0630	1.55	-17.0	0.1418	0.858	6.83	11.4	22.0K	509	266	12.1
0.0787	1.44	-17.0	0.1469	0.853	6.71	11.2	21.6K	564	211	9.8
0.0945	0.928	-15.0	0.1502	0.850	6.62	11.1	14.4K	610	163	11.3
0.1260	0.497	-11.4	0.1527	0.847	6.56	11.0	7.9K	656	114	14.4

This means that the fluid drag term is actually lower than it would be if the theoretical value were used. If this term were increased in Equation (30), the force due to the mechanical properties of the fibrous structure would be lower than the tabulated values of F_2. However, if creep were responsible for this difference, an increase in F_2 would be expected. Therefore, these differences cannot be attributed to creep during this initial time interval.

The assumption was made that the mat porosity at any time was constant throughout the mat. Since the fluid drag forces tend to compress the fibers at the top of the mat while relatively little change is introduced near the septum, this assumption is not entirely valid. It is probably more in error near the start of the run, since at this time relatively little of the load is supported by the fibrous structure; most of this load results in fluid-fiber movement. As the mat becomes compressed, more and more of the load is supported by the fibers and less is required for fluid-fiber movement. Therefore, this assumption of uniform porosity is more nearly correct when the mat has been somewhat compacted. Of course, some error is introduced by the fitting of a polynomial expression to the distance-time data. This source of error is probably responsible for the observed variations of K near the end of each run.

The possibility of water flow through the mat edges could also be responsible in this low value of resistance, since this would add more possible area over which flow could occur, and the resistance to flow in this direction is less than the resistance in a direction perpendicular to the plane of the mat. This factor would also be of greater

importance during the initial stages of compression, or when dealing with a mat of higher basis weight.

Even though the usefulness of this expression is subject to these limitations, it is of considerable value in understanding the importance of creep at these short times. For example, when a higher basis weight is used (Run 1-D), values of $\underline{K}$ at times equal to or greater than about 0.07 second indicate that at least over this time range creep is not a significant factor in determining the mat deformation behavior. When a lower basis weight is used (Run 1-H), and not as much time is required for the mat to compress sufficiently for Equation (30) to apply, $\underline{K}$ values are in good agreement starting at about 0.04 second. From these considerations, it appears that at times greater than 0.04 second, the creep of the mat seems to be relatively unimportant in comparison to the rate-controlling fluid flow mechanism. If the equations used could be modified to be applicable at still shorter times (this would require the introduction of terms to account for the variations in porosity within the mat due to the fluid drag forces present, and also for any flow of water through the edges of the mat;, it is probable that the relative unimportance of creep could be demonstrated at even shorter times. These data give no indication that such accelerated creep does exist.

MAT BEHAVIOR FROM THE STANDPOINT OF DAMPED VIBRATIONS

It was pointed out in an earlier section that if a combination of low basis weights and high compressive forces were employed, the short time data showed the existence of a marked oscillation. Although this

behavior is somewhat analogous to the situation of a damped vibration in that the mat structure serves as the mechanical resistance to movement, analogous to the usual spring constant concept, and the water flow is a viscous element analogous to the simple dashpot, such an analogy cannot be applied quantitatively to this system. In the more simple case, the drag force due to fiber-water movement would be dependent only upon the relative velocity between fiber and water. However, in the actual case, the area over which these particular velocity gradients exist changes as the mat is compacted so that this simple constant no longer relates the velocity and the total drag force. Also, it is assumed in the more simple case that the mechanical restoring force (or the elastic element in the model) is directly proportional to the displacement of the element from its equilibrium position. In this system, neglecting creep effects, the restoring force is proportional to a function of the mat solids concentration. Since this concentration is proportional to the reciprocal of the mat thickness, the mat thickness and the restoring force are also related through this same function, so that the restoring force is not directly proportional to the displacement. Actually, the vibratory nature of this system should be more nearly given by Equation (30), although the assumptions discussed earlier would still be involved. Considering F_1 to be the force due to fluid-fiber friction and F_2 to be the force due to the mechanical strength of the fiber network, it is seen that the same type of differential equation is obtained as when treating the simpler vibratory system.

In summary, it may be said that creep appears to be of relatively little importance during this initial period of rapid mat deformation.

There is no indication that the creep rate increases above the rate observed at longer times. The entire system during this initial period may be considered to be essentially a special case of damped vibration; when dealing with low basis weights, the drag forces are not as great as at higher basis weights, and eventually a point is reached at which the system is underdamped. Under these circumstances, an actual oscillation is observed at short times.

POSSIBLE MECHANISMS INVOLVED IN MAT COMPRESSION

It has been shown previously that water-fiber frictional considerations are responsible for determining the rate of mat compression during the initial rapid compression stage. Once this initial stage has been passed, there appear to be at least three mechanisms by which the mat can undergo further compression. These mechanisms deal with the geometry changes in the over-all fiber network as related to movements of individual fibers, and do not consider the behavior of individual molecules which make up the fiber except as these molecules influence the over-all fiber behavior.

First, there is the possibility of the slipping of one fiber past another which would result in new fiber positioning and hence would be a nonrecoverable deformation. This behavior would be very difficult to evaluate theoretically, and although it is probably of considerable importance, it will not be considered further.

There is also the possibility of reversible fiber-fiber slippage, in which only one end (or one segment) of the fiber moves relative to its neighboring fibers while the remainder of the fiber is held fixed. This type of slippage could be recovered when the applied stress has been removed; at the present time, this type of slippage cannot be separated from deformations within the individual fibers and therefore will not be considered in these developments. While this assumption of negligible fiber slippage does impose certain restrictions on the value of the developments which follow, it is felt that they will still be of value in describing at least a part of the deformation mechanism;

without such an assumption, the system would not readily lend itself to such a treatment.

In addition to deformation resulting from fiber slippage, a second probable mechanism of deformation is the bending of the fibers within the bed when subjected to stresses applied at points of contact with surrounding fibers. If this situation is to be treated quantitatively, it must be assumed that the ordinary beam equations can be applied to this situation. Such an application makes it necessary to assume that the deflections are small enough so that there is no appreciable difference between the original beam length and the projection of its deflected length. Also, for purposes of simplification, it is assumed that the "beam" is uniform throughout its entire length, both in cross-sectional dimensions and in elastic properties. It is also assumed that the fibers are oriented in the bed so as to be at random in the plane perpendicular to the direction of liquid flow during formation; no fibers can be at an appreciable angle to this plane. This last assumption is probably not much in error since sheets formed by the filtration technique do have fibers which exhibit this approximate orientation. This can be observed by watching individual fibers as they are deposited on the surface of the mat during formation. The other assumptions may be difficult to justify in the case of a wet fibrous bed since the fibers are quite flexible and some will probably be deformed a great deal. However, it is hoped that by such an evaluation, even with its obvious limitations, some insight may be gained as to the mechanisms involved in mat compression.

In addition to the assumptions which must be made at the outset, it is necessary to make certain other assumptions during the course of this development. These include:

1. The system behaves as though the same distance existed between all points of fiber-fiber contact.

2. The points of loading are assumed to be equidistant from the points of support (this is really a consequence of Assumption 1).

3. The fibers are cylindrical in shape and are not significantly deformed in cross section during the deformation.

4. A definite relationship exists between the mat solids concentration and the unsupported fiber length.

5. Each intersection supports the same fraction of the total applied load.

6. Each "layer" is the same as all other "layers," contains the same number of intersections and is deformed by the same amount under any applied apparent stress as all "layers."

Since these assumptions are at best only approximately correct, it must be realized that the application of such a treatment to a system as complex as a pulp fiber network cannot be expected to describe the exact quantitative behavior of such a system.

MATHEMATICAL DEVELOPMENT

Consider a fiber supported at several points along its length. The distance between points of support is denoted by ℓ; the fiber is considered fixed at these support points.[a] When a load, dP, is applied midway between these supports, a deformation, dL, occurs.

---

[a] The same final form would be obtained if the beams are considered free at the points of support, except that the constants would change. However, since many contacts would be involved along the length of any fiber, the assumption of fixed supports seems realistic. Actual behavior would probably occur somewhere between these extreme cases.

If there are N_1 total fibers per unit area in the mat, the projected number of intersections per unit area (p.n.i.)(this refers to the total number of possible points of intersection that would be observed if the mat structure were viewed from the top) can be calculated as follows (27):

> Consider a fiber of length b placed in unit area. A second fiber of length b is now dropped so that it makes an angle between θ and $\theta + d\theta$ with the first fiber. If the center of this second fiber lands within the parallelogram shown in Fig. 22, the two fibers will come in contact; if the center of the second

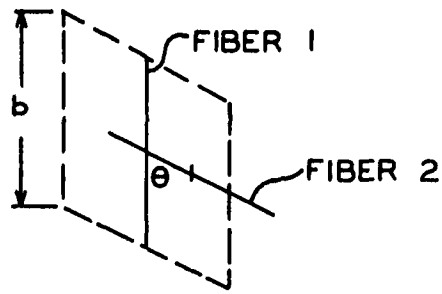

Figure 22. Fiber-Fiber Intersections

> fiber lies outside this area, no contact can be made. The probability of this particular fiber falling so that its center does lie within the parallelogram is:

$$P_1 = \frac{\text{parallelogram area}}{\text{total (unit) area}} = b^2 \cdot \cos\theta. \qquad (36)$$

> However, only a small fraction of the total fibers dropped will be contained in the angle between θ and $\theta + d\theta$. The probability of a fiber landing in this angle is:

$$P_2 = \frac{\text{angle involved}}{\text{total possible angle}} = \frac{d\theta}{\pi} . \qquad (37)$$

The over-all probability of contact between the two fibers is given by the product, $p_1 \cdot p_2$. Since a fiber could land at any angle, θ, between $\theta = 0$ and $\theta = \pi$, the resulting expression must be integrated over these limits. Hence,

$$P_t = p_1 \cdot p_2 = \frac{b^2}{\pi} \int_{\theta=0}^{\theta=\pi} \cos\theta \, d\theta = \frac{2b^2}{\pi} \int_{\theta=0}^{\theta=\pi/2} \cos\theta \, d\theta = \frac{2b^2}{\pi} . \qquad (38)$$

For N_1 fibers per unit area, all of length b, the projected number of intersections is merely the product of this probability for one dropped fiber multiplied by N_1, or

$$(\text{p.n.i.}) = \frac{2N_1 b^2}{\pi} . \qquad (39)$$

But W/A = wt. of fiber/unit area = (no. of fibers/unit area)(wt./fiber)

or,

$$W/A = (N_1)(\pi r^2 b \rho_f) = \pi r^2 N_1 b \rho_f ,$$

where

ρ_f = apparent fiber density, grams of dry fiber per unit volume in water,

r = fiber radius (assuming cylindrical fibers) when in equilibrium with water, cm.,

W/A = basis weight, g./sq. cm., and

b = fiber length in water, cm.

Therefore,

$$N_1 = (W/A)/\pi r^2 b \rho_f . \qquad (40)$$

Substituting this value of N_1 in Equation (39), we obtain

$$(p.n.i.) = \gamma 2(W/A)b/\pi r^2 \rho_f. \qquad (41)$$

Now, consider the mat to be made up of a number of layers of fibers. In the unstressed state, these fibers might be considered to be arranged in a pattern as shown in the sketch below. Let the number of these layers in the mat be denoted by m. Then the weight of fiber per unit

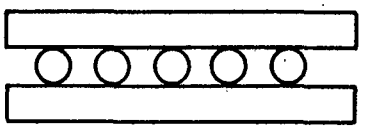

area per layer is $(W/A)/m$. We now introduce a term, c_o', which represents the mat solids concentration at zero compacting pressure.[a] In the unstressed state, the volume of one layer per unit area is equal to $2 \cdot r$. Then,

$$2 \cdot r = \frac{(W/A)/m}{\text{solids concentration in the mat}} = (W/A)/m \cdot c_o'.$$

From this,

$$m = (W/A)/2rc_o'. \qquad (42)$$

(As the mat is compressed, c_o' will increase to some value, c. However, the volume per layer will decrease to a value given by $2rc_o'/c$. Therefore, the number of layers, m, will remain constant throughout the compression.)

---

[a] This is the same c_o' referred to in the discussion of first-creep behavior, but at the present time, it cannot be assumed identical to c_o, the value obtained from first-creep data for this fibrous system.

For fibers within the bed, the actual number of points of contact is given by

$$\text{no. of contact points/layer} = 2(\text{p.n.i.})/\underline{m} = 8\underline{b}\underline{c}_o'/\pi^2\underline{r}\rho_{\underline{f}} \quad . \qquad (43)$$

Within any layer, there are $\underline{N}_1/\underline{m}$ fibers of length $\underline{b}$ so that the total fiber length per layer is $\underline{N}_1\underline{b}/\underline{m}$. Substituting for $\underline{N}_1$ from Equation (40) and for $\underline{m}$ from Equation (42):

$$\frac{\underline{N}_1\underline{b}}{\underline{m}} = \text{total fiber length [(layer)(unit area)]} = 2\underline{c}_o'/\pi\underline{r}\rho_{\underline{f}} . \qquad (44)$$

The distance between fiber-to-fiber supports at zero compacting force is given by

$$\underline{\ell}_o = \frac{\text{fiber length/layer}}{(1/2)(\text{no. of contacts/layer})} = \frac{(2\underline{c}_o'/\pi\underline{r}\rho_{\underline{f}})}{(8\underline{b}\underline{c}_o'/\pi^2\underline{r}\rho_{\underline{f}})} = \frac{\pi}{2\underline{b}} \quad . \qquad (45)$$

At any degree of compaction beyond this initial unstressed state, the number of fiber-to-fiber contacts must be related to the solids concentration within the mat at this compaction. This relationship is unknown at the present time. It is assumed that the distance between points of support is related to mat solids concentration by:

$$\ell = \underline{K}_2/\underline{c}^{\alpha} \quad . \qquad (46)$$

Then, $\underline{\ell}_o = \underline{K}_2/(\underline{c}_o')^{\alpha}$, or $\underline{K}_3 = \underline{\ell}_o(\underline{c}_o')^{\alpha}$. Therefore,

$$\ell = \underline{\ell}_o\left(\frac{\underline{c}_o'}{\underline{c}}\right)^{\alpha} = \left(\frac{\pi}{2\underline{b}}\right)\left(\frac{\underline{c}_o'}{\underline{c}}\right)^{\alpha} \qquad (47)$$

where ℓ = average distance between support points at a mat solids concentration of $\underline{c}$.

From beam theory, for a beam with fixed supports which is centrally loaded (28),

$$\delta\underline{L} = \text{beam deflection} = \frac{\delta P \cdot \ell^3}{192\underline{E}\underline{I}} \qquad (48)$$

where

$\underline{E}$ = modulus of elasticity of the beam material,

$\underline{I}$ = moment of inertia with respect to the centroidal axis,

and $\delta\underline{P}$ = the load applied at the midpoint of any two points of beam support.

To evaluate $\delta\underline{P}$ in Equation (48), the total load applied to the bed must be divided by the total number of points which support this load. Since only half the total intersections must support the downward load while the other half will support the equal upward component, the number of supports involved is obtained from Equation (43), with the appropriate correction for changes in mat solids concentration:

$$\text{no. of supports/layer} = \left(\frac{1}{2}\right)\left(\frac{8\underline{b}\underline{c}_o'}{\pi^2\underline{r}\underline{\rho}_{\underline{f}}}\right)\left(\frac{\underline{c}^{\alpha}}{\underline{c}_o'}\right) = \frac{4\underline{b}\underline{c}^{\alpha}}{\pi^2\underline{r}\underline{\rho}_{\underline{f}}}$$

$$(\underline{c}_o')^{1-\alpha} \qquad (49)$$

or,

$$\delta\underline{P} = \frac{\underline{P}}{\text{no. of supports/layer}} = \frac{\pi^2\underline{r}\underline{\rho}_{\underline{f}}\underline{P}}{4\underline{b}\underline{c}^{\alpha}(\underline{c}_o')^{1-\alpha}}. \qquad (50)$$

Also, the total deformation of the mat must be equal to the sum of the deformations of each individual layer. Thus,

$$(\delta \underline{L})_{\text{total}} = \underline{m} \cdot (\delta \underline{L})_{\text{av.layer}} = \left(\frac{\underline{W/A}}{2\underline{r}c_o'}\right)\left(\frac{\delta \underline{P} \cdot \ell^3}{192\underline{EI}}\right). \quad (51)$$

If we now substitute for $\delta \underline{P}$ from Equation (50) and for ℓ from Equation (47) in Equation (51), it becomes

$$(\delta \underline{L})_{\text{total}} = \left(\frac{\underline{W/A}}{2\underline{r}c_o'}\right)\left(\frac{\pi^2 \underline{r}\rho_f \underline{P}}{4\underline{b}c\ c_o'^{1-\alpha}}\right)\left(\frac{\pi^3 c_o'^{3\alpha}}{8\underline{b}^3} \cdot \frac{1}{\underline{c}^{3\alpha}}\right)\left(\frac{1}{192\underline{EI}}\right)$$

For a differential load, $d\underline{P}$,

$$(d\underline{L})_{\text{total}} = \left[\frac{\pi^5 \rho_f (c_o')^{4\alpha-2}(\underline{W/A})}{1.23 \times 10^4 \underline{EI}\underline{b}^4}\right]\left[\frac{d\underline{P}}{\underline{c}^{4-\alpha}}\right]. \quad (52)$$

However,

$$d\underline{L} = \frac{\underline{W/A}}{\underline{c}^2} \cdot d\underline{c} \qquad [\text{from } \underline{c} = (\underline{W/A})/\underline{L}].$$

Substituting into Equation (52) for $d\underline{L}$, rearranging, and setting limits of integration, we obtain

$$\int_{c_o'}^{\underline{c}} \underline{c}^{4\alpha-2}\, d\underline{c} = \left[\frac{\pi^5 \rho (c_o')^{4\alpha-2}}{1.23 \times 10^4 \underline{EI}\underline{b}^4}\right] \int_0^{\underline{P}} d\underline{P}.$$

Integrating,

$$\underline{c}^{4\alpha-1} - c_o'^{4\alpha-1} = \left[\frac{(4\alpha-1)\pi^5 \rho c_o'^{4\alpha-2}}{1.23 \times 10^4 \underline{EI}\underline{b}^4}\right] \underline{P}. \quad (53)$$

If $\underline{c}^{4a-1} >> \underline{c}_o'^{4a-1}$, this Equation (53) can be simplified to yield

$$\underline{c} = \left[\frac{(4a-1)\pi^5 \rho \underline{c}_o'^{4a-2}}{1.23 \times 10^4 \underline{EI} \underline{b}^4}\right]^{1/(4a-1)} \cdot \underline{p}^{1/(4a-1)}. \qquad (54)$$

Equations (53) and (54) represent the final form of the expression. It is very interesting to note that Equation (54) has the familiar form of the "compressibility" equation, with

$$\underline{M} = \left[\frac{(4a-1)\pi^5 \rho \underline{c}_o'^{4a-2}}{1.23 \times 10^4 \underline{EI} \underline{b}^4}\right]^{1/(4a-1)} ; \quad \underline{N} = \frac{1}{4a-1}.$$

It must be remembered that these equations deal only with the immediate elastic deformations, and say nothing about the time-dependent component of deformation. However, it may be assumed that the total deformation will show the same load dependency as does the initial elastic deformation.

If it is further assumed that $\underline{c}_o'$ can be represented by $\frac{2\underline{r}}{\underline{vb}}$, as indicated by Equation (12), and remembering that $\underline{v} \simeq \frac{1}{\rho_{\underline{f}}}$, Equation (54) can be further reduced to

$$\underline{c} = \left[\frac{(4a-1)\pi^5 \left(\frac{2\underline{r}}{\underline{b}}\right)^{4a-2}}{1.23 \times 10^4 \underline{EI} \underline{b}^4 \underline{v}^{4a-1}}\right]^{1/(4a-1)} \underline{p}^{1/(4a-1)}. \qquad (55)$$

COMPARISON WITH EXPERIMENTAL RESULTS

At this time it is not possible to attempt any quantitative verification of these equations. No means are now available for measuring c_o', the mat solids concentration at zero applied stress. Also, with a nonideal system such as that made up of pulp fibers, correct values of E, I, and even ρ_f (or ν) would be difficult to evaluate with a sufficient degree of accuracy. A distribution of fiber lengths and radii would be encountered, and the effect of such distributions in modifying an equation of this type is not known. The fact that these equations apply only to the elastic deformations within the fibers also limits its comparison with experimental data, since all such data also include delayed, nonrecoverable deformations. However, certain things might be pointed out concerning the trends observed with existing data as compared to the type of results expected if this equation (or some similar form) were to apply.

The "compressibility" constants presented in the following table were obtained from compressibility measurements carried out at The Institute of Paper Chemistry by the Pulping and Chemical Engineering groups as well as from the work done in connection with this thesis on summerwood fibers. These values will be used here for comparison purposes.

First, let us consider the exponent, N. According to the work reported in this thesis, this quantity is independent of time. However, the exponent does depend on the relationship which exists between the mat solids concentration and the unsupported fiber length

TABLE IV

COMPRESSIBILITY CONSTANTS FOR THE EQUATION, $c = MP^N$
(c, g./cc.; P, g./sq. cm.)

Fiber	$M \times 10^2$	N
Nylon (3- and 15-denier)[a]	5.35	0.225
Dacron[a]	3.79	0.254
Bleached southern pine kraft[a]	3.08	0.292
Unbleached southern pinekraft[a]	2.92	0.292
Bleached poplar soda[a]	2.77	0.324
Unbleached poplar soda[a]	2.60	0.324
Unbleached southern pine kraft summerwood[b]	2.55	0.311
Unbleached black spruce bisulfite, unbeaten[c]	1.83	0.437
Unbleached black spruce bisulfite, beaten 35 min.[c]	2.83	0.437
Unbleached black spruce kraft, unbeaten[c]	1.64	0.457
Unbleached black spruce kraft, beaten 40 min.[c]	2.13	0.457

[a] Data obtained from W. L. Ingmanson, Chemical Engineering Group, IPC.
[b] Pulp used in creep work.
[c] Data obtained from N. A. Jappe, Pulping and Papermaking Section, IPC.

within the mat at that concentration. If the constant, α, is truly a constant and is independent of fiber dimensions, this exponent should be constant for all pulps; if α varies with the system being considered, this would not be the case. At this time, this question cannot be resolved. Also, if the exponent obtained from "compressibility" work is compared to that obtained from the creep equation, it will be seen that it varies from 0.311 for "compressibility" to 0.418 for creep. Thus,

the introduction of time as a separate variable may have an important influence on the value of this exponent. It is of interest to note that, for the same pulp subjected to different treatments (bleaching or beating) the value of this exponent as obtained by "compressibility" measurements does not change. This lends support to the theoretical equation which states that this exponent is a constant, at least for any particular fiber system.

The constant multiplier, $\underline{M}$, is dependent on the mechanical properties of the material making up the fiber ($\underline{E}$, the modulus of elasticity) and on the fiber size and geometry ($\underline{I}$, the moment of inertia) and the apparent density (or specific volume) of the fiber. The dependence of void fraction on fiber dimensions is not known; however, it can be shown that for simple systems of assumed fiber orientations, this value is proportional to the ratio of fiber diameter to fiber length. (See Appendix III.) Since this relationship is of the same form as that obtained in Equation (12) from different considerations, this discussion will assume the validity of Equation (55) in which $\underline{c}_o'$ has been replaced by $2\underline{r}/\underline{vb}$. Since the moment of inertia of a cylinder about its axis is proportional to the fourth power of the radius (for hollow cylinders, this is actually the difference of the fourth powers of the inner and outer radii), this may also be included in Equation (55). This modified form may then be written as:

$$\underline{c} = \underline{K}_3 \left[\frac{(4a-1)(2)^{4a-2}}{(\underline{b})^{4a+2}(\underline{r})^{6-4a}\,\underline{E}\underline{v}^{4a+1}} \right]^{1/(4a-1)} \cdot \underline{P}^{1/(4a-1)}. \qquad (55')$$

The term $(4\alpha - 1)$ is not included in the constant, K_3, since it is not known whether this quantity is constant for all systems. If the exponents reported in Table IV can be compared to that obtained theoretically, then the "constant," α, must lie between about 0.8 and 1.4. Under these conditions, all the exponents in the denominator of the M term in Equation (55') are positive. This is important in the discussion which follows.

Table IV indicates that for both a southern pine kraft pulp and a poplar soda pulp the value of M in the "compressibility" equation is increased by bleaching. If a fiber is bleached, at least a portion of the lignin is removed from the fiber structure. This would result in a decrease in the modulus of elasticity. At the same time, such a treatment would tend to increase the fiber radius, r, and the specific volume, v, due to increased swelling. Since M increases, the numerator of the M term in Equation (55') must decrease. Therefore, the decrease in E is apparently greater than the increases in r and v.

During the beating process, it is observed that M increases with unbleached pulps; with bleached pulps, there is no change with beating (10). Several changes undoubtedly take place during the beating operation. First, the average fiber radius must be decreased due to fiber splitting. At the same time, beating would tend to increase the specific volume of the fibers due to increased swelling. Studies comparing the increase in specific surface and specific volume during beating with an unbleached and a bleached pulp indicate that the unbleached pulp shows a higher development of specific surface relative to specific volume than

does the bleached pulp (10). Since the lignin present in the unbleached pulp cements the fiber together, beating probably causes more fiber fracture but less fiber brushing and swelling than with the bleached pulp. Therefore, increases in $\underline{v}$ would probably be of greater importance when dealing with the bleached pulp than with the unbleached pulp. Considering Equation (55'), it appears that decreases in the $\underline{r}$ factor must be compensated for by increases in the specific volume term when dealing with the bleached pulp; the over-all result with an unbleached pulp is a decrease in $\underline{M}$ because of a more significant change in the $\underline{r}$ term relative to the $\underline{v}$ term. Thus, these data again appear consistent with the equation.

In all of these examples, it has been possible to explain the observed experimental results by use of an equation of the same general form as Equation (55'). An example will now be given where such an equation does not apply. The data shown in Table V are for two samples of nylon fibers. Each sample was very uniform with regard to fiber dimensions; the compressibility data for both 3- and 15-denier fibers are shown in Table V.

If the equation derived previously for beam deflections is to apply here, a significant increase in $\underline{M}$ would be expected in going from the 15-denier to the 3-denier fibers. However, the experimental data show no significant change. Obviously, some other factor is responsible for this behavior. If it can be assumed that the modulus of elasticity of the fibers is the same in both cases, and that the exponent, $1/(4\alpha - 1)$, does not vary appreciably, a different deformation mechanism must be in

TABLE V

DIMENSIONS OF NYLON FIBERS[a]

Fiber	Arith. Av. Diam., microns	Weighted Av. Diam., microns	Fiber Length, mm.	D/L
3-denier	19.2	19.4	6.47	3×10^{-3}
15-denier	42.2	42.4	12.18	3.5×10^{-3}

[a] Data obtained from W. L. Ingmanson, Chemical Engineering Group, IPC.

operation in this case.

However, if more cold drawing is involved in the preparation of the smaller diameter filament, the elastic modulus can be increased a great deal, presumably because of increased crystallinity introduced by molecular alignment during the drawing process (3). The history of these filaments is not known; such considerations may be of importance.

Since small, flexible fibers are easily deformable, perhaps only very small loads would be required to bend them. If such were the case, a significant portion of the recorded deformation might be due to the compression of the fibers at points of fiber-to-fiber contact rather than any bending of the fibers. If this were true, it might explain differences between the action of beating on bleached and unbleached pulp "compressibility"; unbleached fibers would be less flexible and therefore the bending properties might influence the "compressibility." Bleached fibers might be so flexible that only a very small load bends them enough so that they have already developed nearly the maximum

number of contacts; further load merely compresses the fiber structure at these points of contact. A similar behavior might be observed with the nylon fibers discussed.

A quantitative treatment of the deformation of two cylinders in contact along their entire length is to be found in the literature (29). However, this treatment assumes parallel orientation of the fibers and also that the cylinders retain their circular cross section except in the region of contact, where all deformation is assumed to occur. Since wet pulp fibers are quite flexible, it appears that an over-all distortion of the fiber would also be likely on compression. Also, the assumption of point contact at zero applied stress is probably not valid due to the irregularity of the fiber exterior. The application of this approach does not yield an equation of the form indicated by the experimental data, but for the reasons pointed out above, this does not mean that this mechanism might not be of importance in the actual compression process.

The treatment in which the fibers are considered as beams yields an equation which is of the same form as the "compressibility" equation. The equation appears to be qualitatively applicable to many "compressibility" results obtained on bleached, unbleached, beaten, and unbeaten pulps. The behavior of nylon fibers differs from the expected behavior, but this may be due to some change in mechanical properties which has not been taken into account.

IMPORTANCE OF CREEP IN THE ESTIMATION OF FILTRATION RESISTANCE

It has been mentioned that the time variable may be of considerable importance in the determination of filtration resistance, since this resistance is a strong function of the solids concentration within the mat. This concentration determines the void space available for water flow, and since this void space decreases as the apparent stress is applied for longer periods of time, this may be an important effect.

In order to gain a quantitative idea of the importance of this effect, the change in filtration resistance in going from 0.001 second of apparent stress application to 600 seconds of application under apparent stresses of 10 and 100 g./sq. cm. will be considered. The two extreme cases will be treated: that of a mat being subjected to its first stress (this would yield the maximum time effect possible) and also a mat which has been mechanically conditioned (creep would be minimized in this case).

The mat solids concentration, $\underline{c}$, is calculated for first creep using Equation (9), and the values for the mechanically conditioned mat are obtained using Equation (19). Equation (32) can be modified by combining all the constant terms to yield the equation for variation in the specific filtration resistance, $\underline{R}$, with $\underline{c}$:

$$\underline{R} = \underline{K}_1 \cdot \underline{c}/(1 - \underline{vc})^3 \qquad (32'')$$

where $\underline{v}$ is the hydrodynamic specific volume of the wet fibers (3.62 cc./g.) and $(1 - \underline{vc})$ represents the void fraction of the wet mat. The relative change in filtration resistance is then calculated as

$$\% \text{ relative change} = [(\underline{R}_{600} - \underline{R}_{.001})/\underline{R}_{.001}] \times 100. \quad (57)$$

Table VI shows how these values change for first creep and creep after mechanical conditioning.

TABLE VI

EFFECT OF TIME ON CALCULATED VALUES OF SPECIFIC FILTRATION RESISTANCE

Apparent Stress, g./sq. cm.	% Relative Change in $\underline{R}$	
	First Creep	Mech. Cond. Creep
10	26	8
100	62	25

Thus, it is seen from this table that the percentage difference between the filtration resistance at 0.001 second and 600 seconds increases very significantly with applied apparent stress (which would be expected since the rate of creep increases with increased apparent stress). Also, this difference is much larger with first creep than when dealing with a mechanically conditioned mat. However, under any set of apparent stress and time variables, it is evident that the severalfold difference in filtration resistance observed during laboratory and machine drainage studies could not be attributed entirely to creep. On the fourdrinier wire, following the first table roll, the portion of the mat formed at the earlier table rolls would be at least partially mechanically conditioned; hence, if creep alone were to explain differences in filtration resistance, these differences should lie somewhere between the values calculated for first creep and creep of a mechanically conditioned mat. Also, since the apparent stress exerted by fluid drag forces varies from

zero at the top of the mat to a value corresponding to the pressure drop across the mat at the bottom, the apparent stress used to compute creep would also vary across the mat, and for any individual fiber this apparent stress would increase as more fiber built up on top of it. At any rate, the maximum difference in resistance attributable to creep would be calculated using the highest pressure drop encountered and applying this to first-creep conditions. Thus, a maximum of a sixty per cent increase in filtration resistance could be attributed to creep in the mat during the time of stress application at an apparent stress of 100 g./sq. cm. (Since the mechanically conditioned mat was conditioned using an apparent stress of 34 g./sq. cm., it is not strictly legitimate to calculate a value of $\underline{c}$ corresponding to an applied stress of 100 g./sq. cm.; at this apparent stress, the mat would no longer be mechanically conditioned and a larger deformation than that calculated would result. However, the conclusion that creep is less significant following conditioning would not be altered by this added complication.)

APPLICATION OF BOLTZMANN SUPERPOSITION PRINCIPLE TO MAT DEFORMATIONS

Leaderman (1) demonstrated that with polymeric materials which contain both crystalline and amorphous regions, the time-dependent deformation is often not directly proportional to applied stress. If the immediate elastic deformation is still directly proportional to the applied stress, the deformation-stress-time relationship can be expressed in the form:

$$\Delta \underline{L} = \frac{\underline{J}\,\sigma}{\underline{E}} + \underline{J} \cdot \underline{f}(\sigma) \cdot \psi(\underline{t}). \qquad (58)$$

This equation also implies that the time variable and the stress variable can be represented by separate functions, $\psi(\underline{t})$ and $\underline{f}(\sigma)$. In this equation,

$\Delta \underline{L}$ = deformation per unit length,

σ = applied stress,

$\underline{E}$ = modulus of elasticity, and

$\underline{t}$ = time.

If the immediate deformation were also not directly proportional to the applied stress but were determined by this same function of stress, $\underline{f}(\sigma)$, Equation (58) would become:

$$\Delta \underline{L} = \underline{L}_{\sigma,\underline{t}} - \underline{L}_{o} = \frac{\underline{Q} \cdot \underline{f}(\sigma)}{\underline{E}} + \underline{J} \cdot \underline{f}(\sigma) \cdot \psi(\underline{t}) \qquad (59)$$

In the present case of the deformation of mechanically conditioned wet pulp mats, it is possible to relate mat solids concentration, $\underline{c}$, to time of application of apparent stress, $\underline{P}$, by the general equation:

$$\underline{c} - \underline{c}_o = (\underline{A} + \underline{B} \log \underline{t})\underline{P}^{\underline{N}} = \underline{A}\underline{P}^{\underline{N}} + \underline{B}\,\underline{P}^{\underline{N}} \log \underline{t} \cdot \qquad (5')$$

It has been pointed out that this equation does not hold at zero time; therefore, the first term of this equation, $\underline{A}\underline{P}^{\underline{N}}$, represents the change in solids concentration at one second following stress application while the second term represents the time-dependent component. A comparison of this equation with Equation (59) indicates that both are of the same fundamental form.

Leaderman represents the Boltzmann Superposition Principle when applied to the general case of nonlinear behavior given by Equation (58) by the equation:

$$(\Delta \underline{L})_{\underline{t}'} = \frac{\underline{J}\sigma_{\underline{t}'}}{\underline{E}} + \underline{J} \int_o^{\underline{t}'} \frac{d[\underline{f}(\sigma_{\underline{t}})]}{d\underline{t}} \cdot \psi(\underline{t}' - \underline{t}) \cdot d\underline{t} \qquad (60)$$

in which $(\underline{t}' - \underline{t})$ represents the elapsed time following the change in the applied stress, and $\underline{t}$ represents the time measured from zero time until this change in stress occurs. If this equation is rewritten to include the nonlinear behavior of the elastic portion of the deformation as given in Equation (59), it becomes:

$$(\Delta \underline{L})_{\underline{t}'} = \frac{\underline{Q} \cdot \underline{f}(\sigma_{\underline{t}'})}{\underline{E}} + \underline{J} \int_o^{\underline{t}'} \frac{d[\underline{f}(\sigma_{\underline{t}})]}{d\underline{t}} \cdot \psi(\underline{t}' - \underline{t}) \cdot d\underline{t}. \qquad (61)$$

If this form is now applied to Equation (5') for wet mat behavior, this becomes:

$$\underline{c} - \underline{c}_o = \underline{A} \cdot \underline{P}_{\underline{t}'}^{\underline{N}} + \underline{B} \int_o^{\underline{t}'} \frac{d\underline{P}_{\underline{t}}^{\underline{N}}}{d\underline{t}} \cdot \log (\underline{t}' - \underline{t}) \cdot d\underline{t}. \qquad (62)$$

Equation (62) can be interpreted as follows. The change in mat solids concentration at any time, $\underline{t}'$, is equal to the sum of the change due to the nontime-dependent component evaluated under the apparent stress present at that time, plus the sum of all the changes in this apparent stress function with due consideration for the time $(\underline{t}' - \underline{t})$ over which this function acts.

If we consider the behavior resulting from the application of an apparent stress, $\underline{P}_1$, at time, $\underline{t}_1$, and an apparent stress, $\underline{P}_2$, at a time, $\underline{t}_2$, Equation (62) becomes:

$$\underline{c} - \underline{c}_o = \underline{A}(\underline{P}_1 + \underline{P}_2)^{\underline{N}} + \underline{B}\left\{\underline{P}_1^{\underline{N}} \log (\underline{t} - \underline{t}_1) + [(\underline{P}_1 + \underline{P}_2)^{\underline{N}} - \underline{P}_1^{\underline{N}}] \log (\underline{t} - \underline{t}_2)\right\} \tag{63}$$

when applied at some time, $\underline{t}$, such that $\underline{t} > \underline{t}_2 > \underline{t}_1$. Here, $(\underline{t} - \underline{t}_1)$ is the time over which the apparent stress, $\underline{P}_1$, has acted and $(\underline{t} - \underline{t}_2)$ is the time over which the combined apparent stresses have acted. Also,

$$(\underline{P}_1 + \underline{P}_2)^{\underline{N}} + \underline{P}_1^{\underline{N}}$$

represents the change in the stress function, $\underline{P}^{\underline{N}}$, resulting from the addition of the apparent stress, $\underline{P}_2$, to the apparent stress, $\underline{P}_1$. Since the constants, evaluated for creep of a mechanically conditioned mat, have the values shown in Equation (19), inclusion of these values in Equation (63) gives:

$$\underline{c} - 0.06738 = 0.00387\left(\sum_{\underline{i}=1}^{\underline{n}} \underline{P}_i\right)^{0.462} + 0.0001742\left\{\underline{P}^{\underline{N}} \log(\underline{t} - \underline{t}_1) + [(\underline{P}_1 + \underline{P}_2)^{\underline{N}} - \underline{P}_1^{\underline{N}}] \log(\underline{t} - \underline{t}_2) + \cdots + \left[(\underline{P}_1 + \underline{P}_2 + \cdots + \underline{P}_{\underline{n}})^{\underline{N}} - (\underline{P}_1 + \underline{P}_2 + \cdots + \underline{P}_{\underline{n}-1})^{\underline{N}}\right] \log(\underline{t} - \underline{t}_{\underline{n}})\right\} \tag{63'}$$

This equation is in the general form and applies for the application of n apparent stresses at times ranging from t_1 to t_n.

In order to check the validity of such an equation in predicting the deformation behavior of wet pulp mats, a loading sequence involving four stages was made on the mechanically conditioned mat. The first two stages involved increases in the amount of compressive stress added, the third stage the removal of a portion of the stress, and the final stage the reapplication of this apparent stress. The first stage, of course, involves just one apparent stress and therefore Equation (63') reduces to the creep equation at a single stress. In this case, excellent agreement was obtained between experimental and calculated results. However, when this technique was applied to the second, third, and fourth stages, the agreement was not good. Although the magnitudes of the values of c agreed approximately within experimental error (± 0.005 g./cc.), the slopes of the calculated and experimental curves were greatly different over the first portion of the time scale involved. The results for the final stage are shown in Fig. 23; the same trends are noted in the other stages. The experimental values fall on a straight line; the calculated values show a nonlinear behavior. At shorter times, the calculated results lie significantly above the experimental results. However, the initial slope of the calculated curve is much lower than that of the experimental curve, and at longer times, these curves approach each other. At the same time, the calculated curve begins to slope upward, so that at longer times, the two curves become essentially identical.

These results indicate that some effect other than those included in the determination of the creep behavior must be influencing the mat

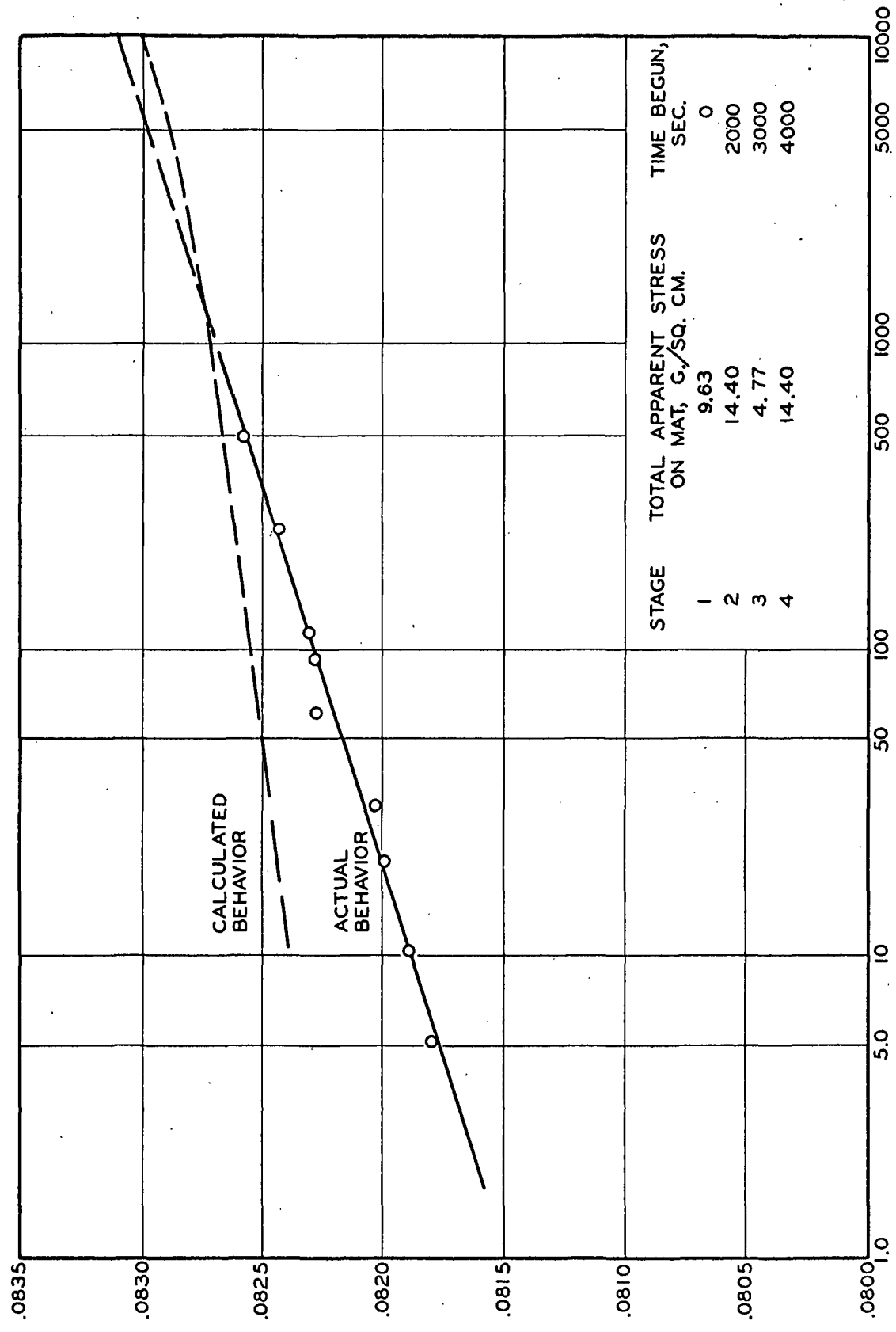

Figure 23. Attempted Application of Nonlinear Boltzmann Superposition Principle to Fourth Stage of Loading Sequence Test

behavior. Again, it appears that the same phenomenon which results in variations between creep and recovery rates under the same apparent stresses may be responsible for this behavior. This behavior, similar to that expected if the crystallinity of the cellulose were increased as the fibers are stressed, appears to make the fibers "stiffer" following the application of a stress than they would otherwise be. Then, when a second stress is added, this increased "stiffness" results in less change in mat thickness than would be predicted using the creep equation. After this second stress has been applied for a short period, the "stiffness" of the fibers begins to approach that of the same mat subjected to no earlier stress, and the two curves begin to approach each other. At longer times, these differences have largely disappeared and the curves are in good agreement.

Since we are dealing with a mechanically conditioned mat, any increase in fiber "stiffness" during creep is entirely lost during the recovery portion of the test. However, if the tests were carried out over shorter and shorter times, this effect would probably be reduced. Some evidence for this has already been presented. This would mean that a mat would exhibit more immediate elastic recovery but less delayed recovery as the time of stress application was decreased.

Although the Boltzmann Superposition Principle applies only to recoverable deformations, it should be applicable as well to systems exhibiting nonrecoverable deformation if the following two requirements are met:

1. The nonrecoverable deformation must be related to the same time and stress functions as the recoverable component.

2. No steps must be involved in the process which require a removal of stress.

If these requirements are met, then it should also be possible to calculate the results of "compressibility" tests from the first-creep data by using Equation (63') and the appropriate time functions. This was done, and it was again found that the calculated results gave higher mat solids concentrations than did the experimental results. Again, this "stiffening" effect may be responsible.

Although the creep of wet mats can be represented by two apparently independent functions of time and applied apparent stress, it appears that an additional effect makes it impossible to predict mat behavior from a knowledge of the loading history. This effect alters the two functions so that these functions evaluated under one set of conditions does not apply under other conditions. Due to slight changes in mat behavior between duplicate runs, probably due to the further introduction of small amounts of nonrecoverable deformation, it is difficult to check the exact validity of such an approach.

POSSIBLE LIMITATIONS OF THE APPLICATION OF THIS WORK TO INDUSTRIAL PROCESSES

At the beginning of this thesis, one of the reasons given for carrying out such a study was that the time variable is an important one when dealing with machine operations. Therefore, it was felt that before these various operations could be understood, the importance of the time of apparent stress application should be studied. At this point, it is necessary to point out some of the differences which exist between the fiber systems employed in this work and those encountered in actual practice. This discussion is certainly not designed to show that measurements obtained in one system have no practical value when applied to the other; it is included merely to point out certain differences which must be kept in mind when drawing analogies between the two systems.

First, although actual pulp fibers have been used in this work, the system has been idealized to a considerable extent by employing classified unbleached kraft summerwood fibers. This is not a major limitation, since similar behavior would be expected with other pulps. However, it would almost certainly not be correct to use the same time-dependent functions on other types of mats, since the magnitude of such functions will very probably be a function of the properties of the fibers which make up the bed.

A second, more important difference would involve differences in fiber orientation. In the mat as formed by filtration, the fibers are oriented almost entirely in the plane perpendicular to water flow, while in the sheet formed on the machine, there would be more chance for fibers

to run at an angle to this plane. Changes in fiber orientation are known to have an effect on sheet permeability (31), and it seems quite probable that the deformation characteristics of the mat would also depend upon this orientation.

Another factor which would be expected to influence the amount of mat deformation observed under any given set of stress-time conditions is the mat thickness, or the number of "layers" of fibers which are present in the mat. Over the basis weight range used in this work (0.02 to 0.08 gram o.d. fiber per square centimeter of mat area) it was concluded that any basis weight effect was negligible. However, when dealing with machine-made sheets, the basis weight may easily be as low as 0.003 gram per square centimeter and there may be as few as ten or less fiber "layers" in the sheet. When mats this thin are used, it would be expected that somewhat different mechanisms of compression would be involved. The extreme case would be a sheet composed of just one layer of fibers; in this case, all the mat compression would be of the nature of actual compression of the individual fibers; no fiber-fiber slippage or fiber bending would occur. It seems, therefore, that as the fiber basis weight begins to approach this limiting case, there would be less relative deformation under any given applied apparent stress and a larger portion of this deformation would probably be recovered once the stress was removed. In other words, when an apparent stress was applied to such a low basis weight sheet, the mat solids concentration at any time would probably be lower. This would mean a decrease in filtration resistance; such is actually the observed behavior when comparing machine and laboratory drainage results. Of

course, at this time one can only speculate as to the importance of such an effect and the basis weight range at which such an effect might become important. However, it should be considered as an important possibility until investigations prove otherwise.

The last point concerns the actual relationship between the size of the mat area being subjected to a "compressive" stress and the size of the entire mat. In the case of the work reported in this thesis (and also in work involving the usual "compressibility" measurement), the entire mat is subjected to the same external load. This is good from an experimental standpoint, since variations from one part of the mat to another are eliminated. However, at the table rolls of a fourdrinier or in the press section, only a small portion of the sheet is actually stressed in the machine direction although the entire width of the sheet is stressed to about the same extent. For example, the pressure profiles obtained by Burkhard and Wrist (19) at table rolls show that the distance along the machine direction which is actually subjected to a suction pressure varies from about one-half inch at a machine speed of 500 feet per minute to about one inch at 2500 feet per minute; the maximum suction occurs over a length much smaller than this. Therefore, when dealing with a continuous sheet of fibers, it seems that if only a small portion of the sheet is subjected to the compressive force, the surrounding fibers would tend to counterbalance these forces and keep the mat from being deformed to as great a degree as would be observed if the entire sheet were "compressed." Such a system would, in effect, spread the applied stress over a wider number of fiber-fiber contacts; the area of the bed involved would increase

from the top of the mat (where it would be just that area over which the stress was applied) to the bottom (where fibers which contact fibers above them would be stressed, thus extending the area of loading outward from the original area) in a pyramid type of arrangement. The extent of such pyramiding of the area exposed to the applied apparent stress will increase with the mat basis weight and with increased fiber length. Again, such behavior would tend to result in a lower value of filtration resistance under machine conditions than during laboratory measurements. While an investigation of the importance of this factor would be difficult due to the variability of systems encountered, it is possibly an important consideration.

From this discussion, it can be seen that differences in mat structure and in the manner in which the mat is stressed may be responsible for some of the observed differences in specific filtration resistance on the paper machine as compared to laboratory measurements. Thus, the entire difference cannot be attributed to creep effects brought about by differences in the time of stress application. As seen from this work, such time effects would account for a significant change but are not large enough to account for the observed differences between the two systems.

SUGGESTIONS FOR FURTHER INVESTIGATIONS

It is felt that this work has been a significant contribution toward the understanding of wet fibrous mats under compressive stress. However, as with most studies involving a relatively unexplored area of research, it has not been possible to make a complete study of all the possible variables, or even to investigate in a preliminary manner just what effect certain of these variables might have. The main significance of this work seems to be the proof that mats under compression do obey certain rules (which are, at the present time, still very empirical in nature) regarding stress applied and time of stress application. One approach toward future work would be to carry out a very extensive study with the aim of determining the effect of the physical variables of the system such as fiber dimensions, temperature, and apparent stress over higher stress ranges. There are indications that the same type of relationship would hold at much higher apparent stresses. Van den Akker, Wink, and Bobb (32) have shown that the linearity of mat solids concentration *versus* log time is still in evidence at an apparent stress of 18,400 p.s.i., although they feel that at least a part of this deformation rate was due to the difficulty in expulsion of water through the small pores present in the mat at this high pressure. Also, when the mats were allowed to reach an equilibrium deformation (up to 214 days were required for this), a plot of log *c* *versus* log *P* yields a straight line (only three values are given, with *P* ranging from 1525 to 7450 p.s.i.), indicating that the "compressibility" equation still holds at these high apparent stresses.

However, it is felt that in future work, the fiber dimensions and physical properties should be well defined so that a more quantitative check might be made concerning the importance of the various possible mechanisms involved. Since the type of equations developed in the section dealing with possible deformation mechanisms are more readily applicable to cases in which the delayed deformation can be neglected and only the immediate elastic deformation need be considered, it is also felt that investigations employing fibers composed of a material having such characteristics would be very valuable. It seems that glass fibers of known (and nearly constant) dimensions would be well suited for such work. The length and diameter of these fibers, as well as the variations encountered in these dimensions, could be readily measured, and the density and modulus of elasticity could also be determined or approximated. With these values all clearly defined, it would be a considerably easier task to determine whether the mechanisms discussed earlier are really applicable to the deformation of wet mats in compression. If the applicability of such treatments can be shown in a simpler case such as this, the next step would be an extension to a fiber system in which creep deformation is appreciable. Again, the physical and mechanical properties of the fibers making up the bed should be clearly defined and should be as nearly uniform throughout the bed as possible. A synthetic fiber, such as nylon, which can be obtained in very uniform sizes would seem ideal.

An extension of this work to pulp fibers, which exhibit large differences in fiber properties within any pulp sample, would be very difficult on a strictly quantitative and theoretical basis. However,

many interesting and valuable generalizations could be drawn from such work, providing that the work on ideal systems had clearly defined the mechanisms involved. If the mechanisms cannot be clearly defined, this work would still be of practical value but would of necessity remain on a more empirical basis. Variables which would be of greatest interest would seem to be apparent stress (extension of the present work to much higher stresses) and effects introduced by changing the properties of the fibers by operations involved in the papermaking process. If it were feasible to use a classified pulp and to make measurements of stiffness and of physical dimensions of the individual fibers as well as the measurements on the mat formed from these fibers, the value of such work would be still greater. Such information would also give an idea of the variability which is present from fiber to fiber, and in this way would indicate just how well simple mechanism theories might apply to these more complex systems.

SUMMARY AND CONCLUSIONS

This study has dealt with the behavior of wet pulp mats when these mats are subjected to a compressive apparent stress applied perpendicular to the plane of the mat and parallel to the direction of water flow during mat formation. All work was carried out on mats formed from classified unbleached kraft southern pine summerwood fibers so that undesirable side effects could be eliminated.

The work was carried out at a temperature of 25.0 ±0.05°C., and the mats were completely submerged in water to eliminate all surface tension effects.

Preliminary creep experiments showed that the creep properties at times greater than about 0.1 second were independent of mat basis weight over the range of 0.02 to 0.08 g./sq. cm. However, at times shorter than this, a decrease in mat basis weight resulted in an increase in the amount of deformation at any time. This indicated strongly that the water flow through the fibrous structure was rate controlling during this initial stage. Creep experiments at different mat diameters showed that this initial period was probably not affected by the mat diameter although errors introduced by working with various diameters make definite conclusions impossible. This probable independence makes it possible to conclude that the water-fiber movement was essentially in a direction perpendicular to the plane of the mat and did not occur to any significant extent in a lateral direction outward through the unrestrained mat edges.

Following these preliminary investigations, the experimental work was directed toward three general areas. First, the creep and creep-recovery behavior of wet pulp mats was studied through the first and second creep and creep-recovery cycles. Secondly, a mat was cycled through several creep-creep recovery cycles in an attempt to reach a state of mechanical conditioning (a material is said to be mechanically conditioned when all of the deformation observed during the creep test is recovered during the subsequent creep-recovery test). Once this mechanically conditioned state was achieved, creep and creep-recovery measurements under different apparent stresses were carried out on this mat. Third, the deformation-time relationship was studied at short times (less than 0.1 second) to determine if creep was an important factor at these short times or whether the water-fiber motion was rate controlling. Since the considerations involved in each of these sections has been thoroughly discussed in the individual sections, only a general description of the work and of the conclusions drawn from this work will be included in this section.

The first and second creep and creep-recovery work was carried out at five levels of applied apparent stress which ranged in magnitude from six to 90 g./sq. cm. of external mat surface. Each creep and recovery test was carried out over a two and one-half hour period. When the results of these runs were plotted as mat solids concentration, c, versus the logarithm of time, both the creep and recovery runs appeared as straight lines following a nonlinear portion at short times. It was found that these data could be correlated using a more general form of the "compressibility" equation:

$$c = MP^N \tag{5}$$

where c is the mat solids concentration, P the applied apparent stress, and M and N are constants. For correlation of the creep data, it was necessary to express M as a function of time, t:

$$M = A + B \log t \tag{8}$$

where A and B are new constants, independent of time. The exponent, N, is also time-independent. It was also necessary to add a constant term, c_o, so that the final form of the modified "compressibility" equation was:

$$c - c_o = (A + B \log t)P^N. \tag{5'}$$

This general equation was found to apply to both creep and recovery over the entire range of stresses employed and at times greater than about 0.1 second. There were several indications that similar behavior would be observed at even shorter times if the water-fiber movement during the initial rapid deformation period were not a complicating factor. (Although this same general equation applied to both creep and creep recovery, the applied apparent stress, P, in the creep equation refers to the total compressive stress while the value of P in the recovery equation refers only to that portion of the apparent stress removed prior to recovery. This is explained in greater detail in the body of the report. Also, the application of this equation to first creep-recovery behavior necessitated the inclusion of a term to account for the nonrecoverable or secondary creep.) If Equation (5') were found to apply down to zero applied stress, the constant c_o would represent the mat

solids concentration under zero applied stress. This constant, when evaluated from the first creep data, is very close to the value estimated for this quantity by other workers; it is probable that this constant does have some theoretical significance.

The slopes and magnitudes of the creep and recovery curves make it possible to speculate as to the probable mechanisms involved in the deformation process. Although the deformation process can be broken down arbitrarily into recoverable and nonrecoverable deformations, these terms in themselves have little meaning since the total nonrecoverable deformation continues to increase until a mechanically conditioned state is reached. It is of greater interest to speak of the sources of the deformations rather than the final over-all result. Contributions to the total bed deformation can be made by fiber-fiber slippage within the bed, by the bending of individual fibers, or by the compression of the fibers at the points of fiber-fiber intersection. Both recoverable and nonrecoverable deformation can result from each of these three mechanisms, and a deformation by one or two of these mechanisms may induce a deformation by the third. Thus, this behavior is very complex. The following results and conclusions were obtained as a result of the first and second creep and creep-recovery studies; some mention is also made of the results of the work done on repeated cycling and the mechanically conditioned mat since this work results in a clearer picture of the mechanisms involved.

First creep proceeds at a significantly greater rate than do any of the subsequent creep tests, as evidenced by the greater slope of the

first creep curves. This is probably due to the large amount of secondary (nonrecoverable) creep which is present during the initial creep test. Following the first four creep tests, no significant change is introduced by subsequent cycles. It therefore appears that essentially all of the nonrecoverable fiber slippage and reorientation has occurred by the end of the fourth creep cycle. The mat exhibits less recovery during each cycle for at least six cycles. The recovery rate is also strongly influenced by the duration of the preceding creep test. This indicates that certain irreversible changes are occuring within the fiber structure which reduce the amount of recovery. The increase in nonrecoverable deformation is probably due at least in part to irreversible fiber slippages. However, the change in recovery rate with changes in the duration of the creep test is more difficult to interpret. This behavior is similar to that described by Leaderman (1) for nylon under high tensile stress, and in this case the behavior is attributed to increases in crystallinity within the filaments during the creep portion of the cycle. The introduction of a partially irreversible crystallinity increase during the creep test would account for the observed wet mat behavior. The presence of water would lessen the probability of the occurrence of such a change, but estimates of the stresses involved indicate that they are high enough to cause such changes.

Work done in an attempt to reach a state of mechanical conditioning indicated that when an applied apparent stress of 34 g./sq. cm. was employed over periods of 24 hours for creep followed by a 24-hour recovery period, cycles became essentially reproducible after six creep-creep recovery cycles. Once this mechanically conditioned state has been reached, creep and creep-recovery measurements (each of two and one-half hour duration) were carried out on the conditioned mat. The four apparent stresses employed ranged from five to 34 g./sq. cm.

As with first creep and creep recovery, the data obtained for creep and creep recovery of the mechanically conditioned mat could be correlated using the general form of Equation (5'). The exponential term, N, was equal for the creep and creep-recovery equations. However, the slope of the recovery curves is again greater than that of the corresponding creep curve. This indicates that the mechanisms previously discussed for first creep behavior are at least qualitatively applicable to the mechanically conditioned state. A comparison of the slopes of the first creep curves and those of the conditioned creep curves shows that the creep rate is more than twice as great in the case of the unconditioned specimen. The corresponding change in the slope of the recovery curves is also nearly twofold; this indicates that not only the rate of nonrecoverable (secondary) creep but also the rate of primary creep is altered by the mechanical conditioning treatment.

The importance of creep during the initial period of rapid mat deformation has been treated by applying a force balance to the system during this period. The deformation is opposed by two forces, one due to the mechanical strength of the fibrous mat network and the other due to the fluid drag forces set up by the relatively rapid fiber-water motion. Although certain assumptions make the application of this simplified treatment quite uncertain when the mat is only slightly deformed, calculations based on the assumption of a negligible creep effect during this time interval are shown to be valid once the mat has been somewhat compacted. From this treatment, it may be concluded that no large increase in the rate of creep is encountered at times between 0.04 and 0.10 second; there is no indication that such increases occur at shorter times.

It has been shown that all of the creep and creep-recovery results can be correlated using a form of the "compressibility" equation which has been modified to include the time variable. Since this general type of equation has been employed by other workers in correlating the "compressibility" behavior of a wide variety of fiber types over a wide range of apparent stresses, it seems likely that this equation has some theoretical significance. In order to explore this possibility further, a treatment of the deformation process was carried out assuming that the fiber network could be treated as a system of beams. Several simplifying assumptions were introduced concerning the uniformity of fiber dimensions and elastic properties, and it was assumed that simple beam equations were applicable to this system. The treatment allows for the increase in the number of fiber-to-fiber contacts as the mat is compressed, but no allowance can be made for the possible slippage of one fiber past another and the resulting redistribution of the applied apparent stress. When this treatment is carried out, it is found that the equation obtained which relates mat solids concentration, c, to applied apparent stress, P, has the same form as does the "compressibility" equation. Although this equation does not include any creep function and therefore applies strictly to only the elastic portion of the deformation, it is speculated that the same general form would also apply to the total deformation if appropriate corrections for creep were included.

This equation indicates that the degree of compaction (as measured by changes in c) should be affected by the dimensions of the fibers making up the bed and also by the modulus of elasticity of these fibers.

This equation is in qualitative agreement with observed changes in "compressibility" which are brought about by such actions as beating or bleaching. It should be pointed out that the exponent, N, in the "compressibility" equation should remain approximately constant according to this equation. The considerable variations in values of N cannot be explained by this equation in its present form; these differences may be due to changes in the amounts of creep which occur during the "compressibility" measurements.

In certain cases, the differences in "compressibility" behavior apparently cannot be explained using this concept of a network of beams. It is possible that the beam concept is applicable to these cases as well, but that differences in certain inherent fiber properties such as modulus of elasticity which are not immediately apparent appear to invalidate this approach. The compression of fibers at points of fiber-to-fiber contact may also be of importance in these cases, but at the present time, this behavior cannot be treated quantitatively.

Since one of the objects of this thesis was to determine the contribution of creep to the differences in filtration resistance which exist between laboratory and machine drainage studies, it is of interest to estimate the magnitude of these changes from the creep data. In order to cover a reasonably wide range of applied apparent stress and degrees of mat precompaction, the calculations were carried out at apparent stresses of ten and 100 g./sq. cm. using the creep equations for first creep and for a mechanically conditioned mat. Times of 0.001 and 600 seconds were used, since these represent the approximate time of

stress application at the individual table rolls of the fourdrinier as contrasted to the time of stress application during laboratory filtration work. Over this time range, the maximum change in filtration resistance due to creep was about 60%. This was under conditions of first creep at an apparent stress of 100 g/sq. cm. The same treatment resulted in a 25% increase with the mechanically conditioned mat. These figures represent the maximum change which could be attributable to creep at this applied apparent stress. From these considerations, it is apparent that while creep effects are very significant under these conditions, they are not large enough to account for the severalfold difference in filtration resistance observed between laboratory and machine drainage results.

While these calculations of possible changes in filtration resistance are useful in determining the importance of creep, there are several differences between the test conditions and actual machine conditions which make any direct absolute comparisons rather dangerous. The fibers used in this work are somewhat idealized, since they represent only a fraction of the entire wood. The orientation of the fibers in the mat is also probably different from that encountered on the fourdrinier wire. The mat thickness (or, more correctly, the basis weight) of the mats used in these studies is large enough so that any differences in the behavior of the fibers at the mat surfaces is of negligible importance in the overall behavior of the mat. However, in an actual sheet of paper, there may be only ten or even fewer thicknesses of fiber through the sheet thickness; in this case, the edge effects may be of considerable importance. Lastly, while the entire mat surface is subjected to a uniform apparent

stress in these creep experiments, the sheet on the paper machine wire is subjected to such stresses only at certain points along its length; fibers adjacent to this area of stress application may actually support some of the applied stress and in this way reduce the amount of deformation.

These effects are very complex and would vary considerably with the composition of the sheet and the processes involved in sheet formation. They are included merely to show that the results of the more simple system studied in this thesis cannot be applied to all other systems without consideration of some of the basic differences involved. Such differences might possibly result in a great change in the apparent stress-time-deformation behavior of the more complex systems.

Since it would be of value to be able to predict mat behavior under a loading sequence, an attempt was made to apply a nonlinear (nonload proportional deformation) form of the Boltzmann Superposition Principle to the wet mat system. However, calculated and experimental results using such a sequence showed that added complications were apparently introduced due to fiber "stiffening" under previous apparent stresses. This same trend was noted when comparing first creep data with "compressibility" measurements. Due to this effect, attempts to predict mat behavior were unsuccessful.

The work and the conclusions drawn from the work presented in this thesis have of necessity been of a rather exploratory nature. Since very little previous work has been done with similar systems, the primary significance of this work is the proof of the existence of a

definite relationship between applied apparent stress, time of apparent stress application, and mat deformation. Although this work, along with work carried out on the apparent stress-deformation behavior of fibrous networks without inclusion of the time variable, indicates that the relationships obtained are of more than empirical significance, the theoretical aspects of such behavior are still almost completely unexplored. If these mechanisms are to be understood, it is felt that further work directed toward the theoretical aspects of the deformation process would be most fruitful.

ACKNOWLEDGMENTS

The author would like to express his sincere appreciation to Dr. Sheldon F. Kurath and other members of the thesis advisory committee for the invaluable advice and encouragement given throughout this investigation.

The assistance of the following is also gratefully acknowledged:

The Chemical Engineering Group of The Institute of Paper Chemistry for assistance in the determination of the drainage properties of the pulp used and for data relating to the compressibility properties of various pulps and synthetic fibers.

The Pulping and Papermaking Section of The Institute of Paper Chemistry for data relating to the compressibility properties of various wood pulps and for assistance in the preparation of the pulp used in this thesis.

The Fiber Microscopy Group of The Institute of Paper Chemistry for determining the fiber length and diameter distributions of the pulp used.

Dr. K. E. Bradway of Union Bag-Camp Paper Corporation for supplying the wood used in the preparation of the pulp which was utilized in this thesis.

NOMENCLATURE

a, b, c, d, e	=	constants in the distance-time polynomial
a	=	acceleration, cm./sec. x sec.
A, B	=	constants in the generalized creep and recovery equations
A	=	external mat area, sq. cm.
b	=	fiber length, cm.
B'	=	constant in filtration equation $= \mu C / A^2 \Delta P_f$
c	=	mat solids concentration, g. o.d. fiber/cc. of mat volume
c_o	=	constant in generalized creep and creep-recovery equations
c_o'	=	mat solids concentration under zero applied stress, g./cc.
c_1	=	mat solids concentration under the precompression stress, 0.0340 g./cc.
c_f	=	mat solids concentration following first creep recovery, g./cc.
C	=	slurry consistency, g. o.d. fibers in filter bed per cc. of filtrate
D	=	fiber diameter, cm.
E	=	modulus of elasticity, g./sq. cm.
F_1	=	force due to frictional drag resistance between fiber and water, dynes
F_2	=	force due to mechanical strength of the fiber network, dynes
g	=	gravitational constant, 980 cm./sec. x sec.
G_f	=	volume fraction of fiber in a wet mat = vc (dimensionless)
G_w	=	volume fraction of water in a wet mat = 1 - vc (dimensionless)
I	=	moment of inertia, $cm.^4$
J	=	constant in Boltzmann Superposition Principle equation

k = Kozeny "constant" in filtration equation

K = calculated quantity in short-time behavior study = $\frac{kS_w^2 \left(\frac{W}{A}\right)\mu}{v}$

K_1 = constant in evaluation of changes in filtration resistance = kS_w^2

L = mat thickness, cm.

$L_{\sigma,t}$ = specimen thickness at stress, σ, and time, t

δL = deformation of an individual fiber or layer of fibers, cm.

ℓ = distance between fiber support points, cm.

ℓ_o = distance between fiber support points under zero applied stress, cm.

m = number of "layers" of fibers within a mat; also mass of piston plus attached weights, g.

M = constant in "compressibility" equation

$M_{max.}$ = maximum bending moment in a beam, g.-cm.

n = number of fibers per unit cell in appendix calculation of c'_o

N = constant in "compressibility" and creep equations

N_1 = number of fibers per unit area in the mat

P_1, P_2, P_t = probabilities in the concept of projected number of intersections

P = apparent stress, g./sq. cm.

P_t = total apparent stress, g./sq. cm.

P_γ = apparent stress removed prior to recovery, g./sq. cm.

δP = load applied at a fiber-fiber contact point, g.

ΔP_f = frictional pressure drop across a mat, g./sq. cm.

q = volume rate of fluid flow, cc./sec.

Q = constant in nonlinear form of Superposition equation

r = fiber radius, cm.

R = specific filtration resistance, cm./g.

R' = modified filtration resistance = $R(W/A)\mu$

R_t = total filtration resistance = $W'_{av}R$

s = distance, cm.

S_w = hydrodynamic specific surface, sq. cm./g.

t = time, sec.

t' = total elapsed time in Superposition equations, sec.

u = machine wire velocity, cm./sec.

u_f = fiber velocity during compaction, cm./sec.

u_w = water velocity during compaction, cm./sec.

$u_{rel.}$ = relative velocity = $u_f + u_w$

u_p = piston velocity, cm./sec.

v = hydrodynamic specific volume, cc./g.

V = volume of filtrate in filtration equation, cc.

V_f = volume rate of flow of fibers during mat deformation, cc./sec.

V_w = volume rate of flow of water during mat deformation, cc./sec.

w = o.d. weight of fibers in a mat from the septum to some arbitrary plane in the mat, g.

W = total weight of fibers in a mat, ovendry grams

W'_{av} = arithmetic average basis weight of sheet entering and leaving table roll area, g./sq. cm.

W/A = mat basis weight, g./sq. cm.

y = distance from beam neutral axis to the most remote element of the beam, cm.

α = constant in equation relating $\underline{c}$ and frequency of fiber-fiber contacts

β = constant in Superposition equation

ϵ = mat void fraction = $1 - \underline{vc}$

θ = angle between two fibers, radians

μ = fluid viscosity, poises

ρ = white water density, g./cc.

$\rho_{\underline{f}}$ = apparent fiber density, g. o.d. fiber/cc. of wet fiber volume

σ = stress, g./sq. cm.

LITERATURE CITED

1. Leaderman, Herbert. Elastic and creep properties of filamentous materials and other high polymers. Washington, D.C., The Textile Foundation, 1943. 278 p.

2. Brezinski, Jerome Phillip. A study of the viscoelastic properties of paper by means of tensile creep tests. Doctor's Dissertation. Appleton, Wis., The Institute of Paper Chemistry, 1955. 242 p.

3. Meredith, R., ed. The mechanical properties of textile fibers. New York, Interscience, 1956. 333 p.

4. Steenberg, B., Svensk Papperstidn. 50, no. 6:127-40(1947).

5. Ivarsson, B. W., Tappi 39, no. 2:97-104(1956).

6. Tobolsky, A., and Eyring, H., J. Chem. Phys. 11:125(1943).

7. Catsiff, E., Alfrey, T., Jr., and O'Shaughnessy, M.T., Textile Research J. 23, no. 11:808-20(1953).

8. Gavelin, G., Svensk Papperstidn. 52, no. 17:413-19(1949).

9. Christensen, G. N., and Barkas, W. W., Trans. Faraday Soc. 51, no. 1:130-45(1955).

10. Jappe, N. A. Personal communication, 1959.

11. Ingmanson, W. L., and Whitney, R. P., Tappi 37, no. 11:523-33(1954).

12. Seborg, C. O., Simmonds, F. A., and Baird, P. K., Paper Trade J. 109, no. 8:35(1939).

13. Seborg, C. O., and Simmonds, F. A., Paper Trade J. 125, no. 15:63 (1947).

14. Seborg, C. O., and Simmonds, F. A., Paper Trade J. 113, no. 7:49 (1941).

15. Brown, R. B., Paper Trade J. 94, no. 13:35(1932).

16. Ingmanson, W. L., Tappi 35, no. 10:439(1952).

17. Taylor, G. I., Pulp Paper Mag. Can. 57, no. 3:267(Convention Issue, 1956).

18. Ingmanson, W. L., Tappi 40, no. 12:936(1957).

19. Burkhard, G., and Wrist, P. E., Pulp Paper Mag. Can. 57, no. 4:100 (1956).

20. Train, D., Trans. Inst. Chem. Engrs. (London) 35:258-66(1957).

21. Ingmanson, W. L., Chem. Eng. Progr. 49, no. 11:577(1953).

22. Ingmanson, W. L., Andrews, B. D., and Johnson, R. C. Internal pressure distributions in compressible mats under fluid stress. Paper presented at the Forty-Fourth Annual TAPPI Meeting, Feb., 1959. New York, N. Y.

23. Den Hartog, J. P. Mechanical vibrations, New York, McGraw-Hill, 1956. 436 p.

24. Daily, J. W., and Bugliarello, G., M.I.T. Technical Report no. 30, 1958.

25. Mason, S. G., Tappi 37, no. 11:494(1954).

26. Susich, G., Textile Research J. 23:545(1953).

27. Van den Akker, J. A. Class Notes, Course A-257, Physical Properties of Fibrous Structures. Appleton, Wis., The Institute of Paper Chemistry, 1957.

28. Singer, F. L. Strength of materials. New York, Harper and Brothers, 1951. 469 p.

29. Marks, Lionel S., ed. In Mechanical engineer's handbook. 5th ed. p. 425. New York, McGraw-Hill, 1956.

30. Ingmanson, W. L. Personal communication, 1959.

31. Brown, Joseph C., Jr. Determination of the exposed surface area of pulp fibers from air permeability measurements using a modified Kozeny equation. Doctor's Dissertation. Appleton, Wis., The Institute of Paper Chemistry, 1949. 146 p.

32. Van den Akker, J. A., Wink, W. A., and Bobb, F. C., Tappi 42, no. 4:340-4(1959).

33. Dixon, W. J., and Massey, F. J., Jr. Introduction to statistical analysis. New York, McGraw-Hill, 1957. 488 p.

APPENDIX I

METHODS USED IN EVALUATION OF CREEP AND CREEP-RECOVERY DATA

All data involving first creep and creep recovery and creep and creep recovery of the mechanically conditioned mat were correlated using an equation of the general form:

$$\underline{c} - \underline{c}_o = (\underline{A} + \underline{B} \log \underline{t})\underline{P}^{\underline{N}} \qquad \text{(A-1)}$$

where

$\underline{c}$ = mat solids concentration at some time, $\underline{t}$,
$\underline{P}$ = applied apparent stress, and
$\underline{c}_o$, $\underline{A}$, $\underline{B}$, and $\underline{N}$ are constants.

This section deals with the methods used in evaluating these constants and in the use of linear regression statistics to determine the best value of the constants and also to determine the certainty of the calculated values.

For first creep and first creep recovery and for creep in the mechanically conditioned state, one method of evaluation was used; for creep recovery in the mechanically conditioned state, a second method was employed. These methods will be discussed here.

The first method involves the following considerations. If Equation (A-1) is differentiated with respect to mat solids concentration, $\underline{c}$, and log $\underline{t}$, we obtain:

$$\frac{d\underline{c}}{d(\log \underline{t})} = \underline{B}\underline{P}^{\underline{N}} .$$

Taking logarithms of both sides,

$$\log [d\underline{c}/d(\log \underline{t})] = \underline{N} \log \underline{P} + \log \underline{B}. \qquad \text{(A-2)}$$

If this relationship is valid, a plot of the logarithm of the slope of the creep or recovery curves *versus* the logarithm of the applied (or removed) apparent stress should give a straight line of slope $\underline{N}$ and intercept, log $\underline{B}$. The results of the application of Equation (A-2) to the first creep data are shown in Fig. A-1.

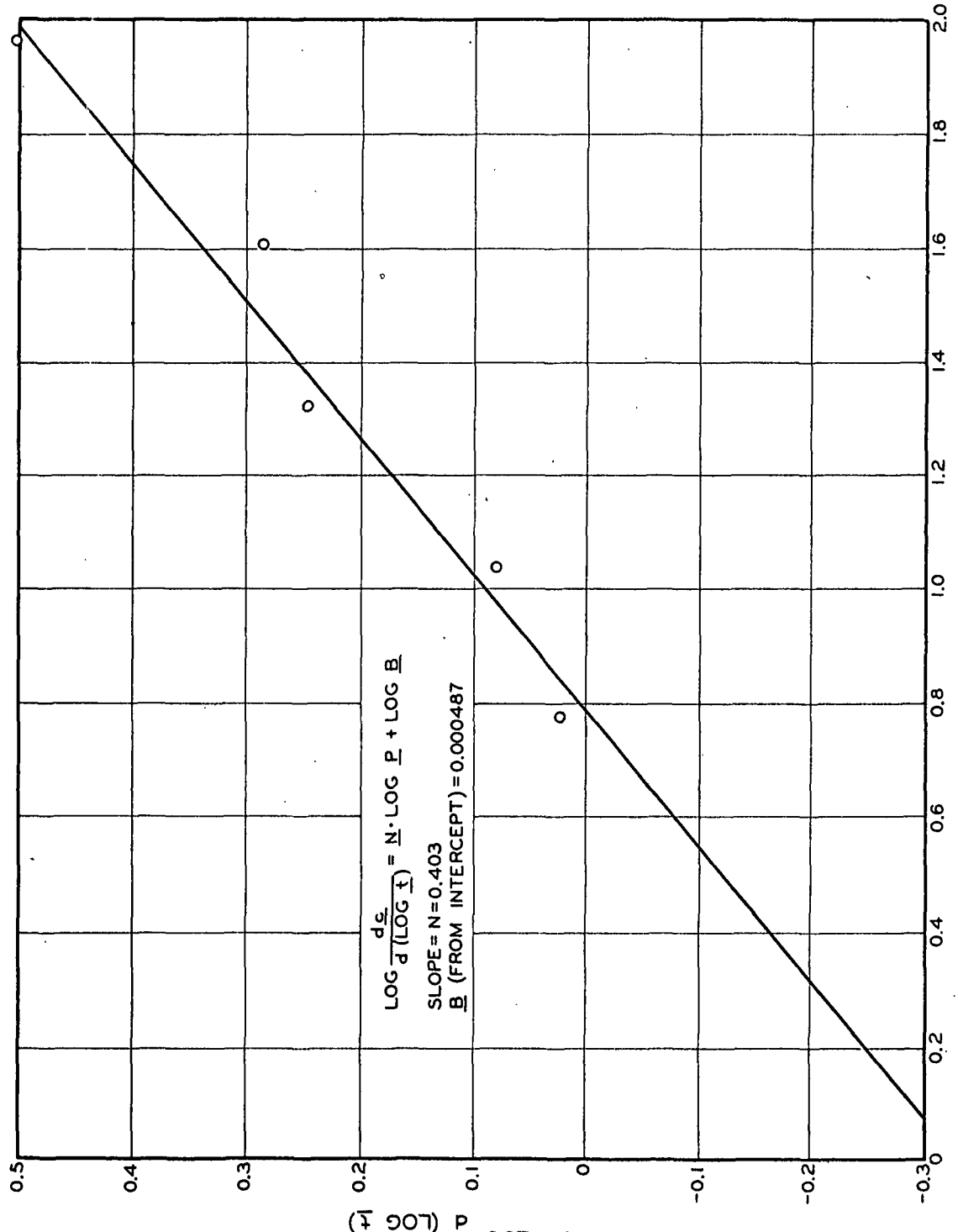

Figure A-1. Evaluation of Constants N and B for First-Creep Data

Equation (A-1) can also be written in the form

$$c - BP^N \cdot \log t = AP^N + c_o. \qquad (A-3)$$

Since all the quantities on the left side of this equation can now be evaluated (B and N are known from the preceding step), this side can be plotted versus P^N; a straight line of slope, A, and intercept, c_o, should be obtained. The results of the application of this equation to the first creep data are shown in Fig. A-2.

This same method was used in evaluating these constants for creep of the mechanically conditioned mat. When dealing with first creep recovery, the additional complication of nonrecoverable deformation is encountered. (The dependence of this nonrecoverable deformation on the times involved in the creep and recovery measurements are discussed in the body of the thesis.) If the nonrecoverable creep is defined by the equation

$$(\Delta c)_{n.r.} = c_f - c_i \qquad (A-4)$$

where

c_f = mat solids concentration following the completion of the recovery run, and
c_i = mat solids concentration before first creep is begun,

it is found that for the times involved in these measurements,

$$(\Delta c)_{n.r.} = 0.00437 P_r^{0.367}. \qquad (A-5)$$

(The constants in this equation are evaluated by plotting the logarithm of $(\Delta c)_{n.r.}$ versus the logarithm of P_r, the apparent stress removed prior to the recovery run; the slope of such a plot is 0.367 and the intercept is the logarithm of 0.00437.)

The time-dependent portion of first creep recovery can be represented by Equation (A-1), but in this case, c represents the solids concentration at any time, t, following the removal of the stress, P_r, and c_o is replaced by c_f, the mat solids concentration at the completion of the recovery run. Thus, the equation becomes:

$$c - c_f = (A + B \log t) P_r^N. \qquad (A-1')$$

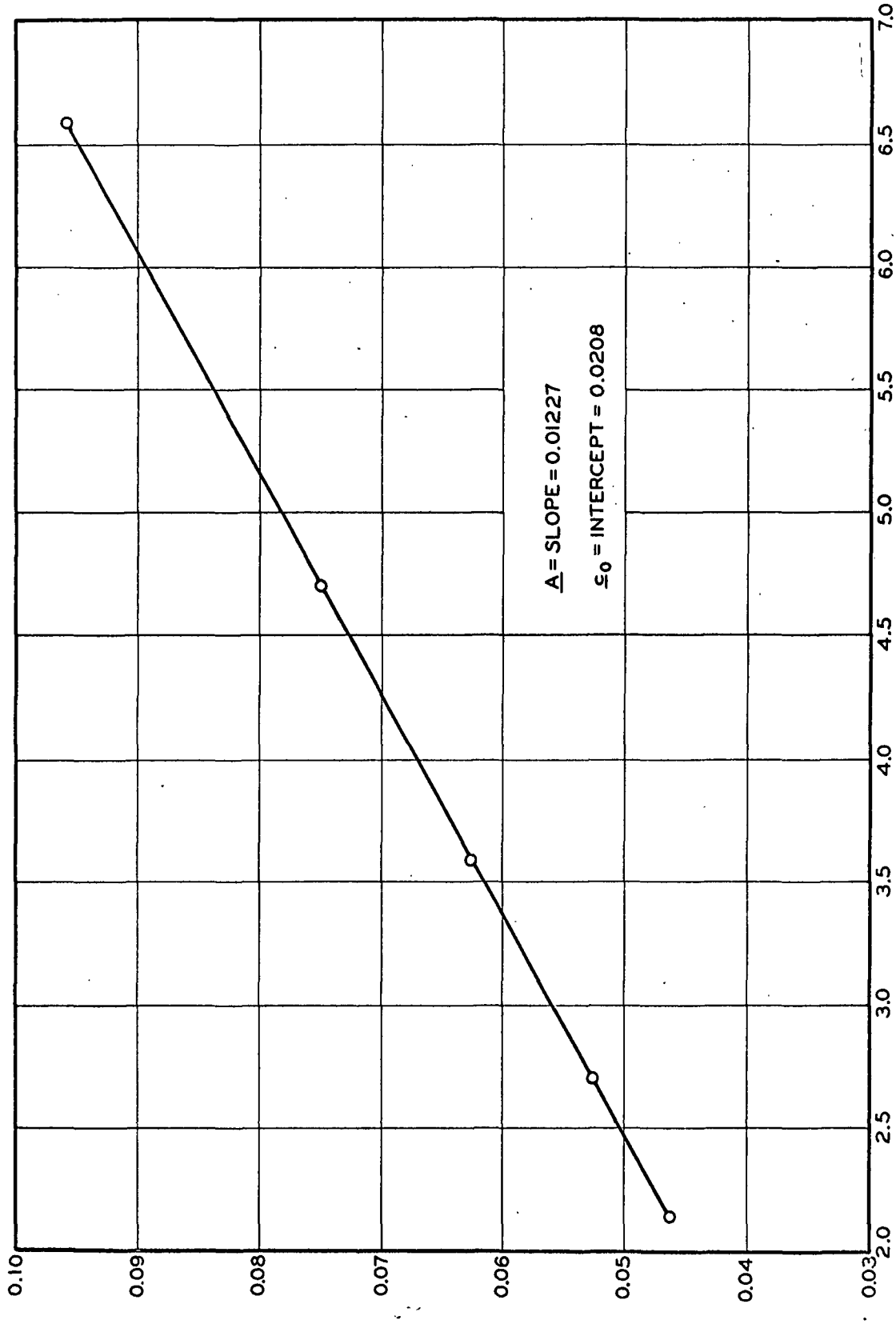

Figure A-2. Evaluation of A and ε_0 for First-Creep Data

If this equation is added to Equation (A-4), we obtain

$$(\underline{c} - \underline{c}_f) - (\underline{c}_f - \underline{c}_i) = \underline{c} - \underline{c}_o = (\underline{A} + \underline{B} \log \underline{t})\underline{P}_r^{\underline{N}} - (\Delta \underline{c})_{n.r.} \qquad (A\text{-}6)$$

Equation (A-19) is evaluated in the same way as was Equation (A-1) for first creep and is then combined with Equation (A-5) to yield an expression for $(\underline{c} - \underline{c}_o)$. In this case, $\underline{c}_o$ refers to the mat solids concentration under the precompression stress ($\underline{c}_o = 0.0340$), since $\underline{P}_r$ in this instance does not include the precompression stress.

For creep recovery of the mechanically conditioned mat, a slightly different approach was used. Equation (A-1) is written for two apparent stresses as follows:

$$(\underline{c} - \underline{c}_o)_1 = (\underline{A} + \underline{B} \log \underline{t})\underline{P}_1^{\underline{N}} \qquad (A\text{-}7)$$

$$(\underline{c} - \underline{c}_o)_2 = (\underline{A} + \underline{B} \log \underline{t})\underline{P}_2^{\underline{N}} \qquad (A\text{-}8)$$

Taking logarithms of each equation yields:

$$\log (\underline{c} - \underline{c}_o)_1 = \underline{N} \log \underline{P}_1 + \log (\underline{A} + \underline{B} \log \underline{t}) \qquad (A\text{-}9)$$

$$\log (\underline{c} - \underline{c}_o)_2 = \underline{N} \log \underline{P}_2 + \log (\underline{A} + \underline{B} \log \underline{t}) \qquad (A\text{-}10)$$

If these two equations are now subtracted, the following equation results:

$$\underline{N}(\log \underline{P}_1 - \log \underline{P}_2) = \log (\underline{c} - \underline{c}_o)_1 - \log (\underline{c} - \underline{c}_o)_2$$

or

$$\underline{N} \Delta (\log \underline{P}_r) = \Delta[\log (\underline{c} - \underline{c}_o)]. \qquad (A\text{-}11)$$

By evaluating $\Delta(\log \underline{P}_r)$ and $\Delta[\log (\underline{c} - \underline{c}_o)]$ at several times and varying values of $\underline{P}_r$, the exponent, $\underline{N}$, can be evaluated. It is found that $\underline{N}$ is truly independent of time, since the same value of $\underline{N}$ is obtained regardless of the times chosen for the calculation.

If Equations (A-7) and (A-8) are subtracted prior to taking logarithms, we have

$$(\underline{c}_1 - \underline{c}_2) = (\underline{A} + \underline{B} \log \underline{t})(\underline{P}_1^{\underline{N}} - \underline{P}_2^{\underline{N}}). \qquad (A\text{-}12)$$

By evaluating $(\underline{c}_1 - \underline{c}_2)$ and $(\underline{P}_1^{\underline{N}} - \underline{P}_2^{\underline{N}})$ at various times, the term $(\underline{A} + \underline{B} \log \underline{t})$ can be evaluated as a function of time. If this term is designated as $\underline{M}(\underline{t})$, we then have

$$\underline{M}(\underline{t}) = (\underline{A} + \underline{B} \log \underline{t}). \qquad (A\text{-}13)$$

Thus, a plot of $\underline{M}(\underline{t})$ versus log $\underline{t}$ enables one to calculate the constants, $\underline{A}$ and $\underline{B}$.

In these developments, general symbols have been used throughout for both creep and recovery. Some clarification of the difference in the meanings to be attached to these values in the various cases should be made. In first creep data correlations, $\underline{P}$ refers to the total applied apparent stress (precompression plus compression), while in all other cases, it refers only to the apparent stress added during the creep portion of the test or removal prior to recovery. Although the lack of evidence in support of the true significance of the term, $\underline{c}_o$, makes it impossible to state definitely what this means in each case, if the equations were to hold down to zero applied stress, $\underline{c}_o$ would represent the mat solids concentration at this point. Thus, with first creep, $\underline{c}_o$ would then represent the true solids concentration at zero applied stress; in all other cases, it would represent the mat solids concentration when the mat was subjected to the stresses exerted by the precompression forces alone.

The following table summarizes the equation obtained for creep and recovery behavior, and also gives the percentile of the significance of the correlation used in the linear regression technique employed in determining the line of best fit. These percentile values are interpreted as follows. When the calculation is begun, it is assumed that the data points to be used are taken from a population of points which can be represented by a certain straight-line relationship. Once the best straight line has been determined, the chance that the actual data points come from the population necessary to give such a line is calculated as this percentage; if a percentage of 95 is obtained, this means that there is a 95% chance that the points on the line and the original data points have come from the same population (33).

TABLE VII

SUMMARY OF CREEP AND RECOVERY EQUATIONS

Type	Equation	Constants Evaluated	Correlation Significance, %
First creep	$\underline{c} - 0.0208 = (0.01227 + 0.000487 \log \underline{t})\underline{P}^{0.403}$	(a) $\underline{N}$ (= 0.403); $\underline{B}$ (= 0.000487); Equation (A-2)	99.5 - 99.9
		(b) $\underline{A}$ (= 0.01227); $\underline{c}_o$ (= 0.0208); Equation (A-3)	>99.9
First creep recovery	$\underline{c} - 0.0340 = 0.00450\underline{P}^{0.360} + (0.00158 - 0.000408 \log \underline{t})\underline{P}^{0.486}$	(a) Nonrecoverable portion; Equation (A-5)	>99.9
		(b) $\underline{N}$ (= 0.486); $\underline{B}$ (=-0.000408); Equation (A-2)	99.5 -99.9
		(c) $\underline{A}$ (= 0.001582); $\underline{c}_o$ (= 0.0340); Equation (A-3)	>99.9
Mech. cond. creep	$\underline{c} - 0.06738 = (0.00387 + 0.000174 \log \underline{t})\underline{P}^{0.462}$	(a) $\underline{N}$ (= 0.462); $\underline{B}$ (= 0.0001742); Equation (A-2)	>99.9
		(b) $\underline{A}$ (= 0.00387); $\underline{c}_o$ (= 0.06738); Equation (A-3)	>99.9

TABLE VII (Continued)

Type	Equation	Constants Evaluated	Correlation Significance, %
Mech. cond. recovery	$\underline{c} - 0.07162 = (0.000865 - 0.000215 \log \underline{t})\underline{P}^{0.462}$	(a) $\underline{N}$ (= 0.462); Equation (A-11)	99.5 - 99.9
		(b) $\underline{A}$ (= 0.000865); $\underline{B}$ (=-0.000215); Equation (A-13)	>99.9

APPENDIX II

ESTIMATION OF MEASUREMENT ERRORS

Although many errors could be introduced throughout the mat-forming and testing procedures, the only types which can be readily estimated are those introduced by the measurement of mat deflection. Since duplicate runs are identical to each other within these calculated limits, it may safely be assumed that no other major sources of error exist.

When taking readings with the micrometer or with the linear variable differential transformer-vacuum tube voltmeter arrangement, the following ranges of reading errors were encountered:

(a) Micrometer readings to ± 0.0005 cm.

(b) Voltmeter readings:

0.1-volt scale, ± 0.0002 volts
1.0-volt scale, ± 0.002 volts
10-volt scale, ± 0.02 volts

(c) Photographed Oscillograph, to ± 0.05 scale divisions, or about ± 0.0015 volts.

The calculation of errors can be divided into two parts; that due to the measurement of the initial mat thickness and that due to the measurement of thicknesses at times greater than zero. Any error made in the first quantity would give a constant error throughout the run, so that the entire curve would be either raised or lowered by a certain amount. The second type of error would cause fluctuations around any curve which was used to fit the data, and would be much easier to visualize from the data.

1. Determination of initial mat thickness.

(a) The micrometer reading involved introduces an error of ± 0.0005 cm.

(b) Since the voltmeter is usually on the 1.0-volt scale, and since the LVDT sensitivity is 0.77 cm./volt, the initial voltage reading would involve an error of $(0.002)(0.77) =$ ± 0.0015 cm.

(c) Since the voltage is set initially at an input value of ten volts, an error of ± 0.02 volts might be introduced here. The error in output voltage due to this

variation is $(E_{out})(0.02/10) = \pm 0.002 E_{out}$. Since E_{out} is usually initially at about 0.9 volts, the error involved here is $(0.9)(0.002)(0.77)$ = ±0.0014 cm.

Total error = ±0.0034 cm.

(This error includes both the measurement of the initial thickness with a micrometer and the conversion to voltage units for future times. The initial mat thickness alone can be determined to ±0.0005 cm.)

2. Determination of mat thickness at times following the initial reading.

(a) If this reading is taken on the 1.0-volt scale, at a value of 0.1 volts, the error involved due to reading the meter is $(0.02)(0.1)(0.77)$ = ±0.0015 cm.

Again, the input must be adjusted to ten volts before a reading is taken. This error is $(E_{out})(0.002)(0.77) = (0.1)(0.002)(0.77)$ = ±0.0002 cm.

Total error = ±0.0017 cm.

(b) If this reading is taken on the 0.1-volt scale at a value of 0.06 volts,

reading error = $(0.0002)(0.77)$ = ±0.00015 cm.
initial setting error = $(0.06)(0.002)(0.77)$ = ±0.00012 cm.

Total error = ±0.00027 cm.

To convert these errors in mat thickness to errors in the mat solids concentration, c, we must assume certain values of basis weight and mat thickness, L. Typical values are:

L = 0.5000 cm.

W/A = 0.04 g./sq. cm.

Then

$c = 0.04/0.50 = 0.08$ g./cc.

For the error involved in the initial mat thickness determination, $L = 0.5000 \pm 0.0034$ cm.

$$c_{min.} = 0.04/0.5034 = 0.07946$$

or $c_{initial}$ may vary by about ± 0.0005 g./cc.

For errors within a particular run:

If the 1.0-volt scale is used, maximum error = ± 0.00025 g./cc.

If the 0.1-volt scale is used, maximum error = ± 0.00003 g./cc.
(These values are calculated in the same manner as that shown for the initial error.)

These values are only approximate, since they are based on assumed average values of voltmeter scale readings, mat thicknesses, and basis weights. However, they should serve as good estimates of the maximum measurement errors involved in this work.

The errors involved in the data obtained from the oscillograph photographs will be approximately the same as those reported for readings made on the 1.0-volt scale; the initial constant error introduced by the measurement of mat thickness will also be the same as previously calculated.

APPENDIX III

DEPENDENCE OF c_o' ON FIBER DIMENSIONS FOR SYSTEMS OF ASSUMED ORIENTATION

Although c_o' has not as yet been evaluated under conditions of random fiber orientation in the plane of the sheet, this quantity can be calculated as a function of fiber dimensions for assumed orientations.

If the fibers are stacked in layers, such layer being made up of parallel fibers and the adjacent layers containing fibers oriented perpendicular to each other as in Fig. A-3, the following calculation can be made.

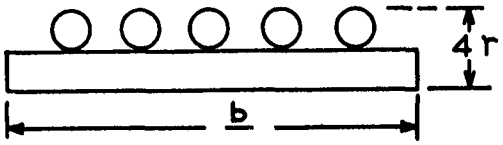

Figure A-3. Stacked Parallel-Perpendicular Orientation

Consider a "unit cell" composed of two layers of such fibers having a cross-sectional area of b^2. If such a system has a void fraction, ϵ, and contains n fibers,

$$\epsilon = \frac{\text{solid volume}}{\text{total volume}} = \frac{(2n)(\pi r^2 b)}{4rb^2} = \frac{\pi n}{2}\left(\frac{r}{b}\right) \qquad \text{(A-14)}$$

Since n is not a function of fiber dimensions (except in the limiting case of a close-packed network), the void fraction is proportional to the ratio of fiber diameter to fiber length. The void fraction at zero applied stress can be related to c_o' by:

$$\epsilon_{\sigma=0} = \frac{\nu c_o'}{} \, . \qquad \text{(A-15)}$$

Combining Equations (A-14) and (A-15), we obtain

$$c_o' = \frac{\pi n}{2} \, \frac{r}{\nu b} \, . \qquad \text{(A-16)}$$

If the fibers are stacked in a triangular fashion, as shown in Fig. A-4, the following calculations can be made.

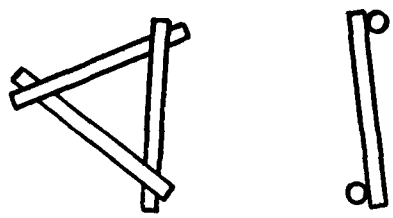

Figure A-4. Triangular Stacking of Fibers

In general, the ratio of fiber length to diameter for pulp fibers is very large. Therefore, the thickness of this "unit cell" can be approximated by $4\underline{r}$.

$$\epsilon = \frac{3\pi \underline{r}^2 \underline{b}}{(4\underline{r})(1/2)(\underline{b})(\sqrt{3}\underline{b}/2)} = \sqrt{3}\pi\left(\frac{\underline{r}}{\underline{b}}\right) \quad \text{and}$$

$$\underline{c}_o' = \sqrt{3}\pi\left(\frac{\underline{r}}{\underline{vb}}\right). \tag{A-17}$$

These two simple types of assumed orientation show that whether the fibers all lie in the plane of the sheet (Case 1) or at small angles to it (Case 2), the mat solids concentration at zero compacting apparent stress is directly proportional to the quantity $(\underline{r}/\underline{vb})$. While these treatments assume that the fibers are straight, such would probably not be the case in actual practice. However, this same assumption was made in the derivation in which the fiber network was treated as a system of beams. When dealing with stiff, unstressed fibers, this assumption may be quite realistic.

APPENDIX IV

TABULATED DATA

TABLE VIII

FIRST AND SECOND CREEP BEHAVIOR (FIGURE 14)

First Creep

Run 4-A (Apparent Stress=5.99)		Run 4-B (A.S.=10.85)		Run 4-C' (A.S.=20.86)		Run 4-D (A.S.=40.42)		Run 4-E' (A.S.=89.52)	
Time(sec.)	c(g/cc)	Time	c	Time	c	Time	c	Time	c
0	0.0348	0	0.0334	0	0.0342	0	0.0328	0	0.0348
.085	.0433	.0391	.0387	10	.0642	10	.0768	10	.0994
.106	.0436	.0782	.0436	20	.0646	20	.0774	20	.1003
.148	.0442	.1173	.0474	30	.0650	30	.0777	30	.1008
.232	.0449	.1564	.0491	60	.0656	60	.0784	60	.1022
.315	.0452	.1955	.0502	90	.0660	90	.0787	90	.1025
.399	.0455	.235	.0510	120	.0662	120	.0790	120	.1028
.483	.0457	.274	.0514	240	.0667	240	.0796	240	.1034
.650	.0460	.313	.0521	480	.0672	480	.0801	480	.1040
.817	.0461	.391	.0522	960	.0676	960	.0805	960	.1044
5	.0468	.469	.0524	1920	.0682	1920	.0810	1920	.1052
10	.0471	.547	.0526	3600	.0689	3600	.0815	3600	.1086
20	.0474	.626	.0527	5400	.0691	7200	.0824	7200	.1091
30	.0476	.703	.0528	9000	.0696	9000	.0828	9000	.1093
60	.0480	5	.0536						
90	.0482	10	.0540						
120	.0483	20	.0544						
240	.0486	30	.0546						
480	.0491	60	.0551						
960	.0493	90	.0552						
1920	.0497	120	.0554						
3600	.0502	240	.0556						
7200	.0506	480	.0560						
9000	.0508	960	.0563						
		1920	.0566						
		3600	.0574						
		7200	.0580						
		9000	.0583						

TABLE

FIRST AND SECOND CREEP BEHAVIOR (FIGURE 14)

Second Creep

Run 4-A		Run 4-B		Run 4-C'		Run 4-D		Run 4-E'	
Time(sec)	c(g/cc)	Time	c	Time	c	Time	c	Time	c
0	0.0419	0	0.0442	0	0.0472	0	0.0507	0	0.0526
.0296	.0440	.00995	.0444	10	.0665	10	.0790	5	.1013
.0692	.0462	.0497	.0496	20	.0670	20	.0795	10	.1018
.1087	.0473	.0895	.0509	30	.0671	30	.0798	20	.1026
.1482	.0480	.1293	.0536	60	.0674	60	.0802	30	.1028
.1875	.0482	.1692	.0541	90	.0677	90	.0804	60	.1036
.267	.0485	.209	.0544	120	.0680	120	.0806	90	.1042
.345	.0487	.249	.0546	240	.0682	240	.0812	120	.1044
.424	.0488	.328	.0546	480	.0684	2760	.0828	240	.1050
.503	.0490	.408	.0547	960	.0686	3600	.0830	480	.1058
.662	.0491	.488	.0548	1920	.0688	7200	.0834	960	.1066
10	.0495	.567	.0548	3600	.0694	9000	.0836	1920	.1071
20	.0496	.647	.0550	7200	.0700			3600	.1078
30	.0498	5	.0554	9000	.0701			7200	.1080
60	.0499	10	.0556					9000	.1086
90	.0501	20	.0558						
120	.0501	30	.0560						
240	.0503	60	.0562						
480	.0468	90	.0563						
960	.0506	120	.0564						
1920	.0508	240	.0566						
3600	.0511	480	.0568						
7200	.0514	960	.0570						
9000	.0515	1920	.0572						
		3600	.0576						
		7200	.0578						
		9000	.0579						

TABLE IX

FIRST AND SECOND CREEP RECOVERY BEHAVIOR (FIGURE 15)

First Creep Recovery

Run 4-A (Apparent Stress=5.99)		Run 4-B (A.S.=10.85)		Run 4-C' (A.S.=20.86)		Run 4-D (A.S.=40.42)		Run 4-E' (A.S.=89.52)	
Time(sec.)	c(g/cc)	Time	c	Time	c	Time	c	Time	c
0	0.0508	0	0.0582	0	0.0696	0	0.0828	0	0.1093
.235	.0465	.0198	.0564	10	.0526	.0207	.0774	.0402	.0968
.273	.0464	.0596	.0545	20	.0519	.0620	.0716	.0804	.0920
.312	.0462	.0993	.0534	30	.0514	.1033	.0688	.1205	.0886
.389	.0460	.139	.0528	60	.0506	.1447	.0675	.1607	.0861
.466	.0459	.179	.0523	90	.0503	.1860	.0666	.201	.0842
.543	.0458	.218	.0519	120	.0500	.227	.0657	.281	.0814
.620	.0456	.258	.0516	240	.0495	.269	.0651	.361	.0802
.736	.0456	.298	.0514	480	.0490	.351	.0638	.402	.0796
.851	.0454	.377	.0510	960	.0484	.433	.0630	.602	.0777
.967	.0454	.457	.0506	1920	.0480	5	.0581	.804	.0789
10	.0444	.537	.0504	3600	.0476	10	.0574	1.007	.0777
20	.0441	.616	.0501	7200	.0472	20	.0564	1.127	.0771
30	.0440	——	——	9000	.0472	30	.0561	1.167	.0748
60	.0436	10	.0482			60	.0552	1.408	.0744
90	.0434	20	.0478			90	.0546	1.609	.0738
120	.0434	30	.0474			120	.0544	1.890	.0728
240	.0431	60	.0470			240	.0535	5	.0688
480	.0428	90	.0466			480	.0530	10	.0673
960	.0426	120	.0464			960	.0522	20	.0660
1920	.0423	240	.0460			1920	.0517	30	.0655
3600	.0421	480	.0456			3600	.0513	60	.0643
7200	.0420	960	.0453			7200	.0507	90	.0634
9000	.0419	1920	.0448			9000	.0507	120	.0628
		3600	.0446					240	.0616
		7200	.0443					480	.0604
		9000	.0442					960	.0596
								1920	.0586
								3600	.0580
								7200	.0572
								9000	.0572

TABLE IX

FIRST AND SECOND CREEP RECOVERY BEHAVIOR (FIGURE 15)

Second Creep Recovery

Run 4-A		Run 4-B		Run 4-C'		Run 4-D		Run 4-E'	
Time	c	Time	c	Time	c	Time	c	Time	c
0	0.0515	0	0.0579	0	0.0701	0	0.0836	0	0.1086
.0300	.0498	.01975	.0574	10	.0551	.0421	.0738	.0201	.1094
.0700	.0488	.0593	.0555	20	.0544	.0842	.0708	.0603	.1044
.1100	.0482	.0988	.0545	30	.0541	.1263	.0692	.1007	.1000
.1500	.0479	.1383	.0539	60	.0534	.1684	.0682	.1408	.0974
.1900	.0476	.1778	.0535	90	.0531	.2105	.0673	.1810	.0954
.2300	.0474	.217	.0532	120	.0528	.252	.0666	.221	.0934
.2700	.0474	.257	.0528	240	.0522	.294	.0662	.302	.0916
.3500	.0471	.296	.0526	480	.0516	.336	.0658	.382	.0898
.4300	.0470	.336	.0524	960	.0512	5	.0616	.543	.0876
.5100	.0468	.414	.0522	1920	.0507	10	.0608	.583	.0872
.5900	.0467	.493	.0521	3600	.0504	20	.0603	.824	.0860
.6700	.0466	.612	.0518	7200	.0500	30	.0598	1.023	.0848
5	.0457	5	.0501	9000	.0499	60	.0592	1.308	.0836
10	.0455	10	.0497			90	.0588	5	.0785
20	.0452	20	.0493			120	.0584	10	.0771
30	.0451	30	.0491			240	.0577	20	.0754
60	.0448	60	.0487			480	.0571	30	.0746
90	.0448	90	.0485			960	.0566	60	.0732
120	.0446	120	.0484			1920	.0560	90	.0727
240	.0444	240	.0480			3600	.0555	120	.0724
480	.0442	480	.0476			7200	.0550	240	.0714
960	.0440	960	.0473			9000	.0548	480	.0700
1920	.0437	1920	.0469					960	.0690
3600	.0434	3600	.0466					1920	.0681
7200	.0433	7200	.0462					3600	.0672
9000	.0432	9000	.0462					7200	.0665
								9000	.0640

TABLE X

MECHANICALLY CONDITIONED CREEP (FIGURE 20)

First Creep

Run 6-A (Apparent Stress=4.77)		Run 6-B (A.S.=9.63)		Run 6-C (A.S.=19.64)		Run 6-D (A.S.=34.04)	
Time(sec.)	c(g/cc)	Time	c	Time	c	Time	c
0	0.0712	0	0.0714	0	0.0717	0	0.0715
5	.0757	5	.0787	10	.0831	5	.0884
10	----	10	.0788	20	.0833	10	.0884
20	.0759	20	.0790	30	.0834	20	.0886
30	.0759	30	.0791	60	.0835	30	.0887
60	.0760	60	.0791	90	.0836	60	.0888
90	.0760	90	.0793	120	.0837	90	.0890
120	.0760	120	.0793	240	.0838	120	.0892
240	.0761	240	.0794	480	.0842	240	.0893
480	.0762	480	.0796	960	.0844	480	.0894
960	.0763	960	.0798	1920	.0847	960	.0896
1920	.0765	1920	.0800	3600	.0848	1920	.0899
3600	.0766	3600	.0801	7200	.0852	3600	.0902
7200	.0768	7200	.0803	9000	.0852	7200	.0906
9000	.0769	9000	.0804			9000	.0906

Second Creep

Run 6-A		Run 6-B		Run 6-C		Run 6-D	
Time	c	Time	c	Time	c	Time	c
0	0.0714	0	0.0714	0	0.0716	0	0.0721
5	.0758	5	.0789	5	.0834	5	.0887
10	.0759	10	.0790	10	.0836	10	.0888
20	.0760	20	.0791	20	.0837	20	.0890
30	.0760	30	.0792	30	.0838	30	.0891
60	.0760	60	.0794	60	.0837	60	.0893
90	.0761	90	.0794	90	.0840	90	.0894
120	.0761	120	.0794	120	.0841	120	.0894
240	.0761	240	.0796	240	.0842	240	.0896
480	.0762	480	.0796	480	.0843	480	.0898
960	.0763	960	.0798	960	.0846	960	.0902
1920	.0765	1920	.0800	1920	.0848	1920	.0902
3600	.0766	3600	.0802	3600	.0848	3600	.0906
7200	.0768	7200	.0804	9000	.0852	7200	.0908
9000	.0768	9000	.0804			9000	.0908

TABLE XI

MECHANICALLY CONDITIONED CREEP RECOVERY (FIGURE 21)

First Creep Recovery

Run 6-A (Apparent Stress=4.77)		Run 6-B (A.S.=9.63)		Run 6-C (A.S.=19.64)		Run 6-D (A.S.=34.04)	
Time(sec.)	c(g/cc)	Time	c	Time	c	Time	c
0	0.0769	0	0.0804	0	0.0852	0	0.0906
5	.0730	5	.0736	5	.0746	5	.0754
10	.0729	10	.0734	10	.0743	10	.0751
20	.0728	20	.0732	20	.0740	20	.0746
30	.0727	30	.0731	30	.0738	30	.0744
60	.0726	60	.0730	60	.0736	60	.0740
90	.0725	90	.0728	90	.0734	90	.0738
120	.0725	120	.0728	120	.0734	120	.0736
240	.0723	240	.0726	240	.0731	240	.0732
480	.0722	480	.0724	480	.0728	480	.0732
960	.0721	960	.0723	960	.0726	960	.0728
1920	.0718	1920	.0720	1920	.0722	1920	.0727
3600	.0717	3600	.0718	3600	.0721	3600	.0724
7200	.0715	7200	.0716	7200	.0717	7200	.0721
9000	.0714	9000	.0714	9000	.0716	9000	.0721

Second Creep Recovery

Run 6-A		Run 6-B		Run 6-C		Run 6-D	
Time	c	Time	c	Time	c	Time	c
0	0.0768	0	0.0805	0	0.0852	0	0.0908
5	.0731	5	.0738	5	.0747	5	.0760
10	.0730	10	.0736	10	.0744	10	.0750
20	.0729	20	.0735	20	.0742	20	.0746
30	.0728	30	.0734	30	.0740	30	.0744
60	.0728	60	.0732	60	.0737	60	.0742
90	.0726	90	.0731	90	.0735	90	.0742
120	.0726	120	.0730	120	.0735	120	.0736
240	.0725	240	.0728	240	.0733	240	.0736
480	.0723	480	.0726	480	.0730	480	.0733
960	.0722	960	.0724	960	.0726	960	.0727
1920	.0720	1920	.0723	1920	.0724	1920	.0725
3600	.0718	3600	.0720	3600	.0722	3600	.0721
7200	.0717	7200	.0718	6900	.0720		
9000	.0717	9000	.0717	9000	.0718		